Summer 2008

In Vivo Murine Melanoma Tumor Responses to Nanosecond Pulsed Electric Field Treatment

Xinhua Chen
Old Dominion University

IN VIVO MURINE MELANOMA TUMOR RESPONSES TO NANOSECOND PULSED ELECTRIC FIELD TREATMENT

by

Xinhua Chen
M.D. June 1999, Xinjiang Medical University
Ph.D. May 2006, Zhejiang University School of Medicine

A Dissertation Submitted to the Faculty of
Old Dominion University in Partial Fulfillment of the
Requirement for the Degree of

DOCTOR OF PHILOSOPHY

BIOMEDICAL SCIENCES

OLD DOMINION UNIVERSITY
August 2008

Approved by:

R. James Swanson (Co-Director)

Karl H. Schoenbach (Co-Director)

Christopher J. Osgood (Member)

Stephen J. Beebe (Member)

ABSTRACT

IN VIVO MURINE MELANOMA TUMOR RESPONSES TO NANOSECOND PULSED ELECTRIC FIELD TREATMENT

Xinhua Chen
Old Dominion University, 2008
Director: Dr. R. James Swanson
Dr. Karl H. Schoenbach

High intensity nanosecond pulsed electric fields (nsPEF) were applied to melanoma tumors to observe functional and structural biological changes and to investigate the possible molecular mechanisms responsible. An animal model was set up by injecting B16F10 mouse melanoma cells into SKH-1 mice. A treatment (T_x) of 100 pulses: 300 nanosecond duration; 40 kV/cm field strength; at 0.5 Hz rate were delivered to melanoma tumors in 120 mice. The nsPEF T_x caused tumor self-destruction with sharply decreased cell volumes and shrunken nuclei. The apoptotic biochemical tests confirmed nsPEF T_x induced apoptosis in a time-dependent manner. Examination of gross vessel and micro-vessel density indicated direct vascular damage to pre-existing vessels and anti-angiogenic consequence on neovascular development concomitant with tumor self-destruction. A five-month survival study on 36 mice showed nsPEF T_x eliminated tumors with no recurrence to the primary site over the five months. In contradistinction to ionization, thermal or electroporation T_x, nsPEFs produced broad impacts on the melanomas *in vivo*, ranging from DNA fragmentation, caspase activation, nuclear damage, apoptosis induction, damage to pre-existing intra-tumoral vessels and neovascular inhibition. These tumor responses were expressed by histological and biochemical changes in both short and long term trials. The data indicate nsPEF T_x acts as non-chemical, non-thermal and non-ligand stimulus that can ablate melanomas *in vivo*.

This thesis is dedicated to my parents
Yongyu Fang and Youzheng Chen
Who made my life possible and meaningful
For their unconditional love and sacrifice

ACKNOWLEDGMENTS

Though my individual name with the designation of Ph.D. will be written on the cover of the dissertation, many people have contributed to the production and completion of this degree. I owe my gratitude to all those who have made this dissertation possible.

I really appreciate my supervisor Dr. R. James Swanson for his generous shepherding. I received amazing grace in having him to direct me in course study, candidate exam, research and defense. Throughout my doctoral work he and Gloria continually helped me not only in academic growth but also spiritual life. They mean much more than the teachers to me but are my American parents. I hope that one day I will become as good an advisor to my students as Dr. Swanson has been to me.

I would like to acknowledge my co-advisor Dr. Karl H. Schoenbach for the kind invitation to join his bioelectric team and give me the chance to know pulsed power. He gave me the freedom to explore on my own and at the same time the guidance to recover when my steps faltered. He set himself as a good example as a scientist for me to develop independent thinking and research skills. Also appreciation goes to Mr. Frank Reidy, who interviewed me in Beijing and initiated my adventure to Norfolk. His passion for science pushed me to overcome many crisis situations and finally finish this dissertation.

I wish to thank my mentor Dr. Stephen Beebe for coaching me to completion of the apoptosis experiment in his laboratory. He stimulated my further thinking of experimental design and greatly assisted me with scientific writing. Dr. Beebe taught me how to question thoughts and express ideas. I am also thankful to him for carefully reading and commenting on countless revisions of my English expression.

I am extremely grateful for the assistance, generosity and advice I received from my boss at home, Dr. Shuseng Zheng and the staff at the First Teaching Hospital, Zhejiang University School of Medicine. Their assistance helped me complete another PhD in China during 2003-2006. I owe a special note of gratitude to Dr. Hao Wen, his wife Jing Xu and the team in Xinjiang Medical University for the kind collaboration. I appreciate Dr. Lei Geng, Dr. Jiangwen Jiang, Dr. Shengyong Yin, Dr. Haiyang Xie and Dr. Lin Zhou, who devoted time aiding me in the candidate exam, mid phase evaluation,

operation skill test and defense. I extend thanks to Dr. Jinjun Li from Shanghai Tumor Institute for his kind offering of expertise and instrument in tissue micro-array.

This research was mainly supported by Frank Reidy Research Center and partially funded by the National Natural Science Foundation of China. (No. 30700778) and Zhejiang Government Grant for Distinguished Young Medical Faculty (No. 2007QN006).

I extend many thanks to Dr. Rich Nuccitelli and Dr. Juergen Kolb, who gave me the first hand help in my project. I would like to acknowledge for numerous discussions and lectures during course study in their class that helped me improve knowledge in the area.

My academic brother, Dr. Shu Xiao, has been always available to listen and give advice. I am deeply grateful to him for the long discussions that broadened my horizon. The same appreciation applies to Dr. Nianyong Chen, who was always ready to comment on my research.

I am also very grateful for having an exceptional doctoral committee and wish to thank Dr. Christopher J. Osgood and Dr. Wayne Hynes for the challenge and motivation.

My sincere thanks to Barbara Carroll and Ruth Lyman. Their good support made my lab work organized. Also thanks for warm hands from Dr. Franck Andre, Angela Bowman and Hunter Baldwin for their great help in the lab. I am also very grateful to Dr. Peter Blackmore and Sandra Anderson for their patient assistance in my lab rotation in EVMS.

My graduate studies would not have been the same without the social and academic challenges and diversions provided by all my student-colleagues in CBE. I am particularly thankful to my friends Yiling Chen, Wei Ren, Fang Li, Liang Yu, Jie Zhuang. Rachael Shevin, Thomas Camp and Wentia Ford. We not only helped each other in course study and journal club but also relaxed, played Ping-Pong and traveled well together. I greatly value the friendship with American and Chinese families from Tabernacle and Larchmont churches that helped me adjust to a new country. I want to say thousands of thanks to my coach Yuming Geng, my dear roommate Dianna Thomas, and my English teacher William Thompson for their consistently taking good care of me without any complaint.

I am greatly indebted to the trusty fellow traveler Dr. Shaohua Fan for his understanding, consideration and encouragement. His faithful commitment and companionship shortens the mile.

The deepest gratitude for my father and mother, elder sister, baby brother, brother and sister in law and my little nephew Baby Tianle. It is the support from sweet family that carries me through.

TABLE OF CONTENTS

LIST OF TABLES

LIST OF FIGURES

CHAPTER I

INTRODUCTION

Melanomas now are the leading cause of death from diseases of the skin. Solid tumors develop from malignant transformation of melanocytes, which are specialized pigmented cells residing in the epidermal basement membrane of the skin.[1]

Malignant melanoma is a very aggressive disease with a high metastatic rate and very poor overall prognosis. The median survival rate is 6 months and 5-year survival rate is below 5%. Annually diagnosed cases of melanoma are reported as 53,600 and 7,400 patients died every year, which represents a 15-fold increase over the past four decades according to the epidemiologic data from American Cancer Society's website.[2]

The present treatment (T_x) of primary melanoma is surgical excision.[3] Complete surgical removal is the most successful and common treatment for melanoma. Excision removes the entire melanoma along with a border. In stages II and III melanoma cases the affected lymph nodes also need to be removed. Such extensive incisions through the dermis cause scarring on the skin.[4] However nsPEF T_x kills the tumor without disrupting the dermis so that scarring is less likely. NsPEF T_x should also be effective on other tumor types located deeper in the body if a catheter electrode can be guided to the tumor.

Besides surgical removal, other treatment options for metastatic lesions vary according to malignancy, nature and stage of the tumor. Melanoma has a high resistance to cytotoxic agents. Only two chemical medicines are approved by United States Food and Drug Administration (FDA) for use in patients with metastatic melanoma: dacarbazine and IL-2. Both agents have an overall response rate well below 20%, with long-term response uncertain.[5]

Dacarbazine was approved by FDA 25 years ago and is now the only FDA-approved single-agent chemotherapy for metastatic melanoma. Dacarbazine is an alkylating agent with no benefit in terms of relapse or survival.[6] Dacarbazine also has high toxicity to all rapidly dividing cells in addition to tumor cells. For example (1) Blood cells: These cells are vital because they fight infection, help the blood to clot, and carry oxygen. When chemotherapy affects blood cells, patients are more likely to get infections. (2) Cells in

---

The journal model for this dissertation is International Journal of Cancer.

hair follicles: Chemotherapy can lead to hair loss. (3) Digestive tract: Chemotherapy can cause poor appetite, diarrhea nausea and vomiting. Patients need to take other drugs for these side effects. Even with these serious side effects, no substantially superior single agent has yet been found a replacement.[7]

Among other therapeutic strategies studied in metastatic melanoma, immunological approaches have yielded the only new FDA-approved agent for metastatic disease, high-dose (HD) bolus interleukin 2 (IL-2).[8] IL-2 was the first immune cytokine to be molecularly characterized as a lymphocytic growth factor. IL-2 is a pleiotropic glycoprotein which is essential in the activation of a specific response to antigens by T cells, but also in triggering the innate immunity by stimulating several functions of NK cells and macrophages. However, like dacarbazine, IL-2 therapy causes high toxicity such as accumulation of fluid, flu-like symptoms, confusion, weight gain, low blood pressure and irregular heartbeat.[9]

Why are melanoma tumors areso resistant to chemical therapy? Some researchers[10] believe that cell hierarchy resides inside melanoma tumors and only a few chemotherapy-resistant cancer stem cells generate the new tumors. Most current therapies target the non-cancer stem cells which makes up the bulk of the melanoma but the resistant stem cells can always escape and survive allowing the tumor to recur after therapy seems effectively progressing. Only those therapies that specifically target the cancer stem cells can completely eradicate melanoma tumors. Studies of cancer stem cell are now focusing on gene-expression patterns which will differentiate them from normal melanoma cells.

Melanoma has traditionally been approached either systemically with chemotherapy, or locally with surgery or radiotherapy. Researchers have recognized the lack of effective therapies and are looking for improve treatments. More physically oriented methods have emerged in cases when surgery is impossible or contraindicated due to high risk. The physical methods accepted in clinical practice as non-surgical methods are minimally-invasive therapies such as localized radiotherapy,[11] Laser ablation [12] and radiofrequency ablation.[13]

The localized radiotherapy-carbon ion beam, which is a high linear energy transfer (LET) beam, has unique physical and biological properties. The range is well-defined and has insignificant scattering which allows focused penetration that can go into tissues.

This energy deposition is localized and can cause oxygenation-independent cell damage. However LET has not yet been fully validated by long-term survival statistics for the adverse effect of the radiation itself.[13]

Laser ablation has the advantage of being rapid and painless. Delivery of the beam however is so invasive that it should be contraindicated except in last ditch efforts. For accurate location, laser ablation often needs to be guided by magnetic resonance. To achieve successful tumor treatment, wide tissue margins around the tumor have to be coagulated which produce necrotic tissue, increasing the risk to vital organs around the tumor.

Radiofrequency ablation (RFA) is a thermal therapy along the order of microwave, laser, high-intensity focused ultrasound, and cryotherapy which use temperature change to kill tumor cells. RFA can raise tumor temperature to lethal levels for tumor cells. Recent developments in radiofrequency ablation technology make large-volume tissue ablation possible for melanoma as an attractive option for patients unable or unwilling to accept surgery. RFA provides safe and effective local treatment of melanomas. The energy causes ionic agitation producing frictional heat, which cooks the tumor and leads to cell death and necrosis. The time for the body to gradually replace the necrosis by fibrosis can be quite lengthy.

One treatment that combines both physical and chemical therapy that has caught people's attention is electrochemotherapy.[14] Electrochemotherapy is a creative combination that uses chemotherapy followed by local application of electric pulses to the tumor. Electric fields have been proven to increase drug delivery into the cells, which combines the physical effect of cell membrane poration with the chemotherapy drug dose.[15]

Electrochemotherapy is special because it uses a pulsed electric filed to alter the tumor cell membrane.[16] Electrochemotherapy requires a generator and electrodes. The generator produces the electrical pulse while the electrodes deliver the pulse into the solid tumor.[17] The general parameter requires hundreds of volts/cm at microseconds duration.[18] These temporary pores originate from the pulsed electric field thus increasing cell membrane permeability which enhanced the chemotherapeutic drugs uptake which

would naturally have a poor permeability without electroporation. When the application of the electric field stops, the temporarily-formed pores immediately close.[19]

In electrochemotherapy, the pulsed electric field is used as a local drug delivery approach.[20] Bioelectric researchers are more interested in using the pulsed electric field alone. They want to develop a chemical free, non-ionizing, non-thermal physical therapy that could trigger apoptosis by a different mechanism or pathway.[21] The recent development of nsPEF produces unique characteristics that may solve the problems caused by heat. NsPEF T_x initialize high electric fields (kV/cm) applied with ultra short durations (nanosecond). Quite different from classical plasma membrane electroporation, nsPEF can produce highly compressed power (billions of watts), ultra short pulse durations (nanosecond), rapid rise times (nanosecond), and high electric fields (kV/cm). The resulting nanosecond pulse is so short that it can penetrate into the cell before the plasma membrane is fully charged allowing nsPEF to have minimal affect the plasma membrane therefore not causing electroporation.[22]

nsPEF has had military applications,its application in biology creates a new academic subject: Bioelectrics, which means applications of ultra-short pulsed electric fields to biological living cells, tissues, and even organs. This new burgeoning branch of research analyzes how biological systems react to high electric fields applied with very short pulse nanosecond duration. NsPEF T_x has been applied in fighting against bacteria and has demonstrated decontamination potential. Only in recent years has it been applied to mammalian cells following careful modeling research and studies using non-mammalian cultured cells.[21] The main characteristics of nanosecond pulsed electric fields are their high power and low energy leading to very little heat production and their special ability to penetrate into the cell to penetrate intracellular organelles.[23] NsPEF T_x is unique because of its non-electroporation effect on the plasma membrane.[24]

During the past years a number of studies have been done to determine biological effects of nsPEF T_x in cultured cells. The results proved that nanosecond pulse stimulation of a variety of cells produces a wide range of physiological responses. *In vitro* studies on cells treated by nsPEF include: (1) p53-wild type and p53-null HCT116 (human colon carcinoma);[25] (2) HL-60 (human promyelocytic leukemia);[26] (3) Jurkat (human peripheral blood, leukemia);[27] (4) B16F10 (murine melanoma);[28] and from a

paper by Stacy, et al., [29] (5) BS-LCL (human B-cell lymphoblastoid line from a patient with bloom syndrome); (6) AT-LCL (Human B-cell lymphoblastoid line from a patient with ataxia-telangiectasia); (7) SV-Normal (Human SV40 transformed normal fibroblasts); (8) SV-AT (human SV40 transformed fibroblasts from a patient with ataxia-telangiectasia); (9) SV-FA (human SV40 transformed fibroblasts from a patient with Fanconi's anemia); (10) SV-XP (human SV40 transformed fibroblasts from a patient with xeroderma pigmentosum); (11) HS578T (BrCa-human ductal breast carcinoma); (12) HeLa (human adenocarcinoma of the cervix); and (13) 3T3(mouse pre-adipocytes). Effects of nsPEFs on cells *in vitro* include: (1) apparent direct electric field effects; (2) induced apoptosis leading to caspase activation and then cell death; (3) nuclear changes and modified cellular functions with delayed plasma membrane effects becoming smaller as the pulse duration is shortened; (4) release of calcium from internal calcium pools and activation of plasma membrane calcium influx channels or capacitative calcium entry (like ligand-mediated responses); (5) induction of DNA and cell cycle anomalies; and (6) diminished cell survival. The biological effect of nsPEF T_x on cells *in vitro* is directly related to the electric filed strength, the pulse number and the pulse duration.

The effect of nsPEF T_x on multicellular tissue or human subjects has not been tested until very recently. An *ex vivo* study on mouse embryonic fibroblasts was the initial approach for testing nsPEF effects on tissues. Fibrosarcoma tumors (B10.2) were injected in the flanks of C57Bl/6 mice and then excised and exposed to nsPEF T_x. Fibrosarcoma B10.2 cells *ex vivo* became reduced in size after nsPEF T_x.[30] Because the tumors were removed from the animals before T_x then sliced and exposed to nsPEF T_x in cuvettes, the experiment was *ex vivo* rather than *in vivo*. Therefore the data cannot substituted for an *in vivo* experiment.

Based on the previous *in vivo* and *ex vivo* work, nsPEF T_x is hypothesized as a highly localized, drug-free, non-thermal physical technique which would be a new therapy for tumor treatment. To apply nsPEF T_x to tumors *in vivo* is an important bridge to connect individual *in vitro* cellular response with future clinical application. This emerging field has unknowns surrounding the nsPEF mechanism of actions on the *in vivo* tumors. Our study provides prospective research data on nsPEF T_x on solid *in vivo* tumors.

Proof of apoptosis induction and anti-angiogenesis sheds light on the mechanism of how nsPEFs work on tumors. Since nsPEFs act as a non-chemical, non-thermal and non-ligand pulse that did not exist in the natural environment, these studies reveal new understandings of apoptotic and angiogenic signaling pathways in tumor tissues.

While a number of studies have been done to determine effects and mechanisms of nsPEFs in cultured cells, much remains to be done to determine nsPEFs effects on tumor tissues *in vivo*.

A previous *in vivo* case study was reported for a single patient. A nsPEF T_x was applied (150 pulses of 20 ns duration, and 60kV/cm) to both normal and malignant cells such as WI-38, a cell line established from normal human fetal lung fibroblasts, and VA-13, the matched WI-38 cells transformed with the SV40 virus (which inactivate sp53 and Rb). Cell viability after pulsation didn't show an immediate response which made them believe the final cell death or slowed cell proliferation were delayed results instead of the immediate response of cell membrane destruction. When nanoelectropulse therapy was applied to AsPC-1 tumors in athymic nude mice, a response was seen in 4, the effective rate was 66.7% and the biological effects included clinically complete remission in 3 of 6 animals. A single male human had nanoelectropulse therapy with 200 pulses (10 pulse bursts every 5 sec, 6.5 kV, 20 ns duration, 20 Hz) applied to a basal cell carcinoma with complete elimination. These trials show interesting therapeutic effects but were limited by the sparse case numbers without repetition or controls and thus without statistics.[28]

Our current project is designed to determine tumor response and molecular mechanisms for melanoma regression with nsPEF T_x *in vivo*. More specifically SKH-1 female mice bearing B16-F10 murine melanomas have been treated with 100 pulses of nsPEF T_x at 300 nanosecond pulse duration, 40 kV/cm electrical density at 0.5 Hz rate. Tumor growth inhibition was observed, the number of survival days was tracked after the nsPEF T_x and the biological effects such as induction of apoptosis and anti-angiogenesis. The mechanism of nsPEF parameters to affect biological results was also studied. This research is a unique prospective animal trial for nsPEF application *in vivo*. Our data, drawn from a large experimental animal population (more than two hundred), tested the pulse effects over three different time frames: (1) short-term observations (minutes after nsPEF T_x); (2) intermediate observation (days after nsPEF); and (3) long-term

observation (5-month survival study). I*n vivo* data were provided that is impossible to gather with *in vitro* cell cultures like vascular changes and tumor regression over a real-time framework. Following nsPEF T_x, the kinetics of tumor regression was determined by using ultrasound analysis of tumor volumes and inhibition of tumor blood flow by Doppler ultrasound. This study not only recorded the tumor response but has also revealed possible mechanisms of actions. Molecular events were also determined to be triggered by nsPEF T_x.

The 5 chapters in the dissertation will test the following specific aims:

1. To analyze the tumor volume quantatively after the nsPEF T_x to study if nsPEFs can cause tumor growth inhibition and ultra structural changes.
2. To determine if nsPEFs can (1) damage nuclei or DNA as measured by H2AX phosphorylation and TUNEL or (2) affect the related proteins such as caspase, 6, 7, bcl-2, BAD expression by immunohistology and western blot, thus allowing the kinetics of molecular events related to apoptosis post-nsPEF T_x to be determined.
3. To compare the tumor blood vessel changes, micro-vessel density and the angiogenesis related proteins such as vascular endothelial growth factor (VEGF), and platelet-derived endothelial cell growth factor (PD-ECGF) expression in the tumors with and without nsPEF T_x.
4. To study long-term animal survival rate after nsPEF Tx in mouse-survival days and tumor growth and recurrence in the primary site.
5. To determine the relationship between the *in vivo* biological effect as related to the nsPEF T_x dose.

Our results produce evidence that nsPEF T_x is an emerging modality that may have a role as a local cancer therapy. Therefore the data will form the basis for future human clinical applications in tumor therapy.

CHAPTER II

NSPEF INHIBIT MELANOMA GROWTH AND PRODUCE ABNORMAL TUMOR MORPHOLOGY

According to epidemic data from American Cancer Society, there are 53,600 newly diagnosed melanoma cases and 7,400 deaths per year, a 15-fold increase over the past four decades in the United States.[31] Treatment options for advanced metastatic melanoma are limited and the clinical prognosis is poor.[32] The only single agent therapy approved by the FDA is a chemotherapeutic medicine, decarbonizes (DTIC). It has severe side effects and brings no apparent survival benefit.[33] The challenges of therapy require new methods. Pulsed power technology has attracted attention for its unique biological effects on tumor growth. The application of high power and low energy makes nanosecond pulses pass the cells exterior plasma membrane but shocks the vital intracellular structures.[34] More recently, it has been shown *in silico* that unique nanopores are formed in all cell membranes including the plasma membrane.

nanosecond pulsed electric field (nsPEF) is a high electric field applied with ultra short pulse duration[35] (20kV/cm at 300 nanosecond in our research). Compressed power is extremely high (billions of watts) while the duration of nanosecond pulses are extremely short thus producing very low energy density with no thermal consequence in living cells.[36]

Prior *in vitro* research in our center has proven that pulses with high-intensity electric fields can affect intracellular structures producing a wide range of physiological responses (e.g., apoptosis, stimulation of calcium (Ca^{2+}) fluxes, changes in membrane potential) in different cell lines such as HL-60 (Human promyelocytic leukemia cells),[37] Jurkat (human T cell leukemia cells)[38] and HCT116 (colon carcinoma cells)[39]. But the *in vivo* proof is still absent.

In the present work, an animal model was set up and investigated the direct tumor response of nsPEF on tumor growth, and examined the morphological characteristics of nsPEF in the treatment of subcutaneous murine melanoma B16F10.

Material and Methods

B16 F10 cells

Murine melanoma B16-F10 cells were obtained from ATCC (Manassas, VA) and cultured in DMEM (Dulbecco's modified Eagle's medium) supplemented with 10% fetal bovine serum (FBS, Atlanta Biologicals), 4 mM l-Glutamine (Cellgro), and 2% Penicillin–Streptomycin solution (Cellgro) at 37°C in 5% CO2.

Animals

In vivo experiments were set up in conformity with IACUC guidelines under applicable international laws and policies (Animal Care and Use Committee of Eastern Virginia Medical School IACUC #04-011, #04-013). B16 F10 cells were implanted subcutaneously in the right and left flank of the SKH-1 female mice using 0.1 ml of cell suspension with 1×10^6 B16F10 cells prepared from *in vitro* cell cultures. Three tumors per mouse were induced; the treated tumor had electrode placement and nsPEF T_x. The sham tumor had electrode placement only without nsPEF T_x. The control tumor had no electrode placement or nsPEF T_x.

In vivo imaging

Before and after the treatment, melanomas were imaged daily by both transillumination and surface photography at 1.2x magnification. Tumor volume was calculated. Tumors were measured daily after the treatment using the formula [40] for prolate spheroid (square of the width x length x 0.52): $V = 0.52 \times D1^2 \times D2$, where D1 and D2 are short and long tumor diameters, respectively *in vivo* using tranillumination and surface photography.

NsPEF T_x

Pulses were generated using 40 KV/cm, 300 nanosecond pulses with a rise time of about 30 nanoseconds by a Blumlein pulse generator designed and assembled at the Frank Reidy Research Center for Bioelctrics. Three tumors induced on the same mouse were randomly selected as control, sham or treated tumor. An area of skin was pulsed in the same way as the treated tumor for safety evaluation and a second area of normal skin was collected without pulse or electrode placement as a skin control. One hundred pulses were applied to the treated tumor and treated skin at a frequency of 0.5 Hz with a needle electrode.

Histology study

Upon euthanasia, tumors were removed and fixed in 10% neutral buffered formalin prior to paraffin processing. Sections were stained with H&E and assessed microscopically for abnormal cell morphology. One hundred nuclei were randomly selected and outlined in ten non-overlapping fields of each section at 600× magnification. The nuclear area was calculated by MATLAB software and summed as the mean ± SD for statistical analysis. Fontana-Masson stain and Iron stain (hemosiderin) followed a routine protocol described.[41,42]

Transmission electron microscopy

After pulsing, the treated and the control tumors, along with the normal skin samples were excised and immediately put into primary fixation (3% glutaraldehyde) for two hours at room temperature and then secondary fixation (1% osmium tetroxide) was carried out in the dark at room temperature for one hour followed by repeated washing (3×) with phosphate buffer. Dehydration was accomplished with a series of 30%, 50%, 90% and 100% ethanol (v/v) for 15 min each. The dehydrated samples were suspended in propylene oxide followed by 1:1 treatment with propylene oxide: resin and finally with pure resin until infiltrated by resin polymerized. The resin blocks were carefully trimmed and various thicknesses (200nm, 300nm, and 500nm) were cut using an ultra microtome. Tissue ribbons were transferred to 300 mesh copper grids stained with uranyl acetate and lead citrate and then analyzed with a Jeol electron microscope at 160 kV.

Result

Tumor growth was inhibited by nsPEF T_x: Histological analysis.

A self-comparison model was set up to avoid the heterogeneity derived from differences mice. Three melanomas were induced on every SKH-1 mouse and decided randomly to be used as control, sham or treated tumor. The pulsed skin around the tumor was also collected to compare with the normal skin for further nsPEF safety evaluation. Altogether 12 mice were included in the 7-day-long tumor growth observation. Histological data showed that 100% of the treated tumors (12/12) responded to the nsPEF Tx compared to the sham and control tumors. The major pathological diagnosis was summarized as Table 1.

TABLE I - OVERVIEW OF H&E AND TEM MORPHOLOGICAL CHANGES SUMMARIZED FROM 120 MICE BEARING MELANOMAS WITH OR WITHOUT NSPEF T_X

	Control tumor	Treated tumor
Tumor structure	Regular nest and cancer cell cord	disordered
Tumor Center	Lobular	dead
Blood supply	Rich	poor
Tumor nest	Complete	destroyed
Nuclear chromatin	Clearly and evenly spread throughout nucleus	aggregated
Cytoplasm	Structured with organelles	cytoplasmic details lost
Nuclei	less pleomorphic with relatively regular contour,	more heterochromatin, condensed, elongated and dark
Nucleoli	regular and well formed	more pleomorphic, compact, prominent, and irregular in shape
Melanin	most located inside the cell	Some within cytoplasm but much scattered extra cellular space

Tumor growth was inhibited with nsPEF compared to the control tumors from the same mouse.

To avoid the individual tumor growth difference due to the immune system, tumors injected on the same mouse were randomly selected as the treated tumors (n=12) compared with controls (n=12) and shams (n=12). One week after nsPEF T_x the volume of tumor size showed significant difference ($p<0.001$). Control tumors on 12 mice grow faster and larger than the treated tumors on the other side. The skin in the tumor area was also pulsed. Edema and bleeding appear after nsPEF T_x and lasted 3 days. The skin damage underwent a week long recovery and eventually healed.

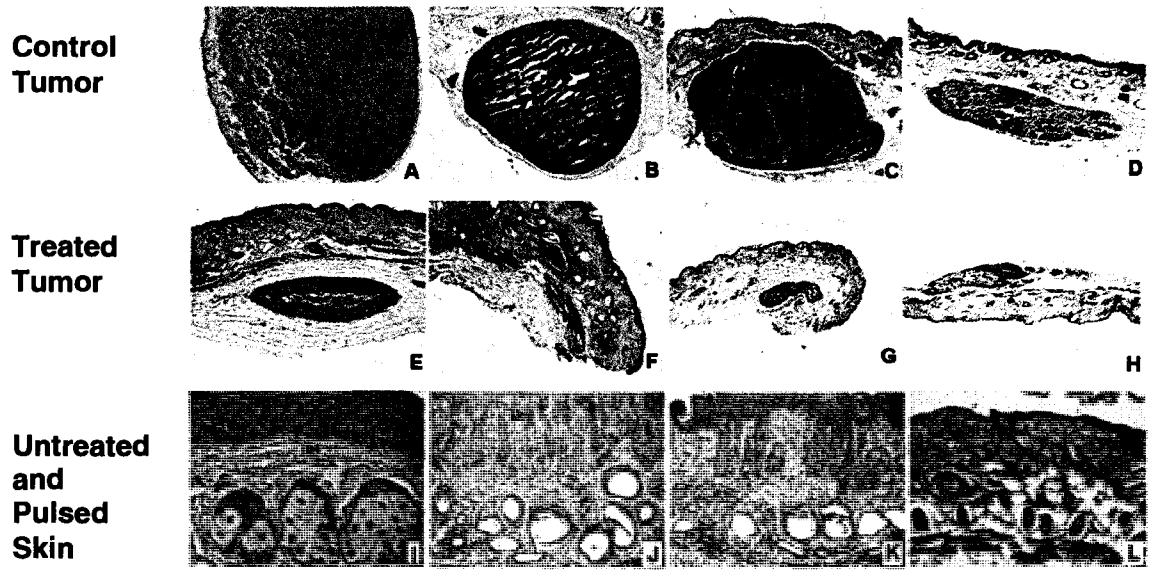

FIGURE 1 - *Tumor growth was inhibited 7 days post-nsPEF T_x compared with control tumors from the same mouse.* H&E comparison of the melanomas with or without nsPEF from the same mouse. For every mouse two tumors were injected on the same mouse but selected randomly one for nsPEF T_x and the other without any treatment used as a self-control. A and E, B and F, C and G, D and H are the tumors grown up on the same mouse (40x). Four different control tumors are shown in the top row; four treated tumors are shown in the middle and the skin in the nsPEF treated tumor areas were shown in the bottom row. I: pre-pulse skin (200x). J-K: post-pulse skin. J: First day post nsPEF T_x (200x). K: Third day post nsPEF T_x (200x). L: Seventh day post nsPEF T_x (40x).

Typical growth change after nsPEF T_x recorded by transillumination and surface photography

Pulsed skin undergoes an acute edema, with local bleeding 10 minutes and 2 days post treatment. On day 2 a shallow scar was observable on the surface, which recovered by day 7. Control tumors size increased continuously on days 2 and 7 maintaining a rich blood supply. Treated tumor growth was inhibited and a surface scar developed and tumor blood vessels disappeared as the tumors shrunk.

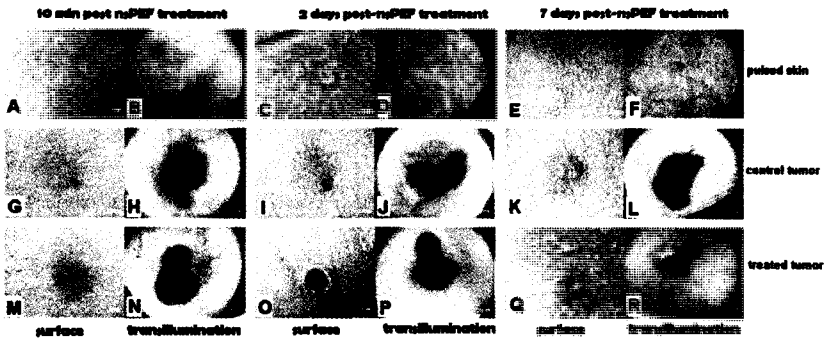

FIGURE 2 - Typical growth change after nsPEF T_x recorded by transillumination and surface photography. The images (1.2 x magnifications) show pulsed skin (top row) untreated control tumors (middle row) and tumors treated with nsPEFs with 100 pulses at 300ns and 40kV/cm (bottom row). Images were taken 10 minutes, 2 days and 7 days post nsPEF T_x as indicated. Images were taken of the surface and with transillumination as illustrated.

Tumor volume changes during 7-day post-nsPEFs treatment

Tumor volume changes during the first week post nsPEF T_x were plotted (Fig.3). Local treatment with nsPEF decreased the tumor volume significantly compared to the self control tumors. The sham was made by putting the electrode on the tumor without delivering the electric field. The sham tumor volume and growth curve had no significant difference from the control tumor, which indication that electrode insertion didn't account for the tumor reduction.

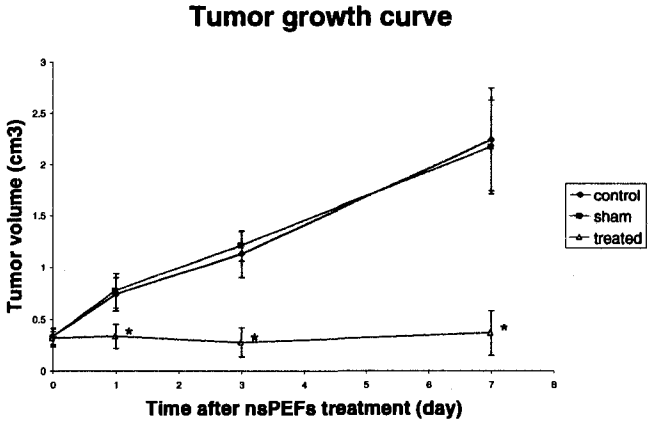

FIGURE 3 - Tumor volume changes during 7-day post nsPEFs treatment. Tumor volume was determined using calipers on days 1, 3 and 7 after treatment with 100 pulses at 300ns and 40kV/cm. Tumor volume for treated (n=12) was compared with controls (n=12) and sham (n=12), calculated and shown as cm^3 as described in Materials and Methods. (* $p < 0.001$)

Inferior view of tumors collected pos- euthanasia.

When the mice were euthanize, all tumors (n=36) were removed and photographed from the epidermal and subcutaneous surfaces. Figure.4 showed the inferior view of tumors. Twelve tumors from control group were large in size and rich in blood supply. The sham was similar to the control group. Twelve tumors from nsPEF treated group showed that tumor size decreased dramatically without an obvious blood supply around the tumors.

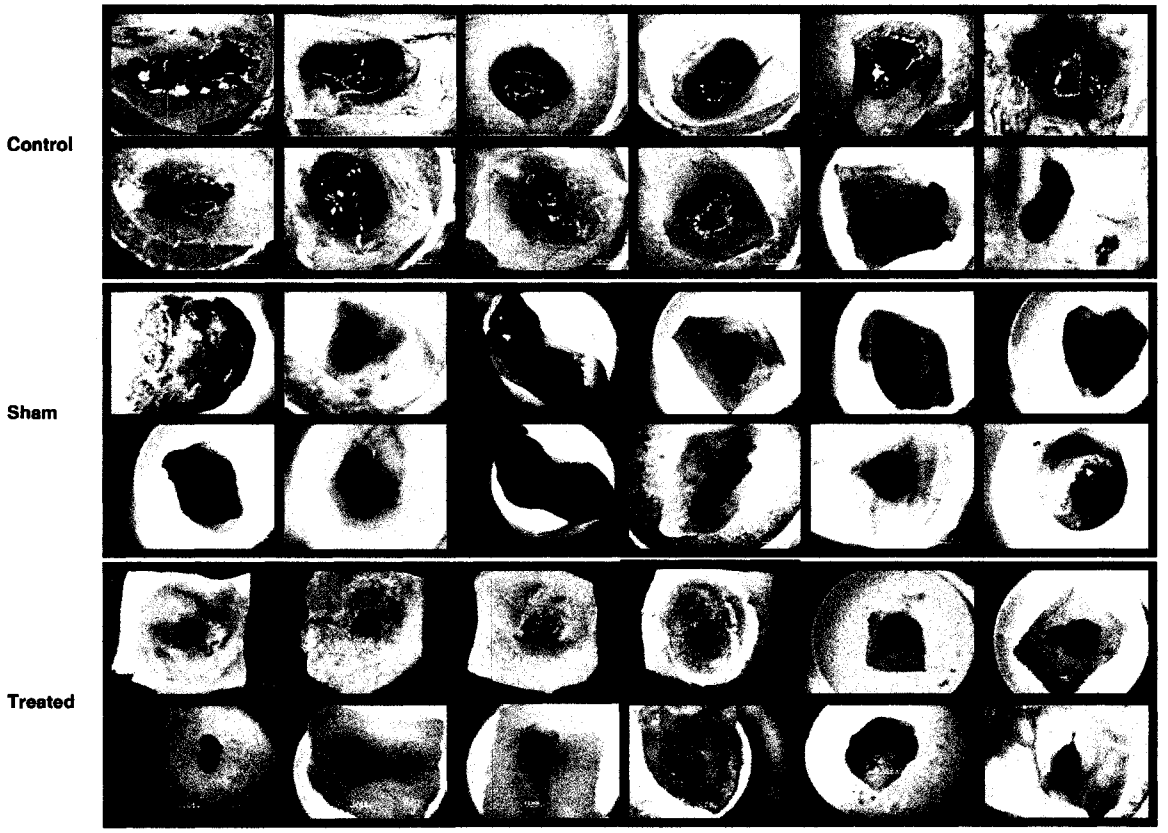

FIGURE 4 - Inferior view of tumors collected post euthanasia. Tumors were removed from the mice after euthanasia. All tumors (n=36, 12 per group) were removed and photographed from the epidermal and subcutaneous surfaces. Tumors were dissected then weighted for statistical analysis. The first frame shows 12 tumors from control group as indicated. The second frame shows 12 tumors from sham group and the third frame shows 12 tumors from nsPEF treated group.

Tumor weights was decreased 14 days post nsPEF treatment compared to the control and sham from the same mouse

Figure 5 showed nsPEF treated tumor volume was inhibited 14.8% of control tumors ($p<0.001$). No differences were observed between control and sham tumors

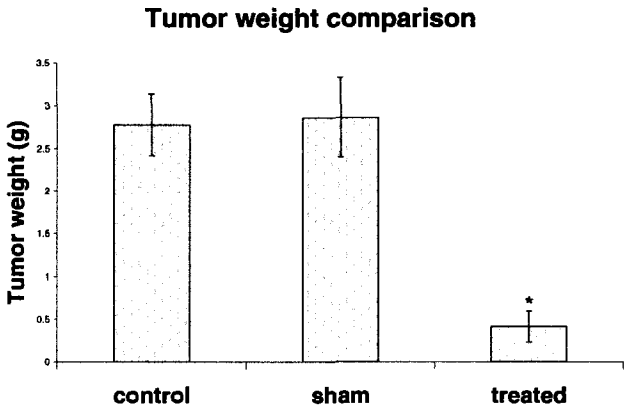

FIGURE 5 - Tumor weights was decreased by nsPEF treatment compared to the control and sham from the same mouse. Tumors were removed from control, sham and treated mice and weighed 14 days post nsPEF treatment (100 pulses, 300ns at 40kV/cm)

Melanoma tumor cell structure and nucleus were changed by nsPEF treatment.

Ultra structure and nuclear change were revealed by H&E. Control tumors showed the aggressive growth, regular nest shape with rich blood supply. The solid tumor was bounded by a thin fibrous capsule and contained internal fibrous bands, demarcating multinodular characteristics. Nests of tumor cells were delineated by well-formed basal lamina, composed of cellular lobules separated by hypocellular, fibrous bands. Nested patterns of growth were identified within these lobules. Tumor cells featured clear and regular nuclei with prominent nucleoli. The cytoplasm is characteristically pink and clear. Pigment suggestive of melanin was identified in an organized shape. Treated tumor nuclei dramatically shrink. Nests break down, losing the cord-like supporting structure on which tumor cells extend. Individual cells elongated and condensed, nuclear to plasma ratio decreased. Dense cytoplasmic bodies make the field dark, unclear and disordered. The arrows point to the tumor nest in the low magnification and the typical tumor cells and melanin in high magnification.

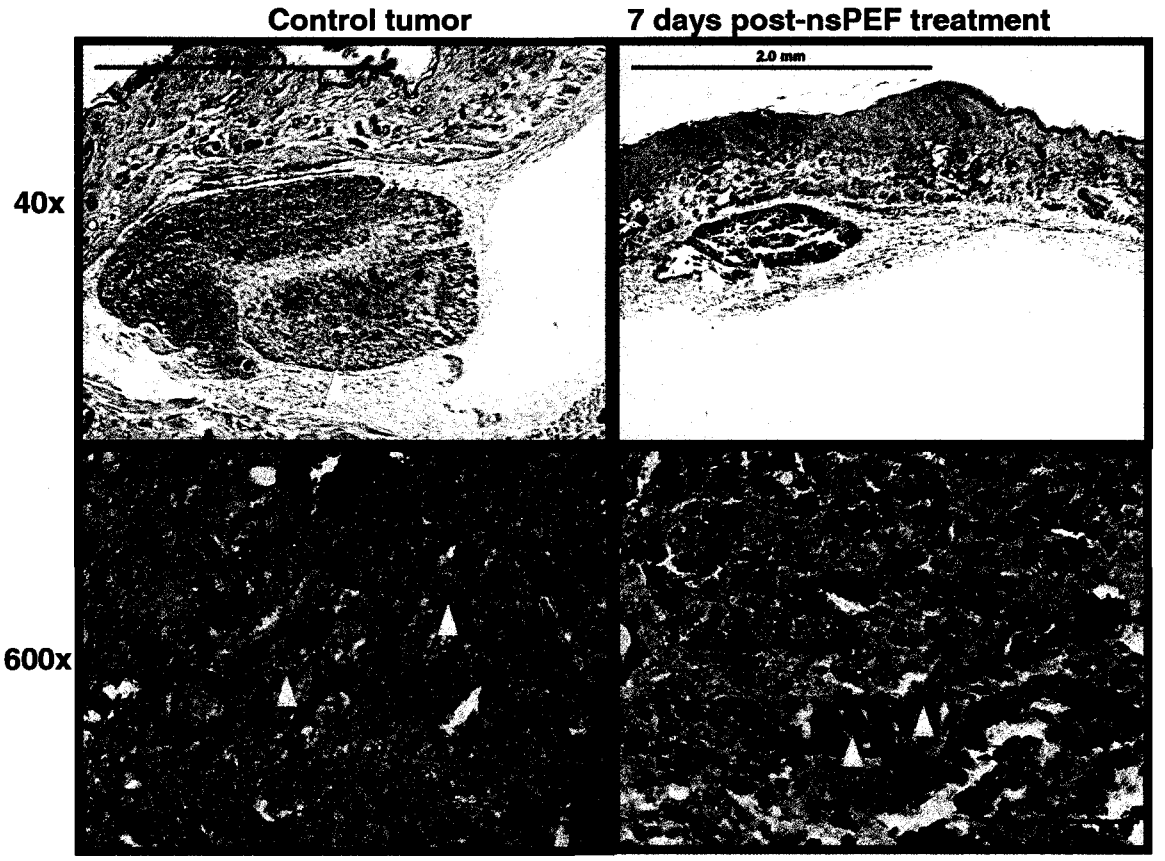

FIGURE 6 - Melanoma tumor cell structure and nucleus were changed by nsPEF treatment. Melanoma cell structure and nuclear changes were analyzed by H&E. Control tumors are stained by H&E and then photographed under 40x and 600x magnification. The arrows point to the tumor nest in low magnification and the typical tumor cells and melanin in high magnification. Bar scale: 2cm on the top line and 50 micro meters on the bottom line.

Melanoma tumors nuclear area was decreased by post nsPEF Tx.

Nuclear area changes of melanoma tumors post nsPEF treatment was shown in Figure.6. Control tumors (n=12) and nsPEF treated tumors (n=12) were compared by their nuclear area. A significantly decreased nuclear area was seen in tumors as indicated 7 days after nsPEF treatment. ($p < 0.05$)

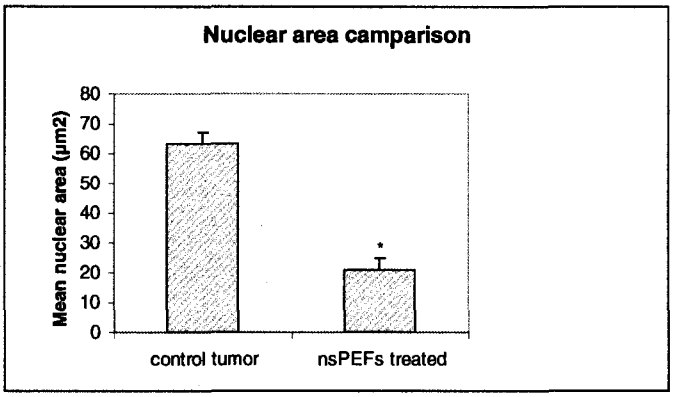

FIGURE 7 - Melanoma tumors nuclear area was decreased by post nsPEF Tx. Specimens were collected when mice were euthanized on the 7th day post nsPEF treatment. Control tumors (n=12) and nsPEF treated tumors (n=12) were routinely stained with H&E and analyzed by a computer-assisted image analysis with MATLAB as previously described. The nuclear area decreased significantly after nsPEF treatment (* $p < 0.05$)

Melanoma tumor cell sub-cellular structures was changed by nsPEF T_x

Sub-cellular structures were analyzed by transmission electron microscopy (TEM). Full-thickness biopsy was made from normal skin, control and nsPEF treated tumor. TEM showed the untreated skin has the typical sub-cellular organelle. The control tumor revealed typical malignant melanoma morphology: regular shaped nucleus with high proliferation and prominent nucleoli in the center, extensive rough endoplasmic reticulum, Golgi stacks, and a large quantity of ribosomes. In contrast, the nsPEF treated melanoma showed: (1) decreased nuclear size but increased nuclear /cytoplasmic ratio, (2) formation of dense cytoplasmic bodies, (3) degenerative tumor cells with fragmentation of nuclei and irregular nuclear outline.

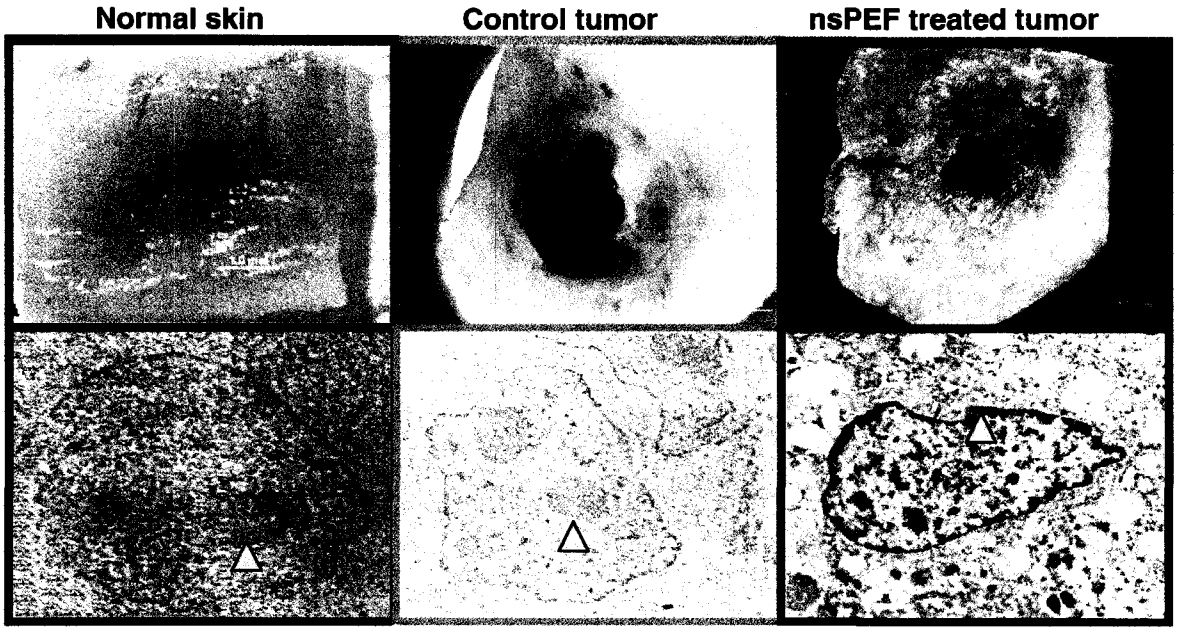

FIGURE 8 – Melanoma tumor cell sub-cellular structures was changed by nsPEF T_x. Melanoma tumor sub cell structure was analyzed by Transmission Electron Microscopy (TEM). Full-thickness biopsy of normal skin, control and nsPEF treated tumor from the same mouse 7 days post nsPEF T_x were dissected as shown in the upper row. The corresponding TEM was shown in the lower row. The first TEM picture on the left shows the mouse skin has the typical epidemic sub-cellular organelle. The arrow points to the nucleolus inside the normal epithelial cell. The TEM picture in the middle shows a control tumor. The arrow points to the nucleolus inside B16F10 cancer cell. The TEM picture on the right shows a treated tumor (100 pulses at 300ns and 40kV/cm). The arrow points to the fragmentation along the cell membrane inside a condensed, shrunken and wrinkled B16F10 tumor cell

Fontana stains for melanin in the melanoma tumors 7 days post nsPEF T_x.

Fontana stain for melanin was shown in Fig.9. Dark spots reveal the melanin layers which were clearly represented with Fontana Stain, a positive, marker for melanin. Control tumors without nsPEF treatment showed a layer of positive Fontana stain which outlines of malignant melanoma. Tumors post nsPEF treatment showed decreased volume with sparse melanin remaining. The staining results suggest nsPEF treatment can reduce or eliminate the melanin in the tumor. Based on the control tumor as a comparison, this staining change is an indirect sign of tumor damage. In tumors where the melanin persist post-nsPEF treatment, the melanin will be aggregated in extra cellular spaces and not within cells which indicates the cell death.

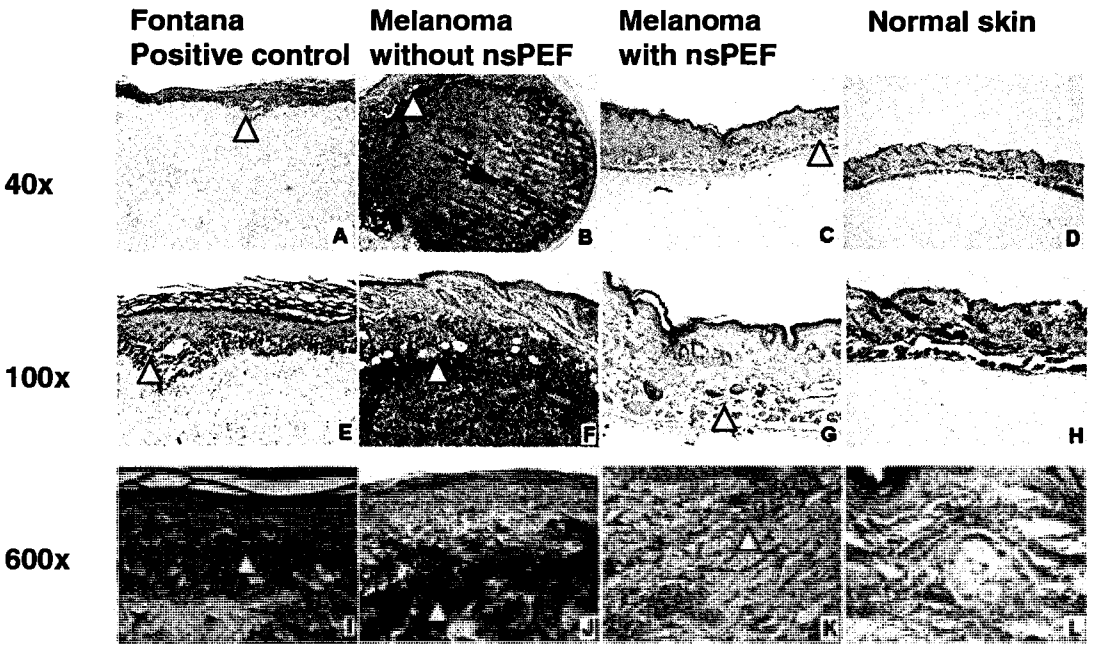

FIGURE 9 - Fontana stain for melanin in the melanoma tumors 7 days post nsPEF T_x. The first column (A, E, I, Fonata positive control) shows the human melanomas without treatment. The second column (B, F, J, melanoma without nsPEF) shows the mouse control tumors without nsPEF treatment. The third column (C, J, K, melanomas with nsPEF) shows tumors post nsPEF treatment. The fourth column (D, H, L, normal SKH-1 normal mouse skin) show negative Fontana stain because the SKH-1 mice are albino and thus almost no melanin in the skin. The arrows point to the melanin layer.

Iron stain for the old bleeding in the melanoma tumors with and without nsPEF T_x.

Iron stain of the mouse melanomas was shown in Fig.10. This extracellular hemoglobin/iron combines the iron stain. Control tumors showed melanin, but no iron. Treated tumor had positive iron staining. The micrographs indicate nsPEF causes some capillaries damage with hemoglobin of red blood cells accumulation within the treated area.

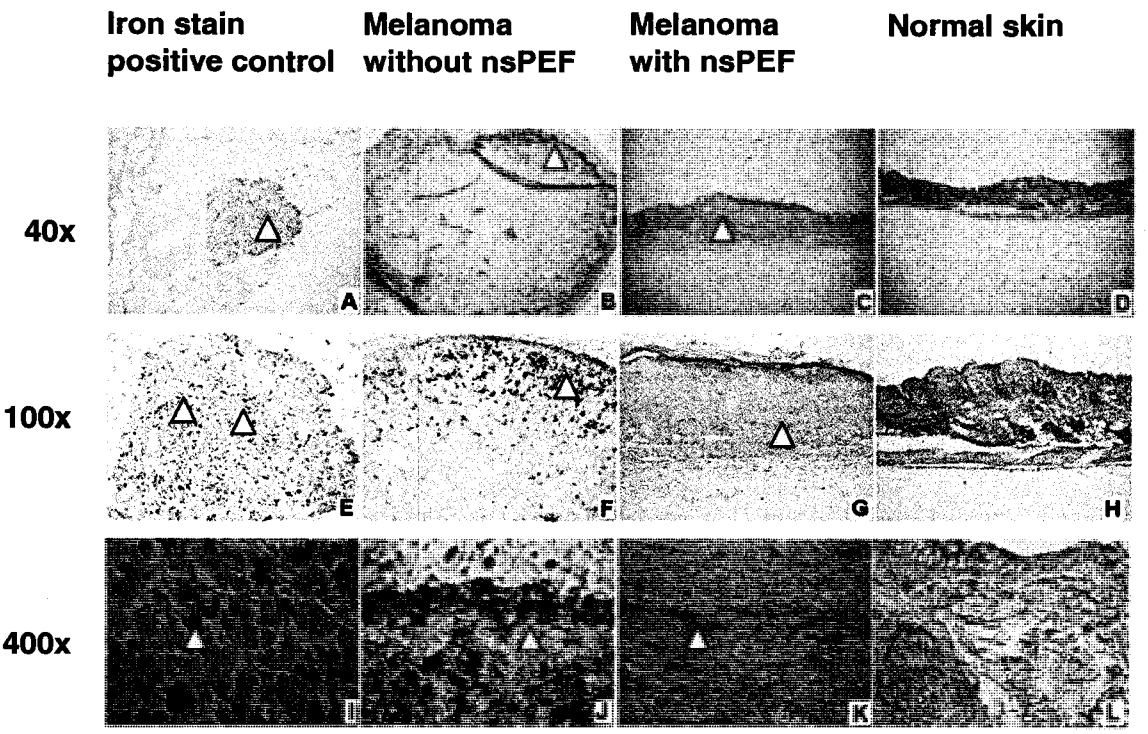

FIGURE 10 - Iron stain for the old bleeding in the melanoma tumors with and without nsPEF T_x. A, E and I (Iron stain positive control) show iron in granules in human melanoma. B, F and J (melanoma without nsPEF) show tumors with melanin, but no iron. C, G and K (melanoma with nsPEF) show layers of positive iron staining. D, H and L are normal mouse skin as the iron stain negative control. The arrows point to the cells which indicate iron stain positive

Discussion

Electric fields applied to living cells cause a number of significant biological effects.[43] The most common application of pulsed electric fields is classical plasma membrane electroporation by which foreign drugs can be introduced into cells through temporary formation of pores in the plasma membrane.[44] Electroporation pulses charge the plasma membrane with millisecond to microsecond durations and low electric fields (V/cm to KV/cm), without significant effects on intracellular membranes. Quite different from classical plasma membrane electroporation, nsPEF is special for its ultra short nanosecond pulse duration, rapid nanosecond rise time, and high electric field (kV/cm). As a result, nsPEF can generate ultra short pulses, which are short enough to penetrate the cell interior before the plasma membrane is fully charged.[45] nsPEF T_x can bypass the plasma membrane because the cell membrane has a relaxation time longer than the pulse duration. Pulses of nanosecond duration in our previous trials showed 100 pulses

increase the temperature of the treated region by only 3 degrees C, ten degrees lower than the minimum temperature for hyperthermia effects.[46] NsPEF T_x shows high power and low energy leading to very little heat production. The consequence of applying intense 300 ns pulses was examined on melanoma bearing mice. This study analyzes melanoma growth and ultra structure post nsPEF treatment. The hypothesis that nsPEF is a highly localized and drug-free physical technique was confirmed. NsPEF could serve as a promising new therapy for tumor.

After nsPEF treatment, the tumor showed delayed development and sharply decreased volume on the first, second and third day compared to control tumors ($p<0.05$). The nsPEF-treated tumor weight was reduced by 85.3%, significantly smaller than the control group ($p<0.001$).

Transillumination and surface photography showed a consistent change after nsPEF treatment while the untreated melanomas were grossly recognizable under the skin surface with round black enlarged appearance on the back. The treated tumors were small and dry with structural shape change and reduction of blood vessel.

H&E and TEM images both showed that without nsPEF treatment, the melanomas kept a regular outline of tumor cells with a pale nucleus and prominent round nucleolus. Cell cytoplasm was finely dusted with melanin and the cells often formed a tumor nest with an active growing center marked by a good blood supply and a well-organized cancer cell cord marked by invading vessels, dermis or muscle fibers. Lymphatic and vascular invasion was present in some control samples, but not as prominent as in the treated group. In nsPEF treated melanomas, solid tumor nest construction was detached, tumor cords were broken and the space in between tumor cells enlarged with shrinking spindle shaped nuclei inside. Regression in size of tumors occurred within 24 hours with surrounding tissue swelling and bleeding. Subcutaneous tissue and skin recovered within 7 days. Skin pulsed with nsPEF showed evidence of typical inflammation in the treated area during the first three days but resolved in one week. Summarizations of pathological comparisons are formed in Table 1.

Fontana-Masson stain was used to assess depigmentation of melanomas after nsPEF treatment. Because melanomas develop from the malignant transformation of melanocytes, specialized melanin producing cells which reside in the epidermal basement

membrane of the skin, melanogenesis is regarded as a functional marker associated with differentiated melanocytes. The data shows the effects of nsPEF on organized melanogenesis and retention of intracellular melanins.

Iron staining can show hemosiderin which is the storage molecule for iron granules so that iron staining can mark recent bleeding by staining the hemoglobin iron released by lysed red blood cells. The data showed iron stain in the treated melanomas, a sign of hemorrhage indicating that nsPEF caused acute blood vessel rupture and bleeding inside the tumor

Melanoma morphological changes revealed that nsPEF can inhibit melanoma growth *in vivo*. NsPEF can significantly delay subcutaneous murine melanoma development by directly damaging the tumor structure and nuclear morphology without significantly affecting the peripheral healthy skin tissue of the treated mice.

CHAPTER III

NSPEF TRIGGER APOPTOSIS IN MELANOMA *IN VIVO*

Previous studies from this laboratory demonstrated that nsPEF could eliminate B16f10 tumors in mice. Our former studies[47] on the first 120 mice with nsPEF T_x show that nsPEF can penetrate into the interior of melanoma cells and cause tumor cell nuclei to rapidly shrink and reduce tumor growth with gradual remission in weeks.[48] Different mechanisms and pathways have been found in the initial apoptosis detection in tumor cells *in vitro*.[49,50] The hypothesis is that nsPEF T_x triggers apoptosis in tumor *in vivo*. Apoptosis differs from necrosis because it is an active process of cellular self-destruction, involves a precisely controlled series of events that become activated in a cell signally its time to die. The current work is designed to find out sequence of molecular events caused by nsPEF in the short term (1-24 hours) post-nsPEF T_x.

Twenty four SKH-1 mice bearing B16-F10 murine melanomas were euthanized at 1, 3, 6 to 24 hours post-nsPEF T_x. The objectives were: to (1) survey the melanoma nuclear morphological changes (2) examine the presence of DNA damage, caspase activation and apoptosis; (3) determine time sequence of the molecular biological events. (4) compare the different biological effects of long pulses versus short pulses.

Material and Methods

Tumor Model

In vivo experiments were set up in conformity with IACUC guidelines under applicable international laws and policies and approved by Animal Care and Use Committee of Eastern Virginia Medical School. In accordance with principles for the ethical use of animals, 24 immunocompetent hairless female SKH-1mice were injected subcutaneously with 100 µl PBS containing $1x10^6$ B16-F10 murine melanoma cells.

nsPEF T_x

A pulser with a Blumlein line configuration was designed and assembled at the Frank Reidy Research Center for Bioelectrics. It can generate 300 nanosecond long pulses with a 30-nanosecond rise time. One hundred pulses were applied to the treated

tumor at 40 Kv/cm and 0.5 Hz. The electrodes for electric field application, pulse generator, voltage and pulsing pattern of nsPEF were described previously.[48]

Sample collection

Specimens were collected for 4 different time points post-nsPEFs T_x (1, 3, 6 and 24 hours). At each time point, 2 groups (nsPEF-treated tumors and the control tumors on the same mouse) consist 6 replicates per group, were studied.

Histology Study

Two tumors induced simultaneously on the back of each mouse were randomly selected as either control or treated tumor. After the nsPEF T_x both control and treated tumor were removed and fixed in 10% neutral buffered formalin prior to paraffin processing. Sections were stained with H&E and assessed microscopically for abnormal nuclear formation. One hundred nuclei were randomly selected and outlined in ten non-overlapping fields of each section.[51] The area of nuclei was measured by the software MATLAB and summed as the mean±SD for statistic analysis.

DNA fragmentation

DNA was extracted by standard proteinase K and phenol/chloroform. Electrophoresis was performed in 1.8% agarose gel in TBE buffer (Tris-borate 89 mM, pH 8.3, EDTA 2 mM) at 30 V for 1h. The DNA was visualized by ethidium bromide staining. B16-F10 cells incubated with Etoposide (Calbiochem, Cat. 341205) used as apoptosis positive control.[52]

Immunofluorescent Staining

Mouse tumor sections were de-paraffinized and then immerged into and boiled in citrate buffer (pH 6.0) for 5 minutes to retrieve antigenic sites masked by formalin fixation. The tissue sections were then placed in 3% hydrogen peroxide for 10 minutes to inactivate endogenous peroxidase. Tissues were blocked with goat serum, and then incubated in a humidity tray with antibodies against phospho-histone H2AX (S139) (RD; 1:500 dilution); caspase 3 (Cell Signaling, 1:500), caspase 6 (Cell Signaling, 1:800), caspase 7 (Biovision, 1:400) in combination for 2h at room temperature. This was followed by incubation of a secondary antibody, Alexa Fluor-488-labeled goat anti-rabbit IgG (Invitrogen, 1:250) for 30 min at room temperature in darkness. Cover slips were mounted with mounting media (Vector Laboratories, H-1200), which contained DAPI to

identify the nuclei. The number of positive cells was scored by manual counting of three sets of at least 100 cells under the microscope. Each experiment was performed twice.

TUNEL Assay

TUNEL (terminal transferase mediated ddUTP nick end labeling) assay was done according to the protocol with Apot Tag Red *in Situ*, an apoptosis detection kit, (Chemicon, Cat No. S7165). Cells with TUNEL-positive nuclei with a cytoplasmic halo were recognized as positive apoptotic cells. For the negative control, no terminal transferase enzyme was added.

Western Blot Analysis

Proteins were resolved over a 15% SDS-polyacrylamide gel and transferred to a nitrocellulose membrane. Gels were transferred electrophoretically to a polyvinylidene difluoride (PVDF) membrane. The blot was preincubated in blocking buffer (5% nonfat dry milk, 1% Tween 20, in 20 mM TBS pH 8.0) for 1 h at room temperature, then incubated with appropriate primary antibodies in blocking buffer for 1 h at room temperature, overnight at 4°C followed by incubation with anti-rabbit or anti-mouse secondary antibodies conjugated with horseradish peroxidase and detected by chemiluminescence and autoradiography using x-ray film. The antibodies against Bcl-2, Bad, beta-actin and caspase-9 demonstrated several bands with the most intense staining at the predicted molecular weight in each case. The antibodies were abtained as following : Bcl-2: (Santa Cruz Biotechnology Inc. Catalog #: sc-23960, dilution: 1:200, molecular weight: 26 kDa,); Bad: (Santa Cruz Biotechnology Inc. Catalog #: sc-8044, dilution: 1:200, molecular weight: 25 kDa); pan-actin (Cell Signaling Technology, Catalog #: 4968, dilution: 1:500, molecular weight: 45 kDa); Caspase 9 (BD, Catalog #: 556585, dilution: 1:200, molecular weight: 46 kDa).

Statistical analysis

Quantitative analysis was based on the nuclear area, immunostaining results of activated H2AX, caspase and TUNEL (positively stained cells *in situ*) as compared between melanoma with and without nsPEFs T_x. The entire samples along 1, 3, 6 and 24 hours post-nsPEF T_x were counted by MATLAB software using fluorescent staining. The number of positive cells was scored by counting three sets of at least 100 cells under a microscope. The differences between treated and control groups tested with two-tailed

Student's t-test and analysis of variance (ANOVA) (SPSS Statistical Program15.0, SPSS Inc., Chicago, IL, USA).

Results

H2AX immunohistochemical staining was used as the early test for early DNA damage. Immunostaining results showed activated H2AX in melanoma with and without nsPEF T_x at the time 1, 3, 6 and 24 hours post-nsPEF. It showed a fine programmed time course of H2AX–positive cells inside melanomas post-nsPEF T_x. Percentages of H2AX-positive cells started to increase 1 hour post-nsPEF Tx, peaked at 3 hours, and then decreased by 24 hours. The *in situ* stain is shown in Figure11 and the quantitative analysis of H2AX phosphorylation is shown in Figure 12. Six different mice were used at each time point in each group. The significant increases of H2AX were at 1 hour and maximum at 3 hours. ($p < 0.001$ vs. control).

Caspase immunohistochemical staining was tested in melanomas post-nsPEF T_x to test the pan caspase activation which play essential roles in apoptosis. Time course shows that percentages of caspase positive cells started to increase 3 hour post-nsPEF T_x, peaked at 6 hours, and then decreased by 24 hours. Quantitative analysis confirmed that immunostaining results of activated caspase 3, 6 and 7 positively stained cells *in situ* and had a significant increase at 3 and 6 hours post-nsPEF T_x. ($p < 0.001$ vs. control)

TUNEL immunohistochemical staining was used in melanomas post nsPEF to detect DNA fragmentation by labeling the terminal end of nucleic acids. Because tumor cells undergoing apoptosis are characterized by a fragmentation of the genomic DNA, many breakpoints can be visualized with the TUNEL reaction. The enzyme terminal desoxynucleotidyl transferase (TdT) adds biotinylated nucleotides to the broken DNA ends. The biotinnylated DNA can then be visualized by fluorescence label. It showed that percentages of apoptotic-positive cells started to increase 3 hour post nsPEF T_x, peaked at 6 hours, and then decreased by 24 hours (Fig.15). Quantitative analysis (Fig.16) confirmed that TUNEL-positive cells showed significant increase at 3 hour and 6 hours ($p < 0.001$ vs. control)

DNA extracted from treated tumor was analyzed by electrophoresis followed by ethidium bromide staining for proof of DNA fragmentation. But the typical DNA

fragmentations, which look like a ladder, were not seen. Only large pieces of DNA were found.

Mean nuclear area measurement was applied as morphology study as well as a quantitative analysis to identify nuclear changes. H&E stain showed tumor construction and nuclear shape changes 1-24 hours post-nsPEF T_x. Control tumor cells exhibited lightly staining pleomorphic nuclei and abundant cytoplasm containing finely dispersed melanin granules. Treated tumors had cell with dense staining, shrunken, darken and elongated nuclei. Cells within the treated melanomas were scattered from the tumor cord. Intracellular melanin granules as well as aggregated extracellular melanin granules were scattered throughout the widened interstitial spaces. Quantitative comparison was made by calculating mean nuclear area (μm^2) between control melanomas and treated tumors during 1-24 hours post-nsPEF T_x. A significant difference exists between the control as compared to 1h, 3h, 6h and 24 h post-nsPEF T_x ($p < 0.001$) as well as between 1 and 3 h times ($p < 0.001$). The data indicate that immediate changes in the tumor following the application of the electric field pulses may be responsible for the tumor regression.

Bcl-2 family protein expression was tested *in situ* at 3 hours post nsPEF T_x because Bcl-2 family proteins play a vital role in regulating apoptosis. Expression *in situ* at 3 hours after nsPEF T_x was determined by immunohistochemistry (IHC). Western-blot analysis of BAD and Bcl-2 protein expression during 1-24 hours post nsPEF T_x after 100 pulses were applied. The time course showed the amount of BAD increased along the hours post-nsPEF T_x while bcl-2 decreased. IHC on 3 hours samples showed that the tumor cells without nsPEF T_x kept the round and regular nuclear shape and size while melanomas with the nsPEF T_x showed condensed and reduced nuclei. Data showed that nsPEF increase BAD expression more than control. Bcl-2 was decreased dramatically after nsPEF T_x. Quantitative analysis of immunohistological staining of BAD and Bcl-2 protein expression showed that BAD was increased while bcl-2 decreased significantly after nsPEF T_x vs. control ($p < 0.001$). Caspase 9 expression was tested by western-blot because it is an important enzyme in extrinsic apoptosis pathway. The time course showed caspase-9 was activated post-nsPEF T_x.

H2AX was activated from 1 to 3 hours post nsPEF T_x

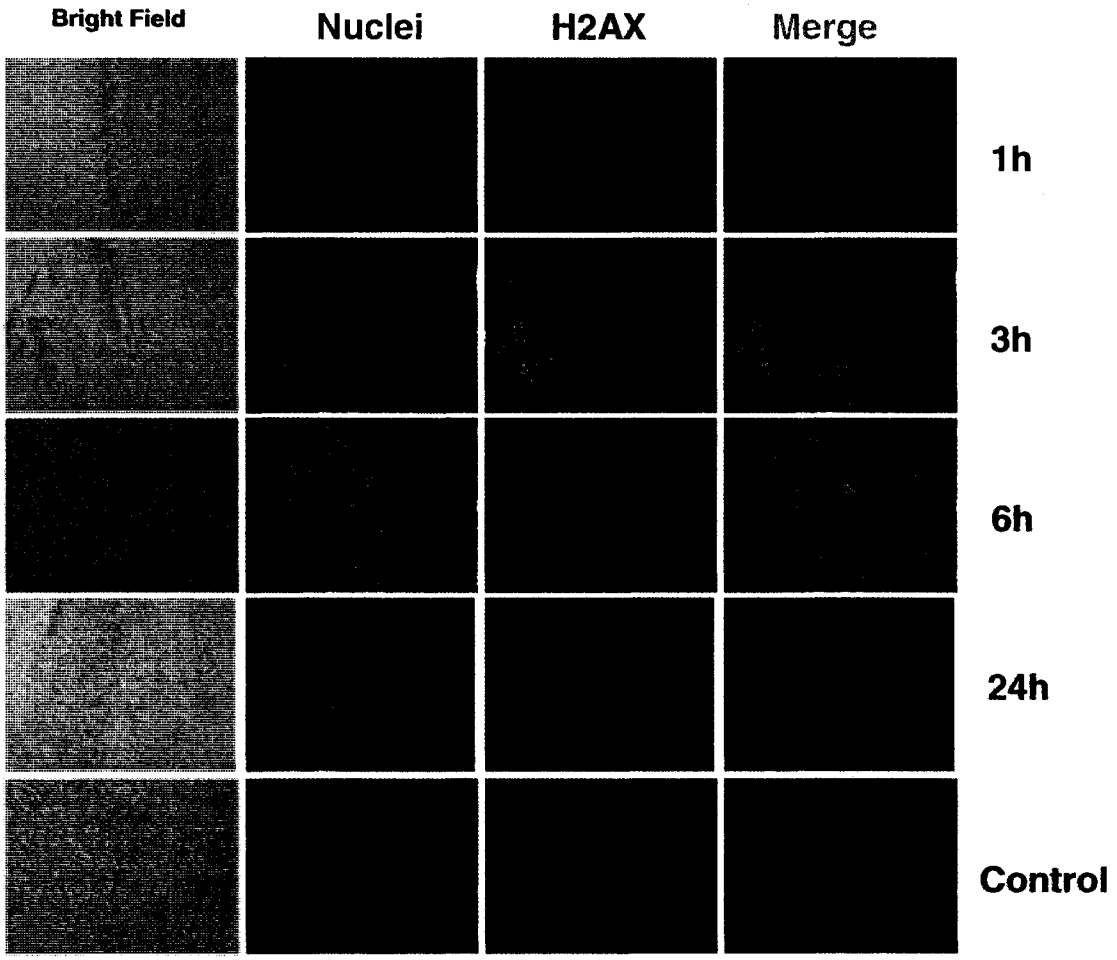

FIGURE 11 - H2AX phosphorylation detected by immuno-fluorescent staining in melanomas post nsPEF Tx. Immunostaining results of phosphorylated H2AX (positively stained cells) in melanoma with and without nsPEF T_x were determined 1, 3, 6 and 24 hours post nsPEF Tx as indicated. A representative experiment is shown. Phospho-H2AX-positive signals were indicated by fluorescence in contrast to nuclei. Phospho-H2AX positive cells are indicated in merged images. Also shown are the corresponding bright field images. Magnification for 1h, 6h and 24h is 200x and the control is 600x.

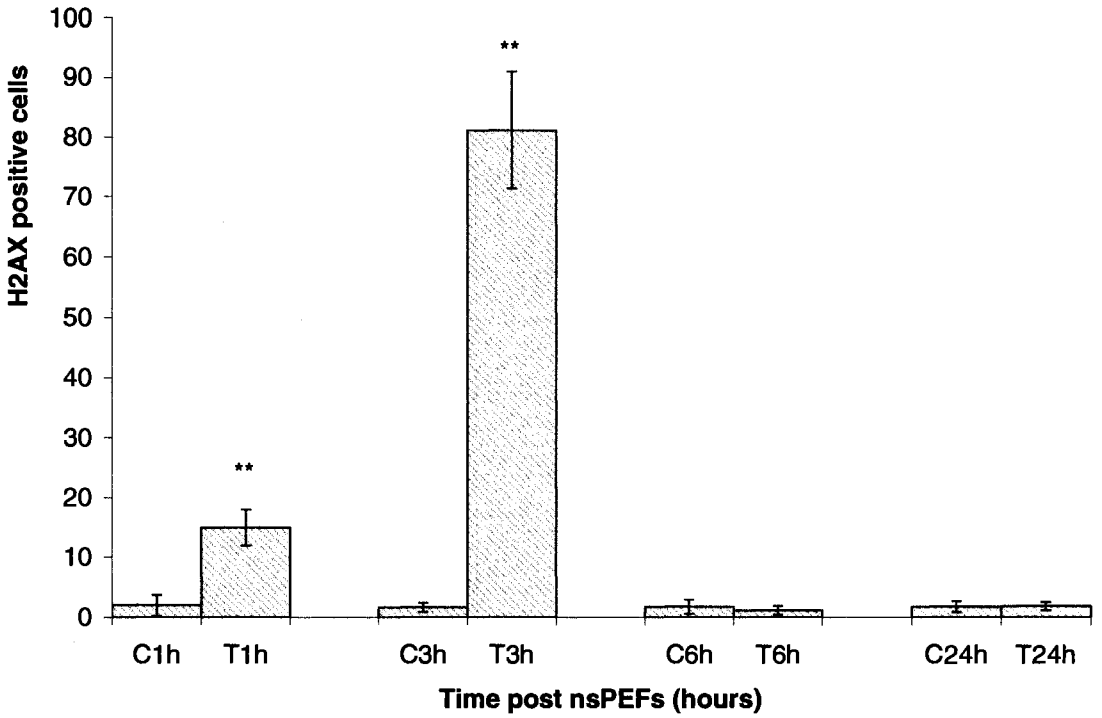

FIGURE 12 - Quantitative analysis of H2AX phosphorylation of melanoma tumors during 1-24 hours post-nsPEF T_x. Immunostaining results of activated H2AX positively stained cells in situ in melanoma without and with nsPEF T_x were determined 1, 3, 6 and 24 hours post nsPEF T_x.as indicated in Materials and Methods. Values are mean±SD. Six different mice were used at each time point in each group * * $p < 0.001$ $p < 0.001$ treated (T) vs. control (C).

Caspase3, 6 and 7 activation post-nsPEF T_x

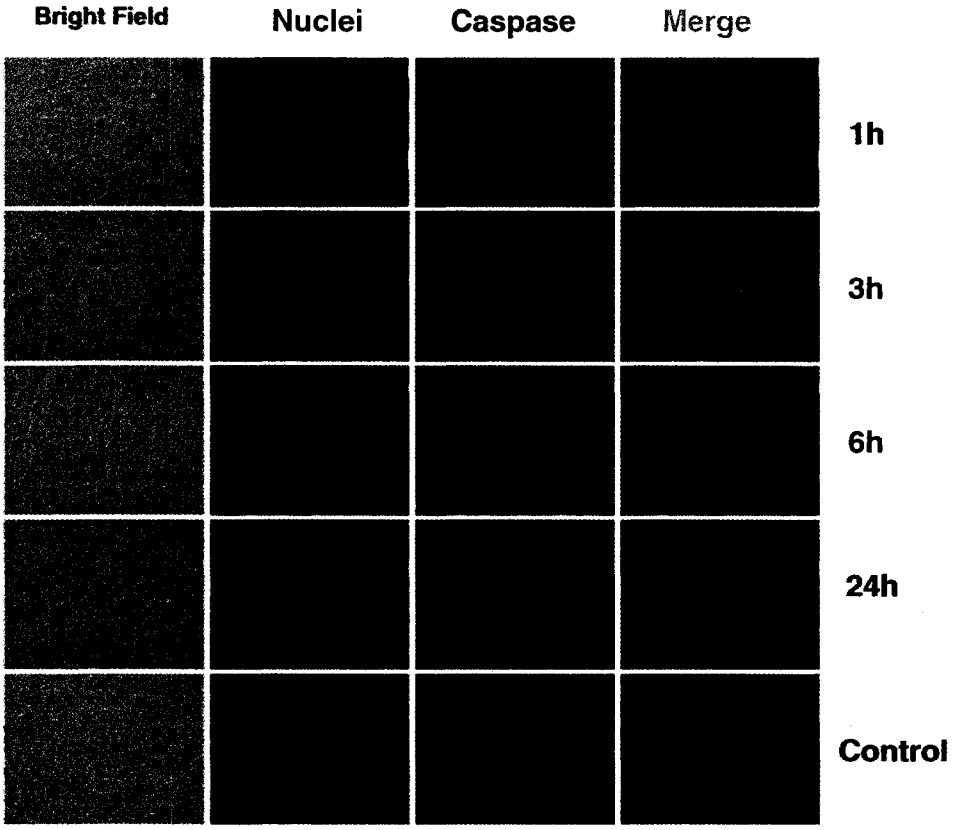

FIGURE 13 - Caspase immunofluorescent staining in melanomas post-nsPEF T_x. Results of immunofluorescent staining for active executioner caspase-3, 6 and/or 7 in melanoma with and without nsPEF T_x 1, 3, 6 and 24 hours post nsPEF T_x are shown as indicated. A representative experiment is shown. Caspase positive signals were indicated by green fluorescence in contrast to red fluorescence-stained nuclei. Caspase positive cells are indicated in merged images as yellow-orange. Also shown are the corresponding bright field images. Magnification is 200x

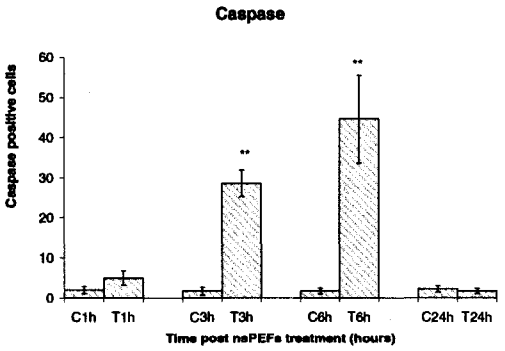

FIGURE 14 - Quantitative analysis of caspase activation of melanoma tumors during 1-24 hours post-nsPEF T_x. Immunofluorescent staining results of activated caspase 3, 6 and 7 positively stained cells in situ in melanoma without and with nsPEF T_x 1, 3, 6 and 24 hours post nsPEF T_x. Values are mean ± SD. Six different mice were used at each time point in each group * *. $p < 0.001$ treated (T) vs. control (C).

TUNEL result for apoptosis detection

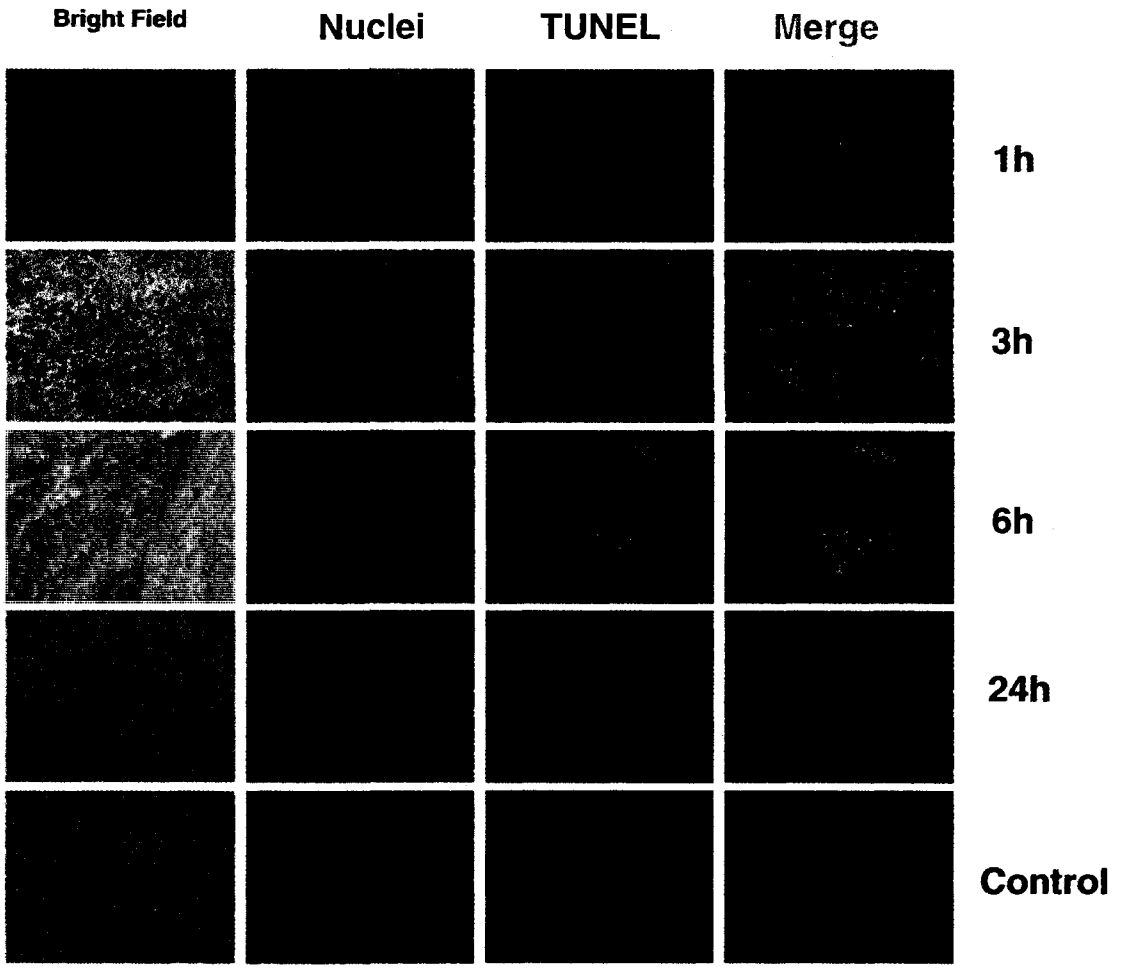

FIGURE 15 - TUNEL immunofluorescent staining in melanomas post-nsPEF T_x. Immunostaining results of TUNEL in melanoma with and without nsPEF T_x are shown 1, 3, 6 and 24 hours post-nsPEF T_x as indicated. A representative experiment is shown. Apoptotic tumor cells are characterized by 3' and 5'broken ends of genomic DNA. The many breakpoints can be visualized with the TUNEL reaction (TdT-dependent dUTP-biotin nick end labeling). The enzyme terminal desoxynucleotidyl transferase (TdT) adds biotinylated nucleotides to the broken DNA ends. The biotinnylated DNA can then be visualized by fluorescence label. Positive signals are indicated by green fluorescence in contrast to red fluorescence-stained nuclei. TUNEL positive cells are indicated by the yellow cells in the merged images. Also shown are corresponding bright field images. Magnification is 200x

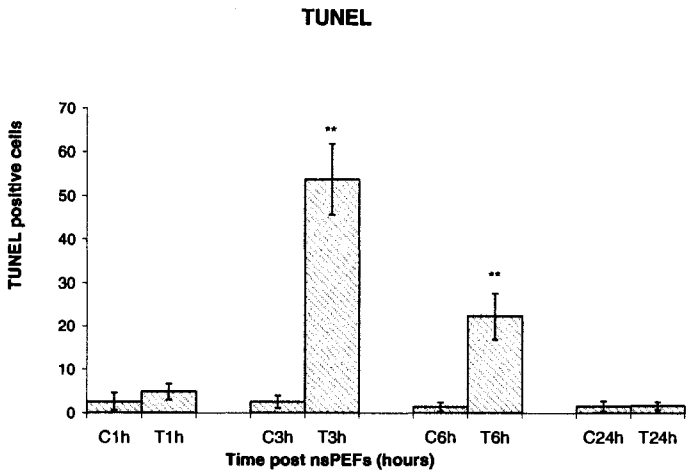

FIGURE 16 - Quantitative analysis of TUNEL in melanoma with and without nsPEF T_x during 1-24 hours post nsPEF T_x. TUNEL positive cells were determined as described in Material and Methods. Values are mean±SD. Six different mice were used at each time point in each group. * * $p < 0.001$ treated (T) vs. control (C).

DNA fragmentations formed post-nsPEF T_x

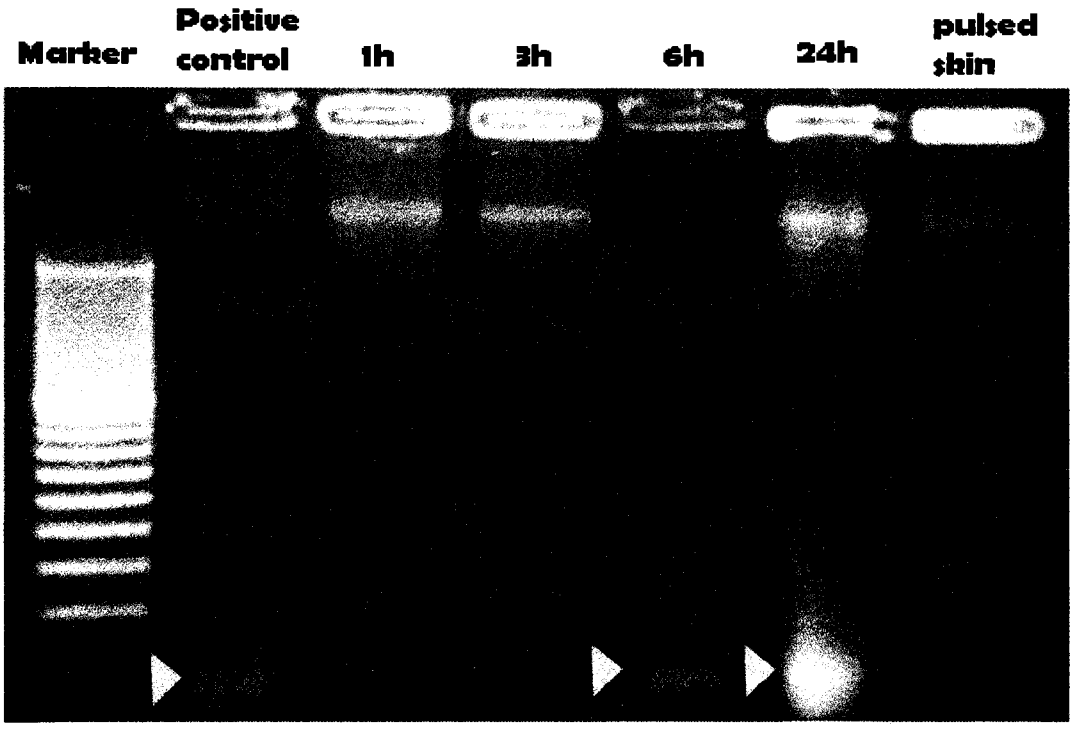

FIGURE 17 – Large DNA fragmentation induced by nsPEF Treatment in melanoma in vivo. B16-F10 cells incubated with Etoposide used as apoptosis positive control. DNA was analysed by 1.8% agarose gel electrophoresis followed by ethidium bromide staining. Data are representative of two independent experiments. B16-F10 cells incubated with Etoposide (Calbiochem, Cat. 341205) used as DNA damage positive control.

Mean nuclear area of treated tumor decreased

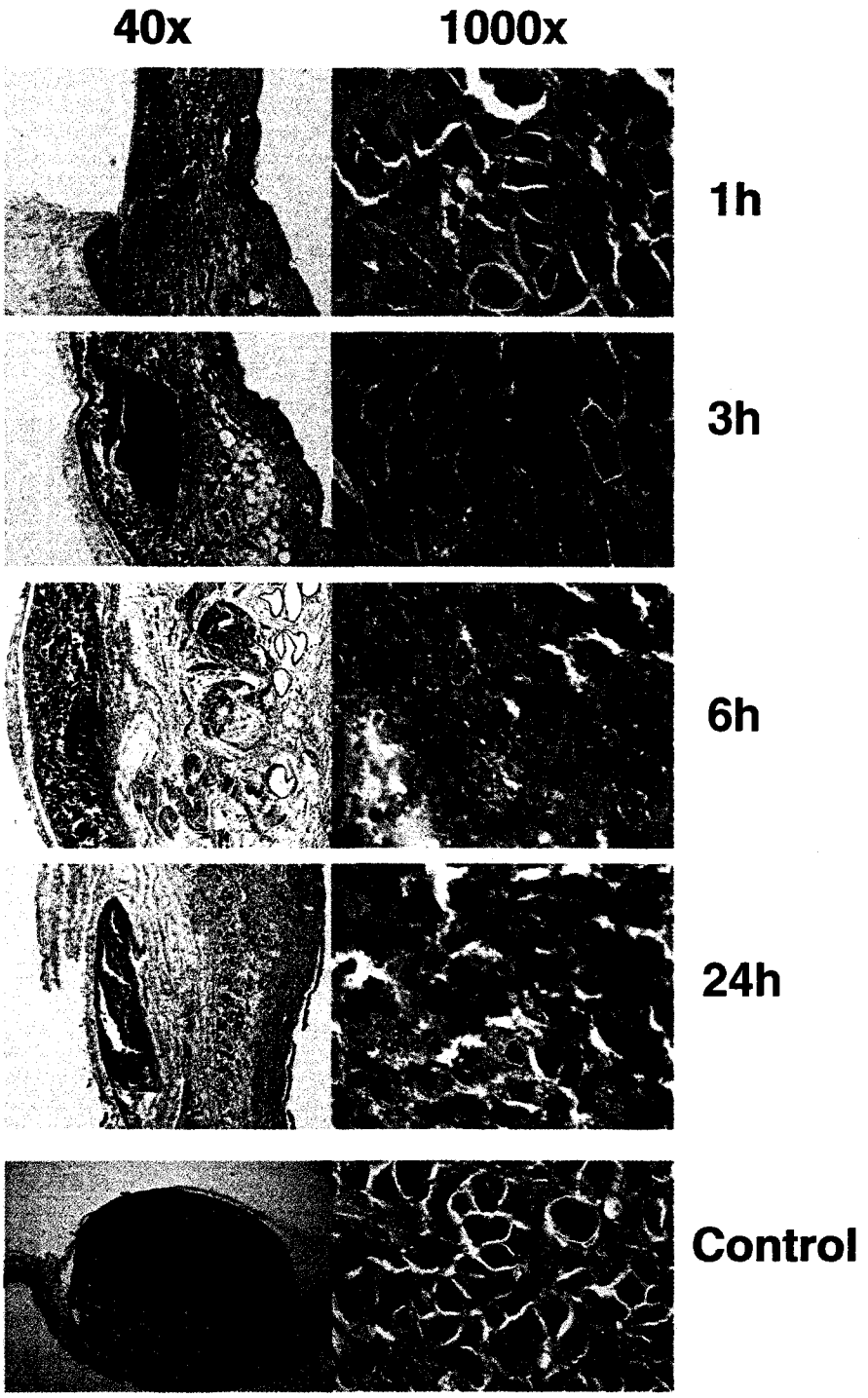

FIGURE 18 - Tumor construction and nuclear shape changes 1-24 hours post-nsPEF T_x. Tumors were treated in vivo with 100 pulses at 300ns and 40kV/cm. Tumors were removed 1, 3, 6 and 24 hours post pulses and prepared for H&E staining Samples at each time point are shown with 40x and 1000x magnification. Histological analysis and determination of nuclear areas are described in the legend to Figure 19 and in Materials and Methods.

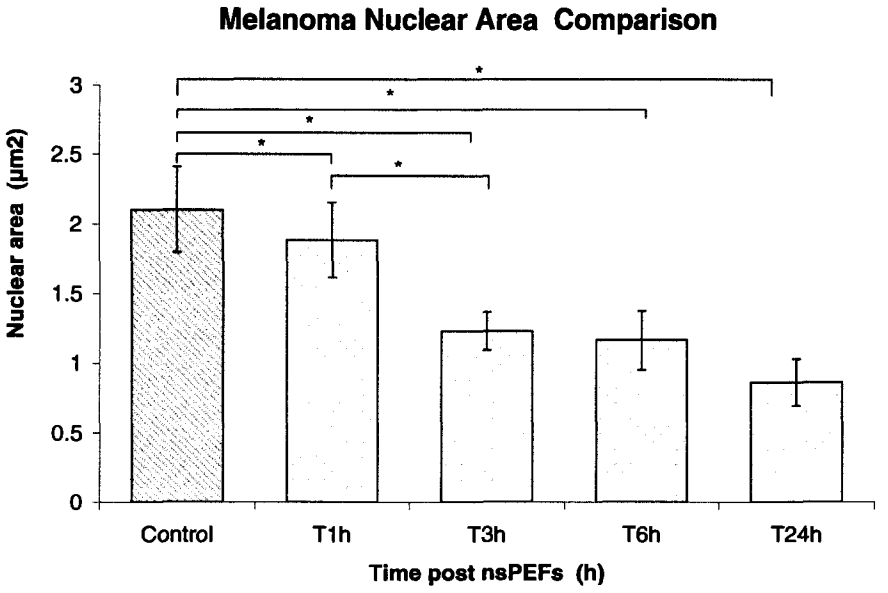

FIGURE 19 - Mean nuclear area (μm^2) comparison between control melanomas and treated tumors during 1-24 hours post nsPEF T_x after 100 pulses at 300ns and 40kV/cm were applied. The number of cell nuclei were measured from 6 mice for each time point and bars represent SEM. Mean nucleus area measurements was applied as in the morphology study as well as a quantitative analysis to identify nuclear changes. Specimens were routinely stained with hematoxylin and eosin and analyzed using a computer-assisted interactive image analysis system MATLAB. Nuclear areas were estimated after manual editing of binary images. * $p < 0.001$ treated (T) vs. control (C).

nsPEF T_x up-regulates BAD and down-regulates Bcl-2 expression.

FIGURE 20 - Western-blot analysis of BAD and Bcl-2 protein expression were determined 1, 3, 6 and 24 hours post-nsPEF T_x with 100 pulses at 300ns and 40kV/cm. A representative figure of Western-blot analysis of BAD, Bcl-2 and actin proteins. After nsPEF T_x or non-treated melanoma tumors were collected and lysed for Western-blot analysis as described in Materials and Methods. Immunoreactivity to b-actin was used as protein loading control.

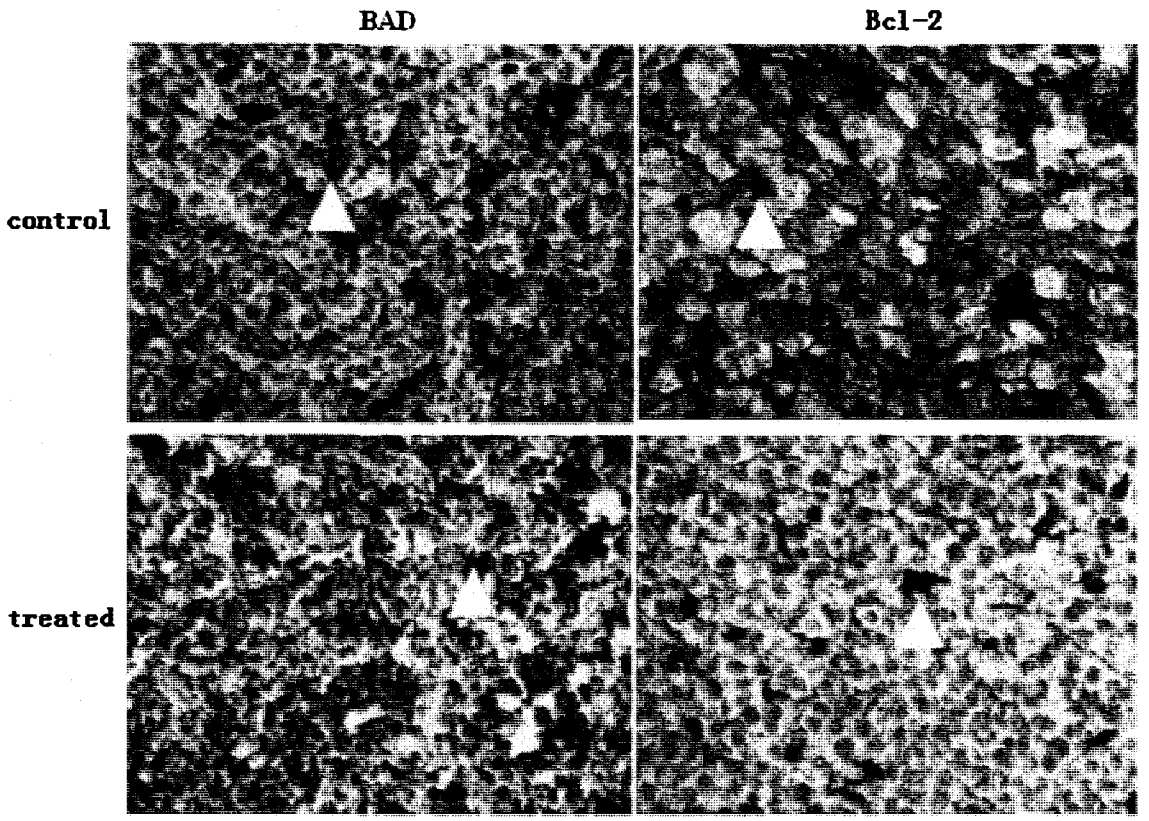

FIGURE 21 – Bad and Bcl-2 protein expression and distribution *in situ* at 3 hours post nsPEF T_x. Bad and Bcl-2 protein expression *in situ* at 3 hours after nsPEF T_x was determined by immunohistochemistry (IHC) using respective antibodies. IHC positive staining is indicated by brown spots overlap the tumor nuclei. Yellow arrows indicate typical positive cells in IHC stain. The specific procedures are described in Materials and methods

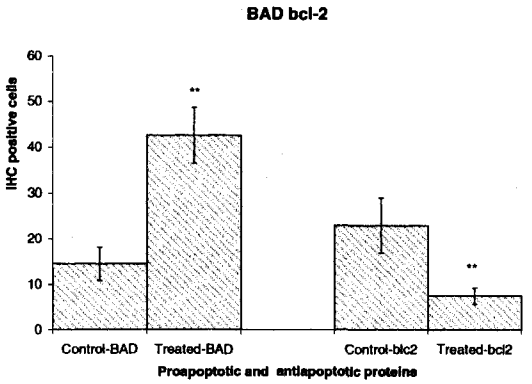

FIGURE 22 - Quantitative analysis of immunohistological staining of BAD and Bcl-2 protein expression in melanoma with and without nsPEF T_x at 3 hours post nsPEF T_x. The positive stained brown cells from IHC staining were counted and calculated as mean±SD. six different mice with melanomas were tested in every IHC trial. Statistical significances are indicated. * *$p < 0.001$ treated (T) vs. control (C).

NsPEF T_x activated caspase 9

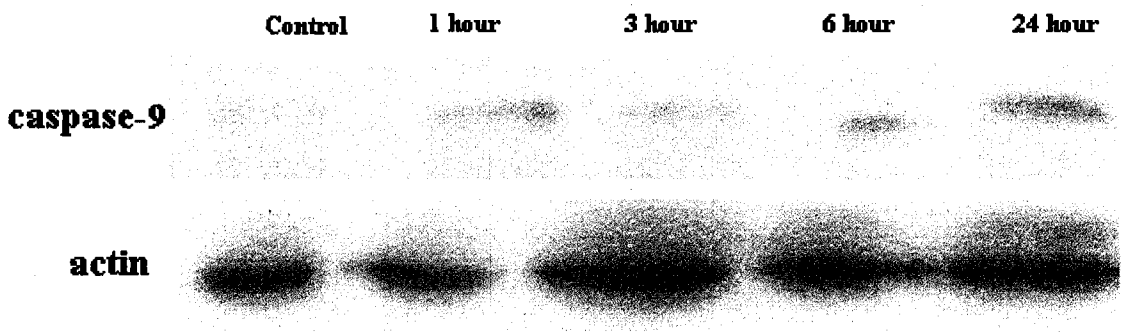

FIGURE 23 - Western-blot analysis of caspase 9 expression. Western-blot analysis of active caspase 9 was determined after nsPEF T_x The melanoma tumors were collected and lysed for Western-blot analysis as described in Material and Methods. Immunoreactivity to beta-actin was used as internal loading control.

Discussion

When the cells become deregulated, such as during tumor formation, the body can induce apoptosis to get rid of them by programmed cell death. [53, 54, 55] In the previous research in tumor cell lines *in vitro*, it was shown that nsPEFs induce caspase associated apoptosis in HL60, Jurkat and HCT116 colon carcinoma by mitochondrial-dependent (Jurkat and HL-60) and mitochondrial-independent (HCT-116) mechanisms.[56] The *ex vivo* trial on mouse fibrosarcoma tumors also proved nsPEF T_x resulted in apoptosis as indicated by caspase activation and TUNEL positive tumor cells. It was further shown that nsPEF treatment could reduce fibrosarcoma tumor size when treated *in vivo*[57] The current work was carried out to determine if and how nsPEF induced apoptosis in melanoma tumors *in vivo*.

Under certain conditions DNA damage can lead to apoptosis inductions. However, for stimuli that induced DNA damage, these markers may appear before caspase activation as a more direct effect on DNA or can occur after caspase activation as apoptosis markers. Figure 11 clearly indicated that nsPEF induced DNA damage as indicated by Histone 2AX phosphorylation as a marker for double strand breaks in DNA. Further evidence for DNA damage was shown by the presence TUNEL positive nuclei (Figure 15), large DNA fragments by agarose gel electrophoresis (Figure 17) and shrinkage of nuclei as indicated by H&E histological examination. All of these DNA damage markers indicated time dependent effects. Histone 2AX phosphorylation and the

presence of TUNEL positive cells peaked at 3 hours, while the presence of significant pyknotic nuclei were evident 3-24 hour post pulse. Caspase activation was shown to peak at 6 hours after nsPEF treatment. These time courses indicate that evidence for DNA damage occurred before caspase activity was at a maximum. This suggests that some damage to DNA was in part due to events that were not related to caspase-dependent apoptosis. This non-apoptotic DNA damage is consistent with the results of Stacy et al.[29], who showed nsPEF-induced DNA damage by comet assay. Further evidence for DNA damage unrelated to apoptosis was indicated by large fragments of DNA after agarose gel electrophoresis. Nevertheless, significant evidence for apoptosis is apparently when using several different apoptosis markers.

Since apoptosis has been demonstrated to occur in response to nsPEFs both *in vitro* and *in vivo*, additional studies were carried out using several different apoptosis markers. One of the best markers for apoptosis is caspase activation. Here activation of executioner caspases-3, -6, and -7 was shown using a cocktail of antibodies with immunofluorescent microscopy. Evidence for caspase activation was obvious 3 hours post pulse, was maximal at 6 hours, but was not observable by 24 hours after treatment. Another apoptosis marker is the presence of TUNEL positive cells. However, while some of the TUNEL positive cells could be related to caspase-dependent activities, at least some of this occurred prior to the peak of caspase activation. However, caspase-positive and TUNEL-positive cells were not determined together. Therefore, based on the studies presented here, it is not possible to correlate caspase activation with apoptosis-dependent TUNEL evidence. This provides evidence that care should be exercised when using TUNEL as an apoptosis marker. However, it should be possible to correlate these apoptosis markers using a more tightly defined time course with assays for caspase-activated DNase (CAD) activity in cells that are caspase-and TUNEL-positive.

Other evidence for apoptosis in treated tumors was provided by histological analysis of pyknotic nuclei, which is a good *in vivo* apoptosis marker. The greatest number of pyknotic nuclear changes possible occurred between 3 and 24 hours post-pulse. Thus, some of these nuclei could have occurred due to apoptosis-related activity. The presence of CAD activity in pyknotic nuclei would help address this issue.

However, additional apoptosis markers indicated that apoptosis was present in some of the tumors after nsPEF treatment. Furthermore, since evidence for apoptosis in tumor cells was present, it was of interest to determine how these processes could be regulated. Increases in BAD, a pro-apoptotic protein and decreases in Bcl-2, an anti-apoptotic protein were observed (Figures 20-22). This finding is consistent with a potential shift in Bcl-2 family proteins toward pro-apoptotic activity. Furthermore, this suggested that the mitochondria could be involved in nsPEF-induced apoptosis. If this were true, we would expect to see caspase-9 activation. In Figure 23 evidence for caspase-9 activity was presented. Thus, the evidences from Figures 20-23 suggest that at least in some tumor cells mitochondria-dependent apoptosis occurred. This could be due to activities through the intrinsic apoptosis pathway, which originates from intracellular stresses such as DNA damage that was observed, or through activities in the type II extrinsic pathway, which originates from the plasma membrane. At the present time, it is not possible to differentiate these two processes. In the future, it will be possible to determine the presence or absence of t-Bid, which connects the extrinsic pathway with the intrinsic pathway through the mitochondria. This is important regarding nsPEF mechanisms, which could occur due to intracellular stress or unique effects on the plasma membrane. If t-Bid were not present it would suggest effects in intracellular structures and functions. On the other hand, if t-Bid were present, it would suggest effects through the plasma membrane.

Although DNA fragmentation into DNA ladders is characteristic of apoptosis,[58] recent evidence indicates that not all cells undergo such extensive DNA fragmentation.[59] NsPEF caused large piece DNA fragmentation instead of DNA ladder. This is because nsPEF T_x does not affect cells in the same way as a long pulse does. Some sensitive tests other than the DNA fragmentation was expected to reveal the early stage changes thought to occur post-nsPEF T_x. TUNEL was used which employs an enzyme TdT (terminal deoxynucleotide tranferase) to tag the cuts in the DNA made by the endonuclease. TUNEL was tested on the control tumors and treated tumors. The data showed TUNEL positive results came at 3 hours, reached its peak at 6 hours, and faded away around 24 hours post nsPEF T_x. This time course is the same as it is for nsPEF-induced caspase activation.

It is reported that H2AX phosphorylation occurs where DNA double-strand breaks by physical attack such as UV or ionizing radiation.[60] H2AX phosphorylation is associated with immediate response to DNA damage and repair. H2AX could be a marker to indicate an early event in apoptosis, even before the caspase activation and the DNA fragments form. Therefore, our experiment was grouped into 4 different time points, 1, 3, 6 and 24 hours post nsPEF T_x with controls to test H2AX activity. These data confirm the hypothesis that nsPEF T_x triggers H2AX activation as an early response and it occurs in a tight time sequence. The immune fluorescent stain *in situ* showed that H2AX can be demonstrated at the first hour after exposure to nsPEF, reaching a peak at 3 hours and regressing over the next to reach a minimum at 3 hours then fell to a low at 24 h after nsPEF T_x.

Histology changes were recorded the same time course. The previous studies on long-term biological effects post-nsPEF T_x had found obvious nuclear morphology changes as well as tumor volume shrinkage.[60] In the current study, histological changes were confirmed even in the short term. Histology data showed that the nuclear area began to change slightly from 1 hour post nsPEF T_x, and the cell shrinkage became very obvious at 3-6 hours. This nuclear change may be the progenitor of the longerterm tumor remission.

One reason melanoma is resistant to traditional chemotherapy is because melanoma cells have low levels of apoptosis *in vivo* compared with other tumors, and are also resistant to chemical medicine –induced apoptosis *in vitro*.[61,62] Little is known about the intracellular mechanism involved in nsPEF T_x induced apoptosis *in vivo*. Because nsPEF is a new physical therapy made by pulse power technique that does not exist in the natural environment, nsPEF T_x would work a different way from traditional thermal anti-tumor therapies.

To summarize, several pieces of evidence indicates nsPEF-induced DNA damage including H2AX phosphorylation, TUNEL positive cells, nuclear pyknosis as indicated by H&E staining and large DNA fragments upon agarose gel electrophoresis. Some of this damage appeared to occur before caspases were activated suggesting that nsPEFs may induce DNA damage itself. However, it is possible that some of the DNA damage occurred after caspase activation as part of the apoptosis processes. However, the absence

of a clear DNA ladder suggests that apoptotic-induced DNA damage did not go to completion. As indicated in the following chapter, it is possible that an interruption in the blood supply to the tumor caused tumor infarction, thus interrupting the apoptosis process. Nevertheless, apoptosis was a cause of some tumor cell death as indicated by the action of execution caspases as well as the initiator caspase-9. The activation of caspase-9, the increase in Bad and the decrease in Bcl-2 suggests that the extrinsic type II pathway and/or the intrinsic, mitochondria-dependent pathways were activated, at least in part. The possibilities of nsPEF-induced DNA damage and a possible involvement of the intrinsic pathway are consistent with nsPEFs affecting intracellular structures and functions, which has been indicated by modeling and experimental data.[24,27,35]

In future work, it will be important to determine if caspase-8 is active and if t-Bid is present. This will suggest involvement of the extrinsic pathway with caspase-8 and differentiate between the extrinsic type II and the intrinsic pathway with the presence of t-Bid.

CHAPTER IV

NSPEF INHIBIT MELANOMA ANGIOGENESIS *IN VIVO*

It has been reported that in solid tumor angiogenesis plays an important role in the growth and metastasis.[63] New blood vessels "feed" the tumor cells with oxygen and nutrients, allowing malignant cells to grow, invade nearby tissue, spread to other parts of the body, and form new colonies of tumor cells.[64] In our initial studies,[65] nsPEF T_x stopped melanoma growth and induced apoptosis. Because melanoma self destruction was always accompanied with interruption of blood flow, it was important in the present study to investigate the intra-tumoral vascular response after nsPEF T_x.

In the initial study,[65] the major change found in melanomas treated by nsPEF T_x was immediately and obvious reduction in blood flow to the tumor. Both transillumination and power Doppler ultrasound reconstructions indicate that the blood flow was stopped within about 15 min after pulsing. Histology confirmed that red blood cells were found scattered within and around the melanoma tumor. After weeks the treated melanoma shrunk to self destruction. The result implies that the intra-tumoral vasculature response is an indispensable part of mechanisms to make tumor finally self destruct.[66] The hypothesis is tested that nsPEF T_x can cause changes at the molecular level that define direct pre-existing vessel damage and also inhibit new micro-blood vessel formation.

Material and methods

Animal model

In vivo experiments were set up in conformity with Animal Care and Use Committee of Eastern Virginia Medical School. Murine melanoma B16-F10 cells were injected under the skin to induce 2 or 4 tumors in the flanks of 66 female immunocompetent hairless SKH-1 mice. When the tumors were 5 mm wide and exhibited angiogenesis, nsPEF was applied on one tumor and the other tumor on the same mouse was kept as control. Freshly isolated specimens were divided into two series, one was fixed in 10% neutral buffered formalin overnight and embedded in paraffin for histological analysis, the other was snap frozen in liquid nitrogen for protein expression tests.

Tissue Micro-arrays Construction

Tissue Microarrays (TMAs) were adopted for homogeneity and high-throughput analysis of all samples.[67] TMAs were constructed with 0.6-mm diameter cores spaced 0.8 mm apart. The tissue array consisted of the treated melanomas, control melanomas and normal skins around the control tumor.

MVD Measurement by CD31, CD34 and CD105 with Immunohistochemistry (IHC)

One section was stained with H&E for histopathological diagnosis prior to IHC. IHC was performed as previously described.[68] The 5 μm-thick sections were deparaffinized in xylene and then rehydrated. Slides were treated with 3% hydrogen peroxide for 20 min to block endogenous peroxidase activity. The primary antibodies were used at the following dilutions: monoclonal rat-anti-mouse CD31 antibody (or PECAM-1, BD PharMingen), 1:50; rabbit polyclonal anti- CD34 (Biovision), 1:250; rat anti-CD105 (BD PharMingen); 1:200. Then, sections were covered with HRP-conjugated antibodies directed against rat or rabbit immunoglobulin.[69] Nonspecific staining was controlled by incubation with mouse or rabbit immunoglobulin instead of the specific primary antibody. 3-amino, 9 ethyl-carbazole (AEC) was used as a chromogen, which provides the red depositions *in situ*. The expression of positive cells was assessed independently by two pathologists, who were blinded to histopathological diagnosis. [70]

Western Blot Analysis

Protein was resolved over a 15% polyacrylamide gel and transferred to a nitrocellulose membrane. The blots were preincubated in blocking buffer (5% nonfat dry milk, 1% Tween 20, in 20 mM TBS pH 8.0) for 1 h at room temperature, then incubated with appropriate primary antibodies in blocking buffer from 1 h at room temperature to overnight at 4°C followed by incubation with anti-rabbit or anti-mouse secondary antibodies conjugated with horseradish peroxidase and detected by chemiluminescence and autoradiography using x-ray film.[71]

Result

Both Tumor blood supply and volume were inhibited by nsPEF T_x

Blood vessels were analyzed first on the pre-existing vasculature . Intra-tumoral pre-existing vasculature was recorded by transillumination photography. Melanoma tumors began with the similar volume and rich blood supply after injection. NsPEF-treated

tumors had the capillary vessels damage on the day nsPEF applied. Tumors stopped growing when nsPEF T_x was applied and the vasculature disappeared along with the tumor shrinkage. Control tumors continued growing with branched blood vessel network. Transillumination photography recorded the typical procedure. Before the T_x, melanomas grew to 5-10mm diameters with rich blood supply after injection of 10^6 B16F10 melanoma cells. One day after the nsPEF T_x, control tumors had blood vessel networks nourishing active growing tumor cells with a large round nucleus. The same day in the treated melanoma, the tumor cells became condensed and volume decreased significantly. The tumor construction was detached, the vessels were broken, and red blood cells scattered or aggregated into the connective tissue. Seven days after nsPEF T_x, the control tumors grew to large volumes with rich capillaries and small venules formed in tumor while the treated tumor dryed out with volume shrinkage and poor vasculature. Tumor blood vessels post nsPEF T_x were tracked. On the day of nsPEF T_x, the tumor network didn't change very much, however 3 days later the blood vessel network was blocked completely. One week later the tumor volume was obviously decreased significantly. The data altogether indicate that nsPEF T_x damaged the pre-existing blood vessels.

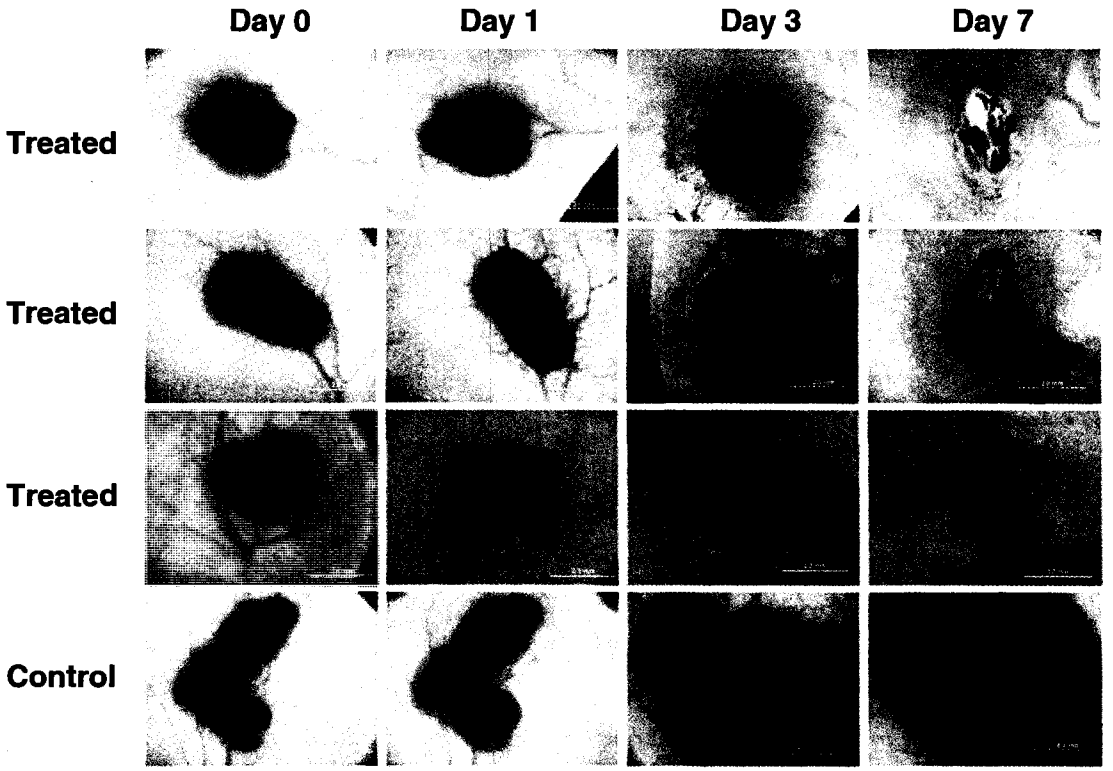

FIGURE 24 – Tumor blood supply and volume were inhibited by nsPEF T_x. Four tumors were induced by injecting B16F10 cells ($1x10^6$). When the tumors grew to diameters around 5mm, nsPEF T_x was delivered to three tumors (300 ns, 100 pulses, 40kV/cm, 0.5Hz). One tumor without nsPEF T_x was kept as control. These four tumors were recorded by transillumination microscopy daily (1.2 x magnifications). The scaling bar is 2.0mm.

NsPEF T_x cut off the pre-existing vasculature

The treated and control tumors came into the study with the similar tumor size and rich vessel network. When tumors developed, the accompanying blood supply grew with it shown as the blood vessels pushed their branches into the tumor. But 7 days post-nsPEF T_x the control tumor achieved a considerable volume with good blood perfusion from arterioles. The treated tumors condensed and the blood vessel dried up. The results are shown from inner side dissection and the corresponding histology under light microscopy.

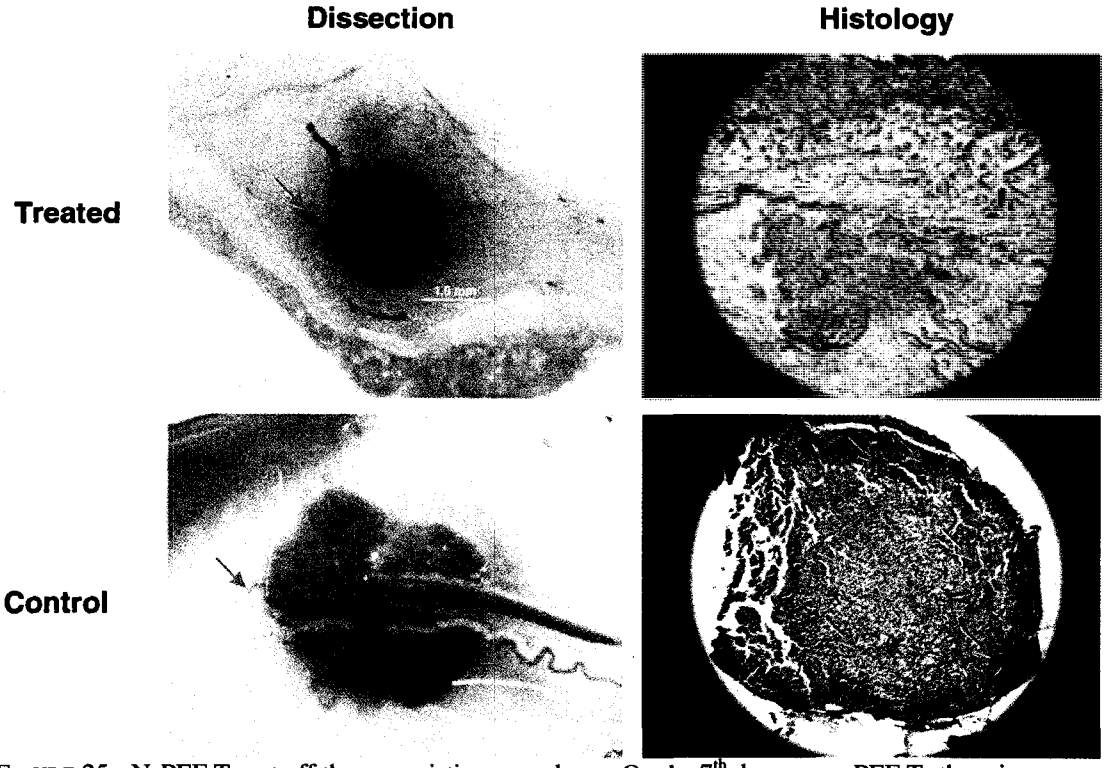

FIGURE 25 - NsPEF T_x cut off the pre-existing vasculature On the 7th day post nsPEF T_x the mice were euthanized and the tumors were dissected. The tumor and the blood vessels were photographed from the inner side. The capillaries were analyzed by histology under light microscopy (H&E, 40x). Arrows point to the pre-existing arteriola and capillaries. Scaling bar is 1.0mm.

Tumor weight decreased in 7 days post nsPEF T_x.

Tumor weight change 7 days post nsPEF T_x was also analyzed. Melanomas grew to similar weight (control group 1.45±0.15 vs. treated group 1.59±0.12) because the same amount of B16-F10 cells ($1x10^6$ cells per tumor) were injected on the same mouse. One day after the nsPEF T_x, treated tumors became slightly smaller (1.41±0.18) than control (1.61±0.25) due to the direct damage of nsPEF T_x. One week later, the control tumor without nsPEF T_x increased twice in weight (2.71±0.17). The treated tumor stopped growing and ended up with decreased tumor weight (0.58±0.21)(the tumor weight is Mean ±SD in gram). The treated tumors had roughly five times more weight than the untreated tumors.

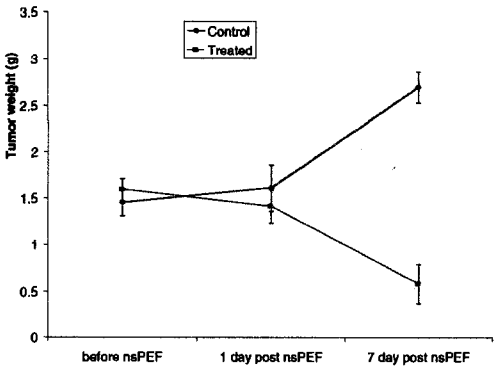

FIGURE 26 - Tumor weight decreased in 7 days post nsPEF T_x(n=66). The tumor weight is expressed as the mean ±SD in gram. Tumors were induced by injecting the same amount of B16F10 cells ($1x10^6$). When the tumors grew to diameters of around 5mm, nsPEF T_x was delivered to three tumors (300 ns, 100 pulses, 40kV/cm, 0.5Hz). On the 7^{th} day post nsPEF T_x, mice were enthanized and the tumors were dissected along the membrane. The tumors were weighted and the mean value of control tumors and treated tumors were plotted along the time.

Intratumoral vessel number changes in 7 days post nsPEF T_x

The numbers of intratumoral vessels were counted following staining with H&E stain. Control melanoma indicated that tumor growth was accompanied by increased vascularity; the vessel number before the T_x, one day and seven days after nsPEF T_x is 23±3, 32±1, 49±2, respectively (Mean±SD). For the treated melanomas, the number of pre-existing vessels dramatically deceased as 25±2, 14±3, 3.0±2, respectively. (Mean±SD).

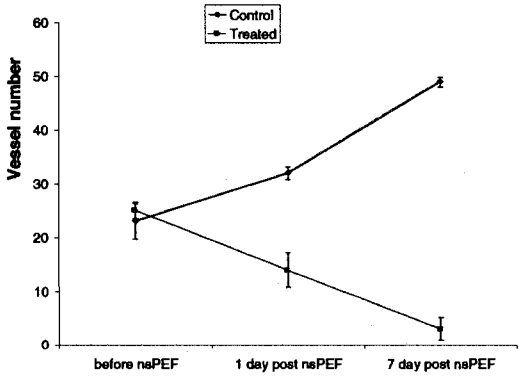

FIGURE 27 - Intratumoral pre-existing vasculature was counted following staining with H& E stain(n=66). NsPEF T_x was delivered to three tumors (300 ns, 100 pulses, 40kV/cm, 0.5Hz). On the 7^{th} day post-nsPEF T_x, mice were enthanized and the number of vessels on H&E slides were counted under the microscope. The mean value of tumor blood vessel number was compared along the time.

NsPEF inhibit micro-vessel density

In order to clarify angiogenesis after nsPEF Tx, the micro-vascular density was evaluated through the expression of CD31, CD34 and CD105, the most common analyzed 3 markers for angiogenesis. CD31 is known as platelet-endothelial cell adhesion molecule, which is used as a pan-endothelial cell marker. CD34 is endothelial cell marker. CD105 is a proliferation-related endothelial cell marker. Figures 28, 29 and 30 exhibit typical expression pattern of CD31, CD34 and CD105 on tissue micro-arrays. Staining for CD31, CD34 and CD105 allowed specific detection of micro-vessels in tissue. Therfore they were used in the current study to estimate the level of functional blood flow in tumors. In all three stains, control tumors showed red staining spots (intensive endothelium) which means neovascular hot areas. These spots were further analyzed under higher power. The red stained areas are endothelial cells or endothelial cell clusters clearly separate from adjacent non-stained tumor cells, while the treated tumors showed significant weak intensive endothelium.

NsPEF inhibit micro-vessel density marked by CD31

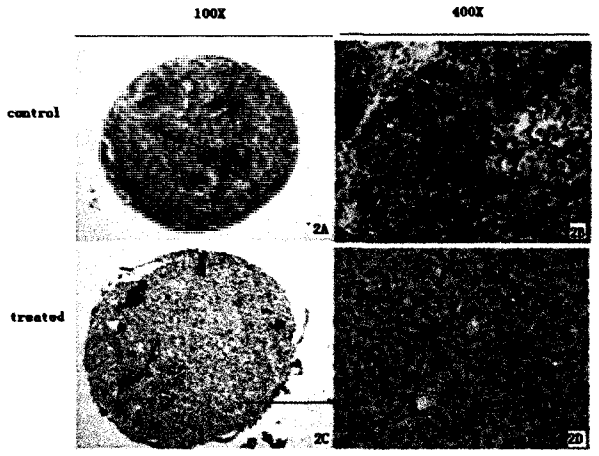

FIGURE 28 - NsPEF inhibit micro-vessel density marked by CD31. The images include magnifications of 100x on the left and 400x on the right, with a control tumor on the top line and a treated tumor on the bottom line. The darker staining spots are endothelia. A and C are the neovascular hot area under 100x magnification. They were further analyzed under 400x magnification in C and D.

NsPEF inhibit micro-vessel density marked by CD34

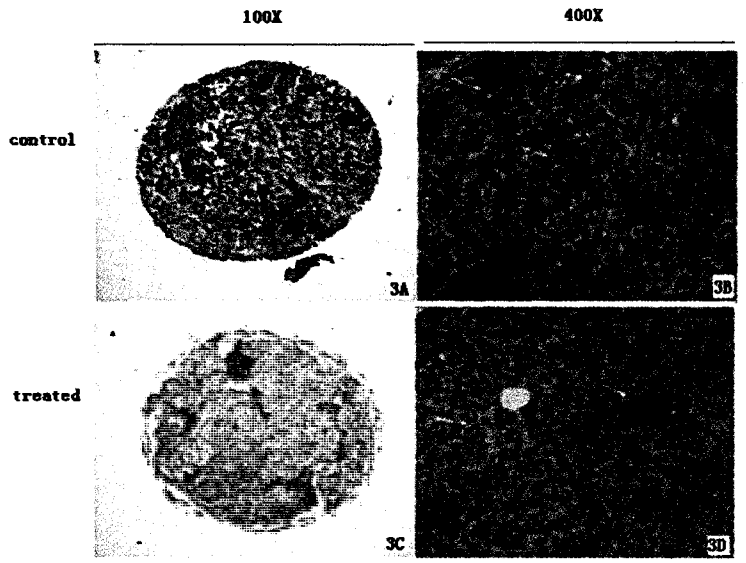

FIGURE 29 - NsPEF inhibit micro-vessel density marked by CD34. The images include a 100x magnification on the left and 400x on the right, with a control tumor on the top line and a treated tumor on the bottom line. The darker staining spots are endothelia. A and C are the neovascular hot area under 100x magnification, they are further analyzed under 400x magnification in C and D.

NsPEF inhibit micro-vessel density marked by CD105

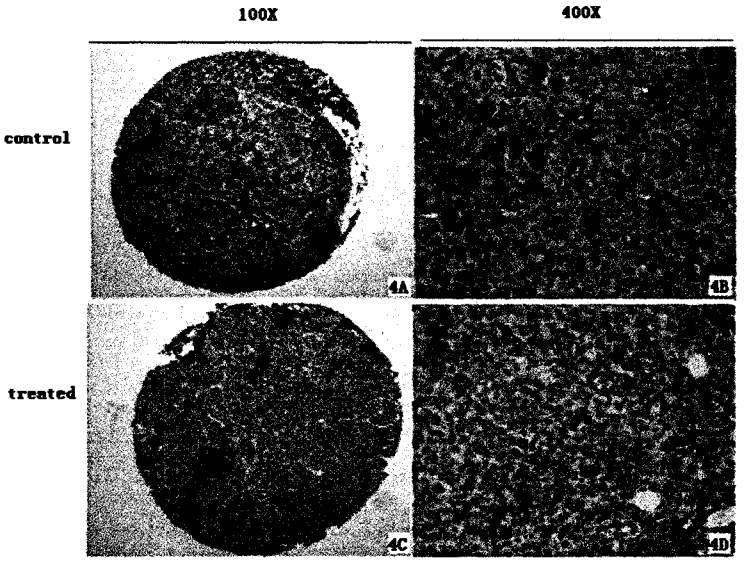

FIGURE 30 - NsPEF inhibit micro-vessel density marked by CD105. The images include a 100x magnification on the left and a 400x on the right, with a control tumor on the top line and a treated tumor on the bottom line. The darker staining spots are endothelia. A and C are the neovascular hot area under 100x magnification, they are further analyzed under 400x magnification in C and D.

The quantitative analysis of MVD marked by CD31, CD34 and CD105 7 days post nsPEF T_x vs. control tumor.

Quantitative analysis of immunohistology positive were determined. Decreased MVD by no matter CD31 (** $p<.0001$), CD34 (** $p<.0001$) or CD105 (* $p<.005$), were noted in nsPEF treated melanomas. The results suggest reduction in the number of intratumoral micro-vessels in the big, medium or small sized vessels. Because CD31 and CD34 are pan endothelial markers, all positive stain of micro-vessels, heterogeneous distribution of large and small micro vessels as well as single immunostained cells throughout tissue sections were included in the micro-vessel count. As a result, the difference between the control and treated groups are more significant. CD105 antigen is a specific marker of activated endothelial cells. MVD marked by CD105 is for detecting newly formed blood vessels. IHC staining indicated CD105 positive cells composed of delicate and ramified vessels. Therefore the CD105 positive marker is not as significant as CD31 or CD34 verses control tumor.

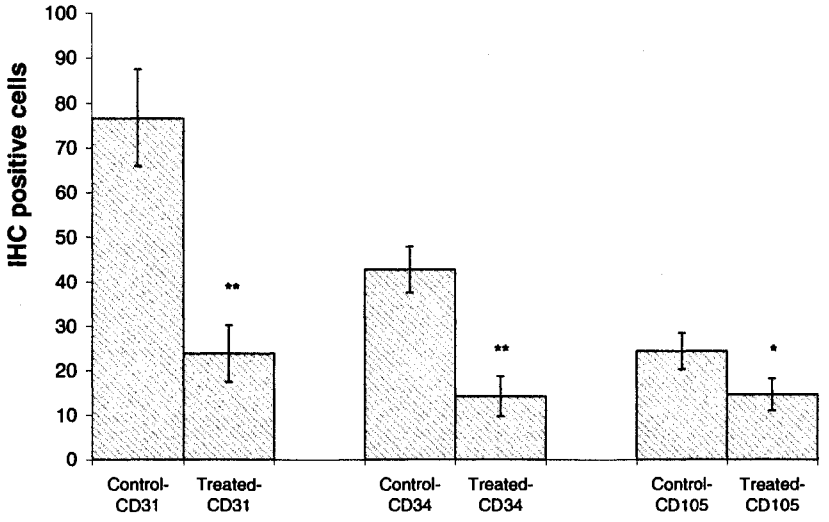

FIGURE 31 -The quantitative analysis of MVD marked by CD31, CD34 and CD105 7 days post nsPEF T_x vs. control tumor. Immunohistology positive cells were counted in five different fields, and the mean number per field was calculated. (** $p<.0001$), CD34 (** $p<.0001$) and CD105 (* $p<0.05$)

VEGF and PD-ECGF protein expression were decreased by nsPEF Tx

Expression of VEGF and PD-ECGF was analyzed by western-blot. Both VEGF and PD-ECGF protein expression decreased after the nsPEF T_x compared to the control tumor from the same mouse (Fig.32).

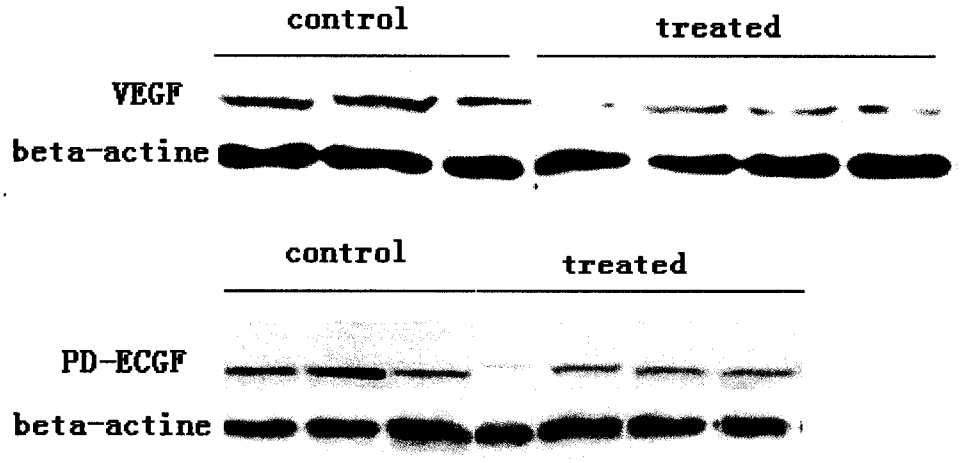

FIGURE 32 - *VEGF and PD-ECGF protein expression were decreased by nsPEF Tx.* VEGF and PD-ECGF protein expression was analyzed by Western-blot. Three mice bearing control tumor and treated tumor were euthanized 7 days post nsPEF T_x. Altogether 7 tumors were dissected. Control tumors (n=3) and treated tumors (n=4) were included. Beta-actin was used as loading control.

Discussion

The use of pulsed electric fields to reduce tumor angiogenesis has been reported previously.[72] Previous research of the anti-tumor effect of nsPEF T_x was confirmed on murine melanoma *in vivo* and nsPEF T_x was shown to cause apoptosis which led the melanoma tumors to self destruct. But nsPEF T_x also caused immediate blood flow reduction and tumor blood supply decrease. Thus the intra-tumor vascular response to nsPEF Tx was studied. The hypothesis is that nsPEF T_x can reduce tumor angiogenesis and might have value as an alternative therapeutic modality for solid tumors with a rich blood supply.

The vascular response of pre-existing vessels were assessed by histology.[73] In this technique, after the selection of a tumor target area, capillaries were visualized by H&E stain and the number of vessels per high-power microscopic field were counted. Before the nsPEF T_x, melanomas were nourished with rich blood supply. One day post nsPEF T_x,

the most obvious effect were blood vessel breakage and red blood cells scattered among condensed tumor cells with nuclear pyiknosis. Seven days after nsPEF T_x, the control tumor grew to a large volume with rich capillaries and small venules formed in the tumor while the treated tumors shrank and exhibited poor vasculature. These results suggest nsPEF T_x can cause direct damage to the blood vessel. Because of the precise location of the electrodes and richer vascular network inside the melanoma, the tumor is subject to greater effects of nsPEF T_x than the normal skin in the area of the tumor. Edema and red blood cells were evident outside the tumor but they recovered within a week. The treated tumor shrank with fewer blood vessels and continued to shrink even beyond the acute damage phase. Therefore beside the direct damage of blood vessel, nsPEF T_x can also inhibit tumor micro-vessel formation.

Angiogenesis has been proposed as essential for the growth of solid tumors.[72] Angiogenesis and the vascular state in tissues are mainly assessed by examining the micro-vessel density, which can be measured using various specific endothelial markers[74]. CD31 has been largely used for immunohistochemical analysis to assess tumour angiogenesis micro vessel density (MVD). As a panendothelial cell marker it represents mature vessels.[75] CD34 marked medium vessels[76] and CD 105 marked newly formed tiny vessels or neoangiogenesis.[77] In our study, no matter what size vessel it marks, MVD in nsPEF treated tumor always decreased significantly versus control tumor on the same mouse.

Our results show that nsPEF Tx caused a decrease in VEGF and PD-ECGF expression, which led to the lower MVD as assessed by CD31, CD34, and CD105. However the degree is different. Interestingly CD105, which is regarded to be a significant marker of neoangiogenesis,[78] indicate a mild decease which was not as significant as CD31 or CD34. This difference was caused by the antigen type. CD105, which is a proliferation-related endothelial cell marker, reflects active angiogenesis.[79] It is a specific marker of activated endothelial cells. In IHC, it recognized tiny newly forming blood vessels. Because CD34 and CD31 are expressed on most endothelial capillaries, they are termed pan-endothelial markers.[69] In IHC, they stained most endothelial cells and also positive for some other mesenchymal cells.

In vitro data suggest that VEGF over expression is a common phenomenon of melanoma cells. [80] Up-regulation of VEGF and hence increased angiogenesis—has been recently shown in melanoma cells undergoing malignant transformation induced by over expression of the survival signaling protein Akt *in vivo*.[81]

Angiogenic cytokines, released by tumor cells have an effect on vessel formation, tumor growth and metastasis;[82] The balance of pro-angiogenic and anti-angiogenic cytokines determines whether endothelial cells remain in angiogenic homeostasis, retrogression, or proceed to the state of neovascularisation to promote tumour growth, migration and metastasis.[83] Since nsPEF T_x can not only affect pre-existing vessels, but also micro-vessels, the hypothesis is that nsPEFs act on the angiogenic cytokines and changed the balance between pro- and anti-angiogenic factors.

Although many important promoters of angiogenesis have been reported, the most heavily studied one is VEGF,[84] apparently the most important angiogenic factors. It is a specific mitogen for endothelial cells and induces capillary tube formation, and increases vascular permeability. It regulates both physiological and pathological angiogenesis in melanoma. In the present study decreased VEGF expression is noted in nsPEF treated melanomas, VEGF was inhibited and expressed less after nsPEFs T_x. It contributes to the corresponding low angiogenic activity. The decreased VEGF expression led to recessive capillary proliferation and therefore neovascularization in melanoma was accordingly down regulated.

Platelet-derived endothelial cell growth factor (PD-ECGF) is a potent angiogenic factor that has been shown to be a thymidine phosphorylase. This enzymatic activity is crucial to its angiogenic activity.[85] PD-ECGF also showed decreased expression in the nsPEF treated melanomas.

One limitations of this study is the length of the follow up period. To set up a strict control, two melanomas were injected on the same mouse to avoid tumor growth difference originating from immune discrepancy between individual animals. However it's necessary to enthanize the animal before the control tumor exceed the maximum tumor burden in the animal protocol (2cm or appearance of ulceration). Nevertheless, despite the relatively short follow up period (7 days post nsPEF T_x), the results

demonstrate a significant impact of nsPEF T_x on the intra-tumoral vessel histology, MVD and the expression of VEGF and PD-ECGF.

It is specifically interesting that nsPEF T_x affected both immediate and delayed blood vessel effects, most likely as a result of several different mechanisms. One of these could be due to direct electric field effects on small blood vessels. Immediate effects on smaller vessels were greater than effects on larger vessels. This would be likely in the event of very high electric fields. Another possibility could be due to apoptosis, which has been shown to occur as early as 3 hours in fibrosarcoma tumors ex vivo (Beebe et al., 2002, IEEE). Likewise, nsPEF induced apoptosis in B16f10 tumors in vivo in the same time domain. Thus it is possible the nsPEF T_x induced apoptosis in endothelial cells to account for delayed effects on tumors vessels. In fact, the presence of apoptosis in endothelial cells from adipose tissue has been observed (S Beebe, unpublished, personal communication). Another possibility is effects on vasovasorium, the small blood vessels that provide blood to large vessels. Effects on PDGF and PD-ECGF are most likely do the effects on tumor cells that re-direct their energy supplies to apoptosis as opposed to growth factor production.

Tumors need nutrients and oxygen supplied by blood vessels in order to grow. They also use blood vessels to spread to other parts of the body. This process, known as metastasis, is the most lethal stage of cancer and the leading cause of cancer-related death. Fighting cancer by starving tumors of life-giving blood vessels has generated great interest in recent years. "Anti-angiogenic" cancer therapies that focus on the tumor's blood supply are not new. However, other such treatments starve tumors of their blood supply indirectly, by reducing blood vessel growth signals.

To summarize, nsPEF T_x directly damaged the melanoma cells and pre-existing blood vessels. As a result, tumor-derived blood vessel growth factors such as VEGF and PD-ECGF were decreased and the balance between pro-angiogenic and anti-angiogenic cytokines was broken. These changes resulted in the inhibition of the new vessel formation. The shortage of blood nourishment induced (1) the tumor infarction and consequently (2) less phagolysis, which interacts with apoptosis and contribute to the melanoma self destruction.

CHAPTER V

TEATMENT WITH NSPEF PROVES LONG-TERM EFFECTIVENESS FOR MELANOMAS IN MICE

Previous research with nsPEFs included 120 mice treated with 100 pulses of 300 ns duration with 40 kV/cm field strength.[86] Observations lasted from 2-4 weeks. These short-term studies showed that nsPEF with a 30 nanosecond rise time caused melanoma tumor cell nuclei to rapidly shrink and also to decrease blood flow to tumors. Melanomas shrank by 90% within two weeks. The treatment caused minor surface skin eschars with edema in the treated area that recovered in 7-10 days. NsPEF T_x deposited energy of 0.2 J/pulse and 100 pulses increased the temperature of the treated region by 3 ℃, 10 degrees below hyperthermia threshold damage.[86] However, the mice were routinely euthanized within a month of treatment for histological analysis. For this study, post-nsPEF treated mice were being observed for 3-5 months as a long-term survival study following complete tumor regression.

Materials and Methods

Tumor Model

In vivo experiments were set up in conformity with IACUC guidelines under applicable international laws and policies (Animal Care and Use Committee of Eastern Virginia Medical School IACUC #06-011). In accordance with principles for the ethical use of animals, the smallest number were used to obtain statistically meaningful data.[87] Thirty-six immunocompetent hairless female SKH-1 mice (albino strain, Charles River, Wilmington, MA , 4-week old) were injected subcutaneously with 10 µl PBS containing $1x10^6$ B16-F10 murine melanoma cells. Before treatment, the mice were randomly assigned to 2 groups[88] (17 in the treated group and 19 in the control group).

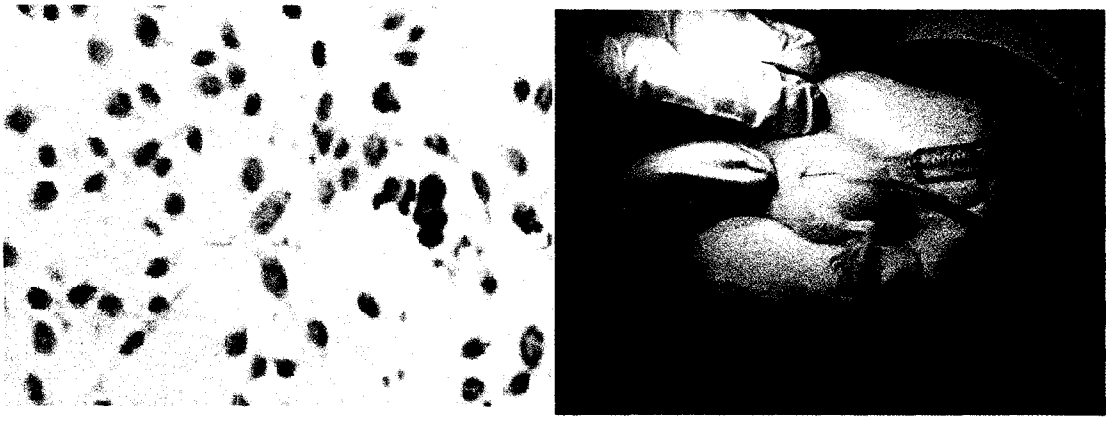

FIGURE 33 - Melanoma-F10 cells in culture and tumor cell injection on SKH-1 mouse. Left murine melanoma B16-F10 cells in culture during log phase (400x). Right B16-F10 melanoma cells being injected under skin of female SKH-1 mouse.

Nanosecond Pulse Generation

The nanosecond pulse generation[89] has an impedance of 75 Ω and consists of 30 pairs of high-voltage capacitors and 30 inductors arranged in a Blumlein configuration. This construction generates a square wave, 300 nanosecond, high-voltage pulse. The voltage across the tumor was monitored using a high voltage probe (P6015A, Tektronix, Beaverton, CA), and the current was measured by means of a Pearson coil (model 2877, Pearson Electronics Inc., Palo Alto, CA). Current and voltage were recorded simultaneously using a digitizing oscilloscope (TDS3052, Tektronix, Beaverton, OR). A single pulse had a duration of 300 ns, field strength of 40 kV/cm at a rate of 0.5 Hz.

Pulse Treatment

Seventeen mice were treated 1-4 times with 300 pulses at 40kV/cm. Each individual treatment of 300 pulses was separated by 2 weeks during which time the tumor was evaluated for nsPEF effects. If the tumor was alive either on the surface by transillumination or by ultrasound imaging at the end of the 2-week interval, another 300-pulse treatment was ordered. For tumor remission, one mouse needed one treatment (7% of the total), two mice needed two treatments (14%), nine mice needed three treatments (65%) and two mice needed four treatments (14%). Euthanasia and tissue collection start-time was calculated from the last treatment day.

In vivo Imaging

Melanomas were imaged daily by external skin surface, transillumination and ultrasound (Visualsonics Vevo 770, Visualsonics Inc., Toronto, Canada) with model 708 scan head at 55 MHz. The power Doppler mode provided blood flow images for each tumor. Pictures were taken every 1-2 days and tumor volume was estimated as O'Reilly experienced equation [$V = (\text{tumor width})^2 \times (\text{tumor length}) \times 0.52$].[90] Vessels supplying the tumor were counted under transillumination microscopy.

Survival Analysis

An animal survival curve (Kaplan-Meier plot) was analyzed using a log-rank test. Differences between treated and control groups were considered as statistically significant at $p < 0.05$. Statistical analyses were done using SPSS 15.0 software.

H&E Staining

Mice were euthanized by CO_2 asphyxiation under anesthesia and dissection was performed under aseptic conditions to collect tumor with overlying skin, liver, lungs and spleen. A red tattooing ink was used to mark tumor location at tumor cell injection sights. Melanoma samples were processed for histology and immunohistochemistry.[91]

Data Collection

After five days post-injection of tumor cells, data were collected every day and summarize according to 5 different time periods (T1 - T5): T1- corresponds to the time of injection to time to treatment; T2- corresponds to the time of final treatment; T3- corresponds to one week post-final nsPEFs treatment; T4-corresponds to 2 weeks post-final nsPEFs treatment; T5-corresponds to the final week prior to animal euthanasia (end of study). The control group data analysis followed the same time course. In summary, T1 = injection, T2 = end of treatment, T3 & T4 = 1st and 2nd week after last treatment respectively and T5 = euthanasia.

Tissue Micro-array Construction

Representative areas of the different lesions were carefully selected on H&E-stained sections and marked on individual paraffin blocks. Two tissue cores (1 mm diameter) were obtained from each specimen. In addition, non-neoplastic melanoma control tumor samples were included as controls. Tissue cores were precisely arrayed into a new paraffin block using a TMA workstation (Beecher Instruments, Silver Spring, MD).[92] An

H&E-stained section was reviewed to confirm the presence of morphologically representative areas of the original lesions.

Histology and Immunohistochemistry for Micro Vessel Density

Six μm-thick, paraformaldehyde-fixed, paraffin-embedded tumor, liver, spleen or lung sections were analyzed. Specimens were deparaffinized, rehydrated and processed for either histology or immunohistochemistry. The antibodies used for blood vessel immunohistochemistry were an anti-mouse PECAM/CD31 polyclonal antibody (M-20; Santa Cruz Biotechnology, Santa Cruz, CA) used at a concentration of 2 μg/ml for 2 hours at 37°C, for 1 hour at room temperature. In negative controls the primary antibody was omitted. The signal was revealed by AEC staining (3-amino-9-ethylcarbozole, red) instead of DAB (3, 3'-Diaminobenzidine, dark brown) to avoid confusion of melanin. Micro-vessel counts were performed on CD31 positive-stained blood vessels.

Western Blotting Analysis for CD31 Expression in Melanomas

The melanoma samples were digested in hypotonic buffer (10 mmol/L Tris-HCl, 1 mmol/L ethylenediaminetetraacetic acid, pH 7.4, with protease inhibitor cocktail tablets; Complete, Roche Diagnostics, Basel, Switzerland). An aliquot of extract was saved for determination of protein concentration and the remainder was boiled in the sodium dodecyl sulfate loading buffer. Eighty μg of protein per sample were separated by 6% gel electrophoresis and transferred to a nitrocellulose filter (Amersham Life Science, Buckinghamshire, UK). Protein detection used (1) a rabbit polyclonal antibody against CD31 (Beijing Boisynthesis Biotechnology CO., LTD) that recognizes both murine and human forms of the receptor and (2) a monoclonal antibody against β-actin diluted 1:1000 (AC-40, Sigma-Aldrich). Detection was performed through a chemiluminescence assay (ECL; Amersham Life Science).[93]

Results

Long term survival analysis

To establish the role of nsPEFs in inhibiting tumor growth *in vivo*, B16-F10 melanoma cells were injected intradermally into the flank of SKH-1 mice (n = 36). Tumor size was measured daily beginning 5 days post-injection of tumor cells when the tumor mass began to be detectable. Control mouse tumors (n = 19) grew exponentially

throughout survival time with dramatic acceleration as compared to nsPEF-treated animals (n = 17). A significant difference was already readily detectable in the 1st and 2nd week after nsPEF T_x. At the experiment's conclusion, melanomas were eliminated in all 17 experimental mice treated by nsPEF and they survived 3-5 months following visible remission. In contrast 13 of the total 19 controls were euthanized within several weeks of B16 cell injection because growth exceeded prescribed size or tumor became ulcerated.[94] In some of these studies, mice were used that were more mature than other mice. These mice were more likely to survive tumor initiation and progression than mice that were younger due to a more mature immune system. It is likely that these mice were responsible for control animal survival greater than 180 days. It should be noted that the tumors in control animals did not decrease in size, but remained at a level that was not deleterious to the animals health as defined by the IACUC protocol.

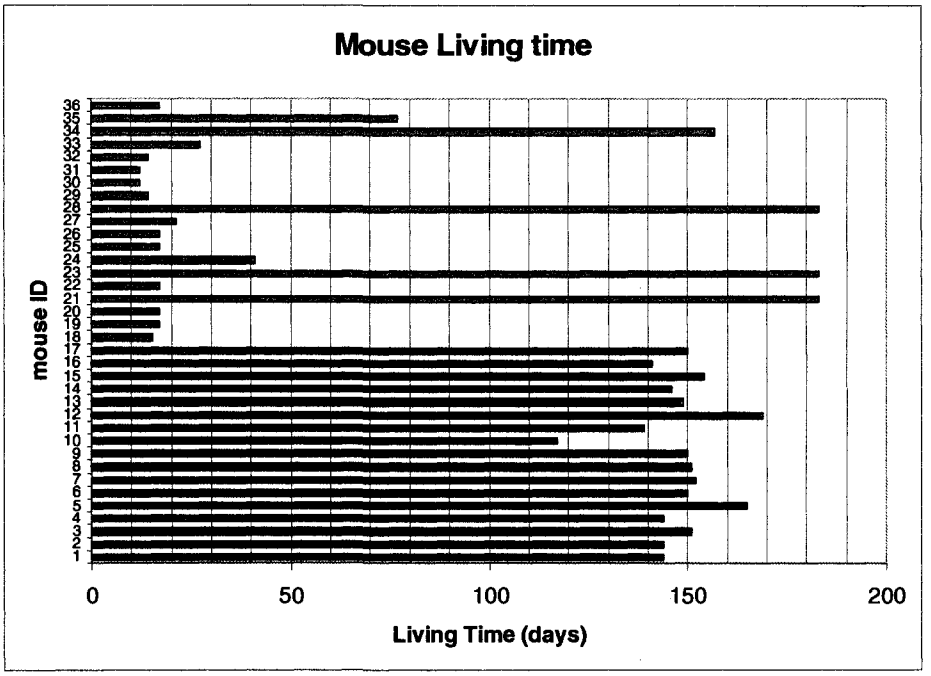

FIGURE 34 - Melanoma Growth Inhibition and Survival Time Post nsPEF T_x. Bars with mouse ID from1-17 indicate animals that were treated. Survival days ranged from 117 to 169. Bars with mouse ID from mouse #19-36 indicate animals that were non-treated controls.

Mouse weighs change during the 5-month survival study

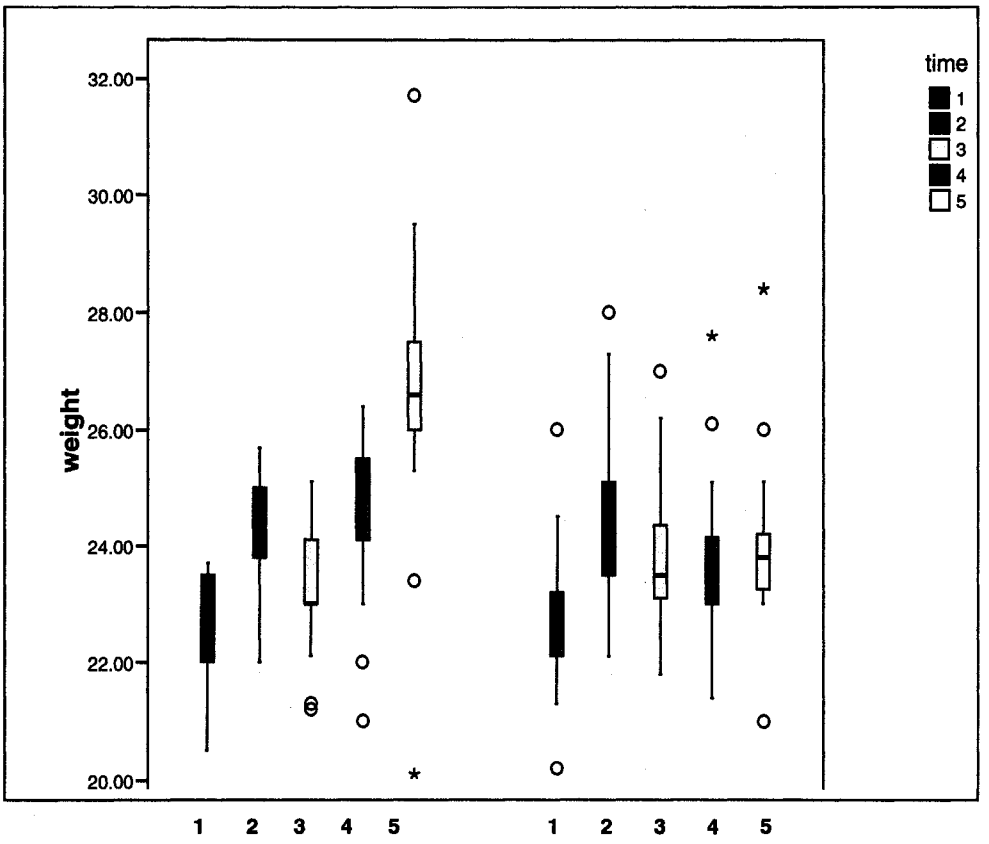

FIGURE 35 - *Mouse weight follow up during the 5-month survival study.* Group 1, treated animal and group 2, control animal. Five boxes in each group represent time period 1-5. Time 1 is injection, time 2 is treatment, time 3 and 4 are the 1st and 2nd week after the last treatment and time 5 is euthanasia. The hinges at the top and bottom of the box generally match the upper and lower quartile of weight measurement of each group. The median is indicated by a thick black line inside the box. The horizontal lines above and below the boxes mark the adjacent values. These are the most extreme values in the sample that lie between the hinges and the inner fences. Data points outside this range should be considered as outliers. Any outliers are marked with a circle and extreme cases with an asterisk.

Tumor volume change after the treatment

When the data was analyzed, the mean value was gotten from 5 time periods which are defined in the legend to Figure 35: Mouse weight change after the nsPEF T_x was measured daily in 5-month survival study. The treated group showed a significant smaller mean weight. A typical tumor morphological change was reflected by surface photograp.

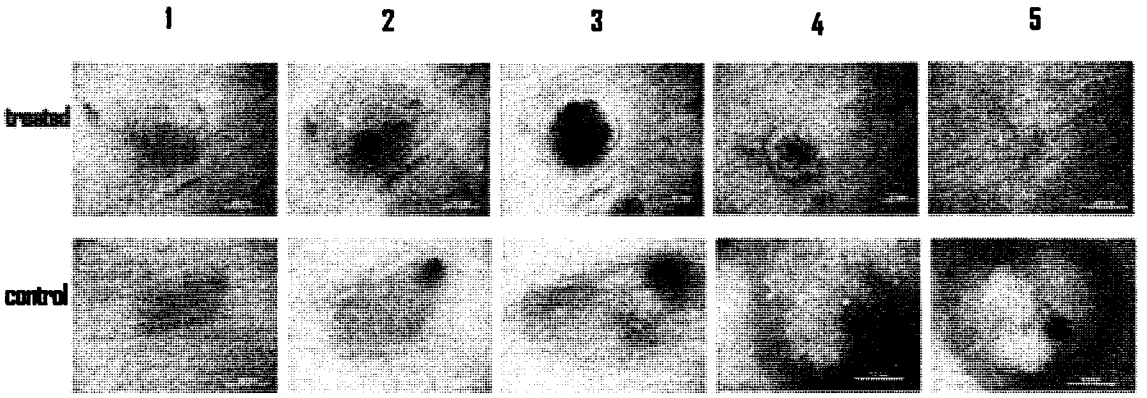

FIGURE 36 - A Typical tumor morphological change reflected by surface photograph. Melanomas were imaged daily and tumor size and appearance were recorded. Time 1 is injection, time 2 is treatment, time 3 and 4 are the 1st and 2nd week after the last treatment and time 5 is at euthanasia. The scale bar is 2mm.

Statistical analysis for tumor volume changes in long term survival study after the nsPEF treatment

Melanomas were imaged daily and tumor volume was calculated by the formulation $V = (\text{tumor width})^2 \times (\text{tumor length}) \times 0.52$. After the injection both groups showed the tumor growth with increased tumor volume. NsPEF Tx changed the growing and tumor volume decreased significantly (p=0.0004).

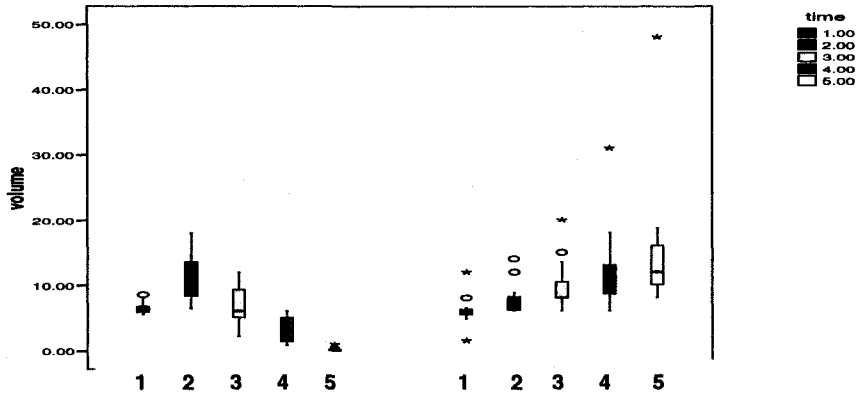

FIGURE 37 - Statistical analysis for tumor volume changes in long term survival study after the nsPEF treatment. Melanomas were imaged daily and tumor volume was calculated by the formulation: $V = (\text{tumor width})^2 \times (\text{tumor length}) \times 0.52$. Group 1, treated and group 2, control. Time 1 is injection, time 2 is treatment, time 3 and 4 are the 1st and 2nd week after the last treatment and time 5 is at euthanasia.

Histological analysis of tumor structure in long-term in survival study

Histological analysis demonstrated that melanomas in the control group were large, round and stuck out of the skin surface. In most cases, the tumors were separated from the overlying epidermis by a thin zone of dermis that appeared highly vascularized. The skin above the big control melanoma mass was often ulcerated, but ulceration did not correlate with a shorter life span. Tumor cells were large with eosinophilic cytoplasm often containing an accumulation of melanin pigment and atypical vesicular nuclei with prominent nucleoli. In comparison, melanomas were hard to find in all 17 treated animals unless a small amount of melanin pigment was left in the tattooed skin area. Tumor net construction and tumor blood supply were totally destroyed with no evidence of the tumors remaining. Only a few masses of atypical melanoma cells were located in the area.

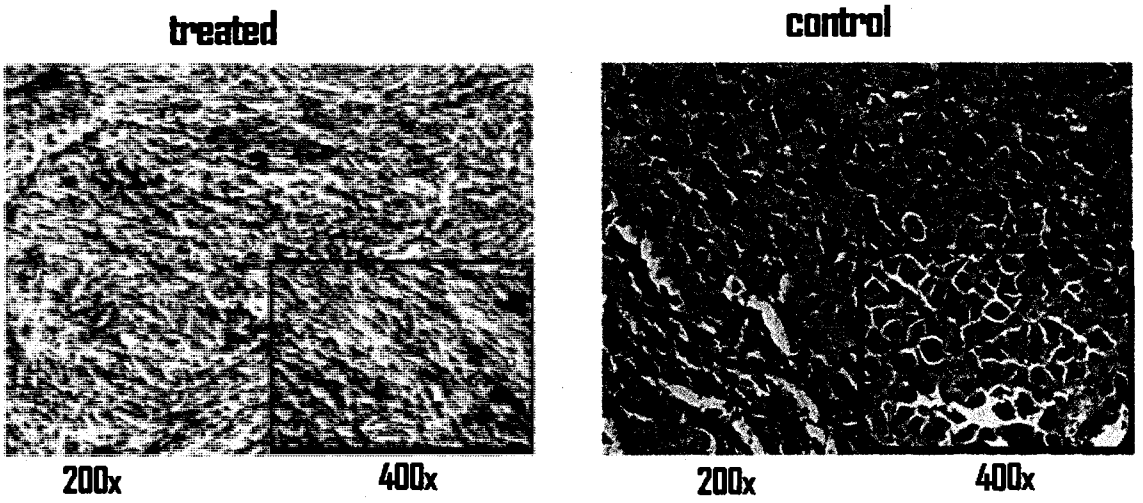

FIGURE 38 - Histology analysis of tumor structure in long term in survival study. The left panel represents a typical treated tumor and the right panel represents a typical control tumor. An area was magnified to 400x to show the tumor cell details in both panels.

NsPEF decreases peritumoral vascularization in long- term survival study

Macrographs revealed that the melanoma mass in control animals was surrounded by an extended area of prominent vascularization while the opposite was found in the treated group, which exhibited a very poor blood supply without surrounding visible vessels at the end of the study.

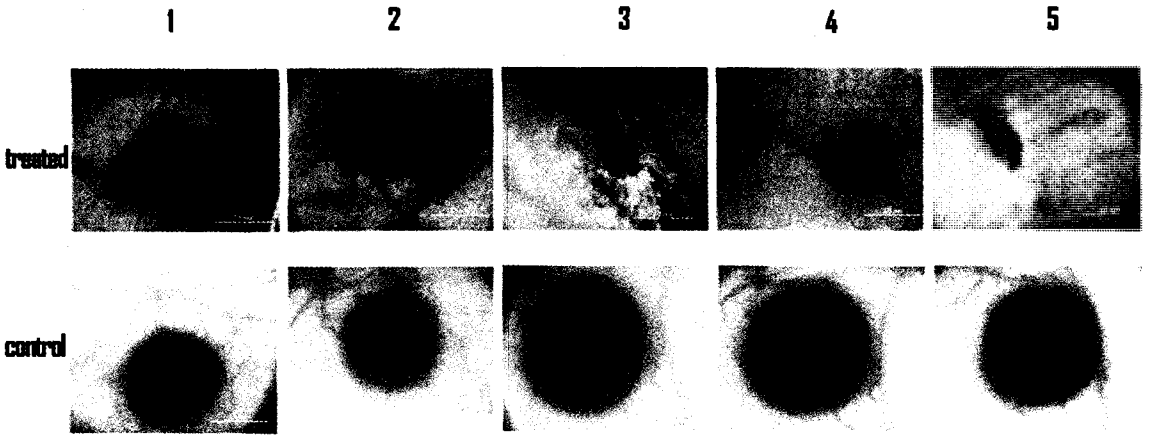

FIGURE 39 - NsPEF decreases peri-tumoral vascularization in long-term survival study. Treated tumors are shown in the top row and control tumors in the bottom. Treatments 1-5 are: Time 1 is injection, time 2 is treatment, time 3 and 4 are the 1st and 2nd week after the last treatment and time 5 is at euthanasia. The scale bar is 2mm.

Quantitative analysis of peritumoral vascularization change in long term survival study after the nsPEF treatment

Vessel number around tumor showed no difference in control vs. treatment groups before nsPEFs treatment (time 1 and time 2) while there were statistical difference after the nsPEF Tx (time 3, time 4 and time 5). Treated tumors analyzed beyond 1 week post-treatment were greater than 6-times smaller than control tumors.

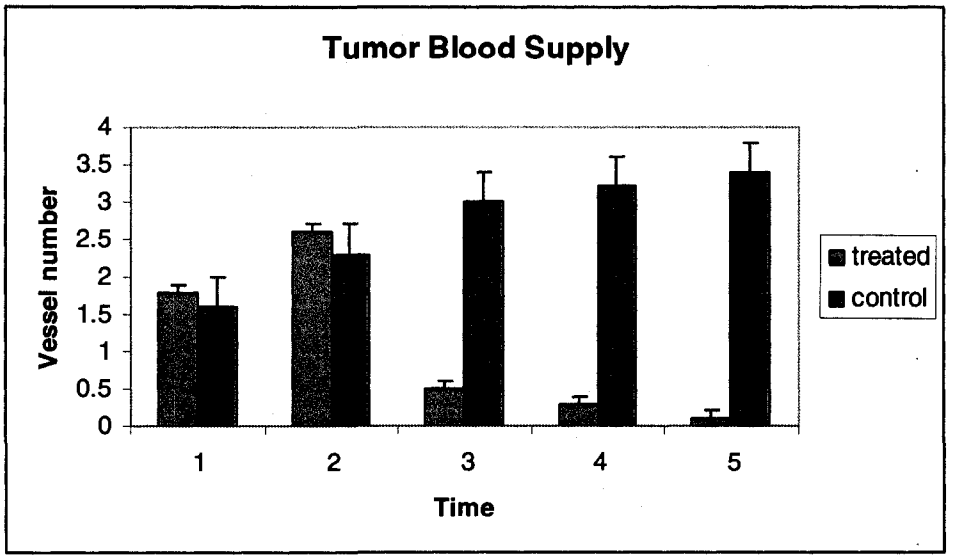

FIGURE 40 - Quantitative analysis of peritumoral vascularization change in long-term survival study after the nsPEF treatment. Vessels around tumor were counted with transillumination microscope and then a mean value was summarized according to the time segment as mentioned above. If there were many blood branches, only those going directly into the tumor were counted. Time 1 is injection, time 2 is treatment, time 3 and 4 are the 1st and 2nd week after the last treatment and time 5 is at euthanasia. A t-test analysis showed vessel number around tumor exhibited no difference before nsPEFs treatment (time 1 and time 2), while there was statistical difference after the nsPEFs treatment (time 3, time 4 and time 5).

Metastatic analysis of melanoma tumors in long-term survival study post-nsPEF T_x

H&E staining of lung, liver and spleen showed metastatic nodules in control mouse ID 196, while in nsPEF treated mouse ID 189, only the liver exhibited metastasis, however, lung and spleen did not exhibited metastasis. For the statistical analysis, the metastatic rate between treated (1/17 and positive rate 5.8%) and control groups (1/19, 5.3%) showed no difference.

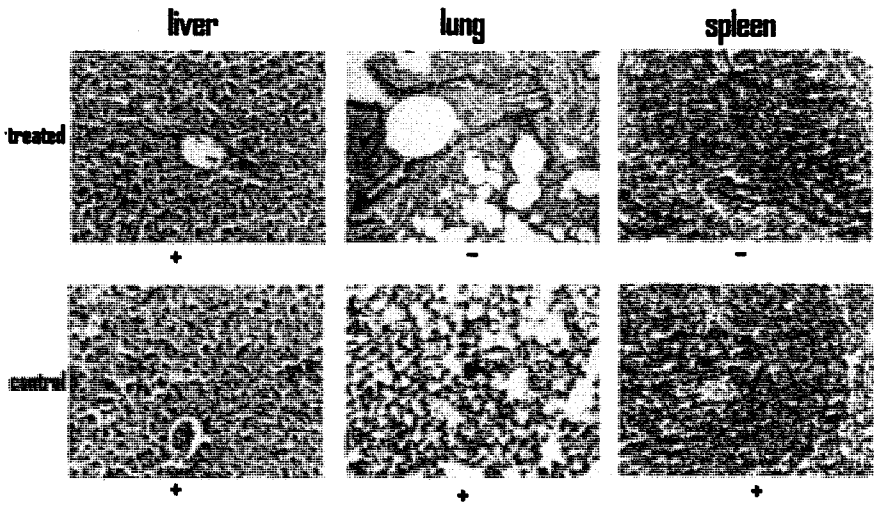

FIGURE 41 - Statistic analysis of melanoma tumors in long-term survival study post-nsPEF treatment. Treated tumor ID 189 is shown in the top panel and control tumor ID 196 is shown in the bottom. H&E staining of lung, liver and spleen are shown as indicated. Original magnifications, ×400.

Angiogenetic analysis of melanoma tumors in long-term survival study post-nsPEF T_x

Tumors from thirty six mice and the lungs, liver, kidney and spleen were put on one tissue-micro array slide for H&E analysis. H&E staining showed the treated tumor had no cancer cells left in the tumor area, only some melanin. The immunohistochemistry (IHC) can show quantitative and qualitative differences in the vasculature of the control and treated tumors by CD31, the pan marker for micro-vessel density. Control tumors had significantly more vessel lumens and capillary endothelial cells than the treated tumor per microscopic field ($p<0.001$). This result was also confirmed by CD31 protein expression by Western-blot which showed high CD31 expression in control tumors (n=3) and low expressed in treated tumors (n=2).

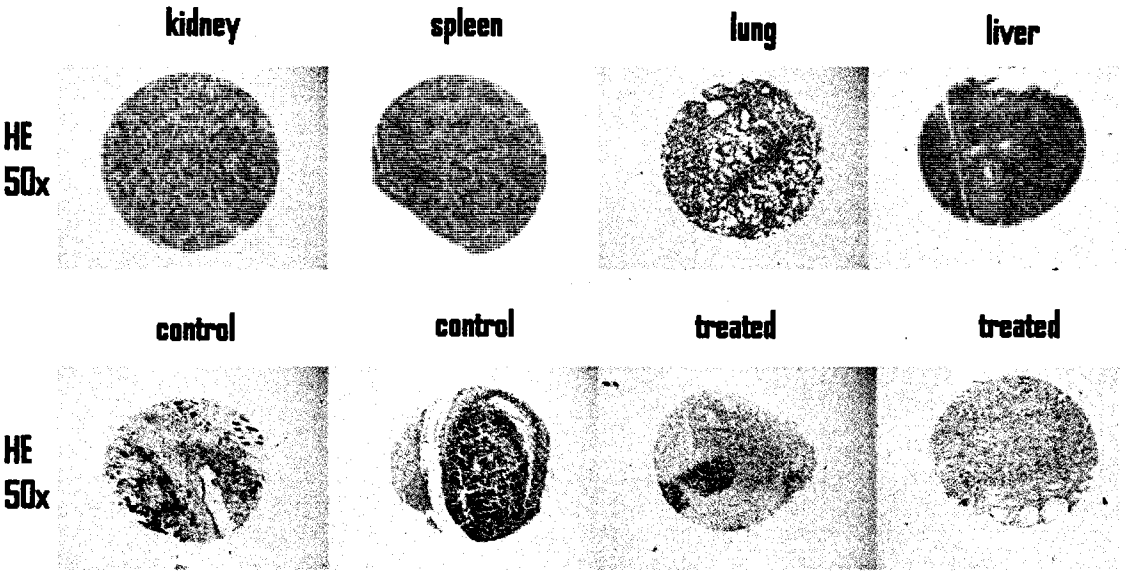

FIGURE 42 - Angiogenesis analysis of melanoma tumors in long term survival study post nsPEF treatment. Angiogenesis was analysis by tissue micro-array and H&E staining. All the tissues collected were constructed on a tissue micro-array so that the same tests were applied to all the samples in the following IHC analysis.

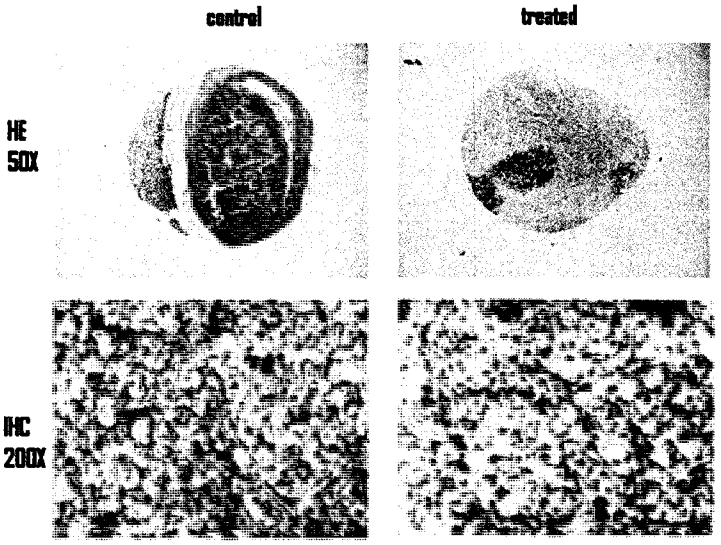

FIGURE 43 - Micro vessel density marked by CD31 with immunohistochemistry of melanoma tumors in long-term survival study post nsPEF treatment. Vasculature within melanoma in SKH-1 female mice. B16F10 mouse melanoma cells were injected subcutaneously into mice, and tumor vasculature was examined by using immunohistochemical staining with anti-CD31. H&E staining showed the tumor volume decreased after nsPEF treatment. Frozen sections of tumors were stained with mouse monoclonal anti-CD31 antibody for total vessel count. The IHC can show quantitative and qualitative differences in the vasculature of the tumors. Micro-vessel counts were performed at ×200 magnification in five microscopic fields. AEC positive staining showing new micro vessels formed inside the tumor. The melanin is a sign of malignant melanoma tumor cells. Positively stained blood vessels by CD31 with lumen as well as cell clusters without a lumen and single cells were considered as individual vessels.

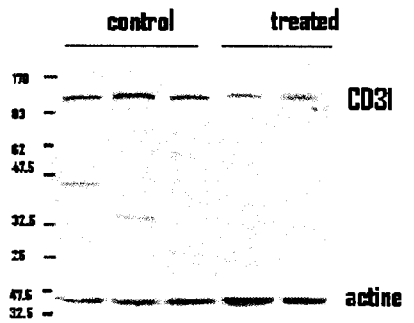

FIGURE 44 - CD31 protein expression by Western-blot of melanoma tumors in long term survival study post-nsPEF treatment. Western blot showed high CD31expression in control tumor (n=3) and low in treated tumors (n=2).

Discussion

Nanosecond pulsed electric fields can induce various kinds of biological effects that are essentially different from conventional plasma membrane electroporation with lower electric fields and longer pulses, [95]especially the interactions of nanosecond pulsed electric fields with living cells.[96] Based on these effects, some applications of pulsed electric fields in cancer therapy, gene therapy, and delivery of drugs were reviewed in details.[97]

However most investigations of the effects of nsPEFs on mammalian cells were *in vitro* studies. The previous *in vivo* study, which involved nsPEF treatment of murine fibrosarcoma tumors indicated the short term biological effects of nsPEFs on tumor including apoptosis markers for caspase activation and TUNEL. However, longer term effects were not considered. In the studies reported here, the data suggest that nsPEFs eliminate tumor by apoptosis and decreased peritumoral vascularization.

Survival curves reflect an obvious difference between the treated and control groups. The accumulative survival rate in treated group was 100%, with all 17 mice living 3-5 months after melanoma tumors vanished. In contrast, 12 control animals died in 17 days for the large tumors including those that were ulcerated. The therapeutic effect of nsPEFs comes from its unique character of high power and low energy density (non-thermal). The nanosecond pulses are too short to cause plasma membrane electroporation. Instead they modulate intracellular structures and functions and work as a form of non-ionizing radiation and are special for cancer treatment because of faster rise time (30 nanosecond) and shorter pulse duration (300 nanosecond).The charging time

on the cell membrane is so short that it can penetrate into the cell interior.[98,99] The hypothesis is that the internal field will generate a current that can kill the tumor cells and blood vessels by the large field strengths (40KV/cm).

The data here also showed statistic change of tumor volume and blood supply. Tumor growth and metastatic spreading depends on the formation of new blood vessels that provide oxygen and nutrients.[100] To promote new vessel development, tumor cells secrete angiogenic growth factors that act on the neighboring endothelial cells, inducing proliferation and migration.[101] According to the histology, nsPEF destroyed the tumor and blood vessel at the same time. Our transillumination pictures showed that adult vessels around the tumor decreased dramatically after nsPEFs treatment. The vessel structure was damaged and bleeding could be seen. After multiple nsPEF T_x, no visible tumor and blood vessel could be found. B16F10 melanomas are highly invasive in part because formation of micro vessels is very efficient. It is clear that micro vessels play a very important role in metastasis. It has been reported that intratumoural microvessel density (MVD) marked by CD31 has prognostic significance in melanoma. To evaluate MVD in nsPEFs treated and control melanomas, the immunohistochemical expression of CD31 was assessed using the tissue micro-array technique so that all samples could be tested under the same condition. CD31 expression was significantly, higher ($p< 0.001$) in control group compared to nsPEFs-treated group. Also CD31 protein expression was tested by immunoblot analysis confirming and the result agreed with the IHC findings.

Tumor angiogenesis is a complex phenomenon that depends on the action of pro- and anti-angiogenic factors, proteinases and their inhibitors, and adhesion molecules. Endothelial cells are able to secrete their own growth factors, but also other cell types, including tumor cells, cells of the tumor stroma and infiltrating inflammatory cells could produce factors that stimulate angiogenesis.[102] NsPEF treatment is non selective on cell type and it targets all cells in the plate electrode area. NsPEF damaged both endothelial cells and tumor cells and as a result, the angiogenetic function is hindered. It is highly likely that the direct damage to blood vessels and tumors is a major mechanism to stop tumor growth. However, the effects of nsPEF are non-thermal and does not cause a heat response from tumor and the normal tissue around the treated areas are not affected by

thermal changes. In a previous study, the mild bleeding and edema around the plate electrode was found, but recover in one week.

Application of nsPEFs makes a significant difference on tumor volume and blood supply. However, effects on metastasis showed no difference in control and treated group. The reason for absence of metastasis in this study is likely due to the injection of B10F10 cells subcutaneously instead of via tail vein.[103] B16F10 is very metastatic when injected into the circulatory system,[104] but not so invasive when implanted as a solid tumor. This may be why so few metastatic sites were found (in 36 mice only 2 cases of metastasis found). An isolated sub-line, BL6 is very aggressive in metastasizing from a solid tumor but less so from direct injection into veins.[105] B16F10 line used here may lack mutations in genes that facilitate tissue breakdown, which they must have to escape the primary tumor. If they are injected instead in the tail vein, they will bypass the need for tissue breakdown and proceed rapidly to metastasis.[106]

Because of the low metastasis rate in control tumor group, the study can not provide strong proof for anti-metastasis effects of nsPEFs. The weight difference between control and treated mice is not very meaningful even though the data showed that the weight of the nsPEF treated group had decreased statistically. Because the treated group lived 3-5 months, the SKH-1 mice began the experiment when they were 4-week old and had plenty of time to gain weight. While most of the control group just died in 2-3 weeks after the B16F10 injection, their time to gain weight was negligible. The present survival study for metastasis issue is therefore incomclusive. But the metastasis issue can be further studied in future trials with the more aggressive melanoma cell lines. Nevertheless, the metastasis issue does not detract from the fundamental conclusion that nonthermal nsPEF T_x can cause electrical, biochemical, functional and histopathological changes in melanomas *in vivo* and in long-term studies, tumors did not reoccur at the primary site.

In summary, melanoma is a malignant skin cancer, which causes the most skin cancer-related deaths in humans. In its advanced stages melanoma is resistant to existing therapies. The effect of a unique non-thermal nsPEF T_x on murine B16F10 melanoma cells *in vivo* in a long-term survival study provides evidence for long term survival. The data showed that nsPEF T_x can decrease tumor volume and blood vessel number and

finally total tumor elimination, not returning to the primary site after 3-5 months. The survival days for the treated group are significantly different from control group. This suggests that nsPEF T_x could be used as a therapeutic treatment for melanoma and furthermore its long-term effectiveness is proved.

CHAPTER VI

PARAMETER STUDY OF NSPEF

In the former experiments, the primary objective was to see if nsPEF T_x had any effects on *in vivo* melanomas. Thus the same treatment condition was used from preliminary experiments: pulse duration was 300 ns, pulse number was 100, the electric field was 40 kV/cm and the frequency was 0.5 Hz. The data confirmed that this condition caused apoptosis, inhibited angiogenesis and eliminated the tumor. Only the treatment conditions mentioned above were used. Different treatment conditions for pulse number, energy density and pulse duration may result in different values of biological responses. Therefore the parameters were changed to study the corresponding biological effects. First, for all conditions tested the energy density was kept at the same level, but the pulse duration was varied to compare how longer pulses (1ms) and shorter pulses (300 ns) affected tumor growth. Second, the pulse duration was kept as 300 ns while the voltage and pulse number was changed to see if there was a dose-effect relationship.

Material and Methods

Electrical conditions for nanosecond pulse and millisecond pulse

Eight mice bearing tumors derived from B10F10 GFP (green fluorescence protein) cells were studied to compare long pulses (pulse duration 1ms) with short pulses (pulse duration 300 ns). Five days after the subcutaneous injection of 1 x 10^6 B16F10 GFP cells were injected and tumors having a mean diameter of 5 mm were treated. The same electric energy was delivered to 2 tumors injected on the left and right flanks of the same mouse but one treated with a long pulse (1ms, 150V, 48 pulses) and the other with a short pulse (300ns, 6kV 100pulse). The animals were euthanized and dissected tumors were visualized by florescence microscopy.

Quantification of caspase-3 enzymatic activity

Melanomas were placed on dry ice (5–10 min) and lysed in Tris buffer with 0.5% Triton, pH 7.5, containing general protease inhibitors. An aliquot was diluted with a solution containing interleukin 1B converting enzyme (ICE) buffer and the fluorogenic

caspase-3 enzymatic activity was determined by Ac-DEVD-AFC (N-acetyl-aspartate-glutamate-valine-aspartate-AFC, 7-amino-4-trifluoromethyl coumarin) .[107] Fluorescent emission (excitation 400 nm and emission 505 nm) was measured after incubation for 45 min at 37°C. Blanks were evaluated to determine background fluorescence. Standards containing 0–500 pmol/l AFC were used to determine the amount of fluorochrome released. Fluorescence was measured at λmax = 505 nm using a SpectraMax Gemini XS (Molecular Devices, Sunnyvale, CA, USA). Caspase activity was expressed as pmol/min/mg protein. Murine melanoma B16F10 treated with 1 mmol/l cycloheximide were used as positive controls.

Fluorescent tumor model

To compare the long and short pulse differences clearly, B16F10 cells were replaced by a B16F10 GFP cell line, which continually expresses the GFP protein.[108] Because melanomas derived from this cell line were clearly detected under the animal's skin upon fluorescent microscopy, tumor margin and tumor volume were easily defined. This enabled *in vivo* imaging of the tumor volume and fluorescence intensity over time after treatment.[109] These tumor cells have an expression of GFP gene less than 100%, but the majority do have green fluorescence which makes this animal model able to provide the green fluorescence quenching as a biological effect.

Results

Comparison of long pulse and short pulse.

Before pulses were delivered, the tumors had bright green fluorescence. When the 1-ms PEF (150v, 48 pulses) was applied to the tumor, GFP quenching happened immediately. In contrast, when the 300-ns PEF (6 kV, 100 pulses) was applied to the tumor, the GFP began to fade gradually. After 3-6 hours most of the green fluorescence disappeared. After 24 hour post-nsPEF Tx the fluorescence vanished. This time sequence matches caspase activation, TUNEL detection and histological changes, which were discussed in Chapter III. Thus, both pulse conditions had quenching effects on tumor, but the long pulse effect was immediate, suggesting a direct effect on GFP fluorescence. In contrast, the short pulse effect on quenching was delayed and coincident with apoptosis, suggesting that the GFP was degraded with other proteins in response to

apoptosis. Furthermore, the short pulse conditions inhibited the tumors more effectively then the longer pulse conditions.

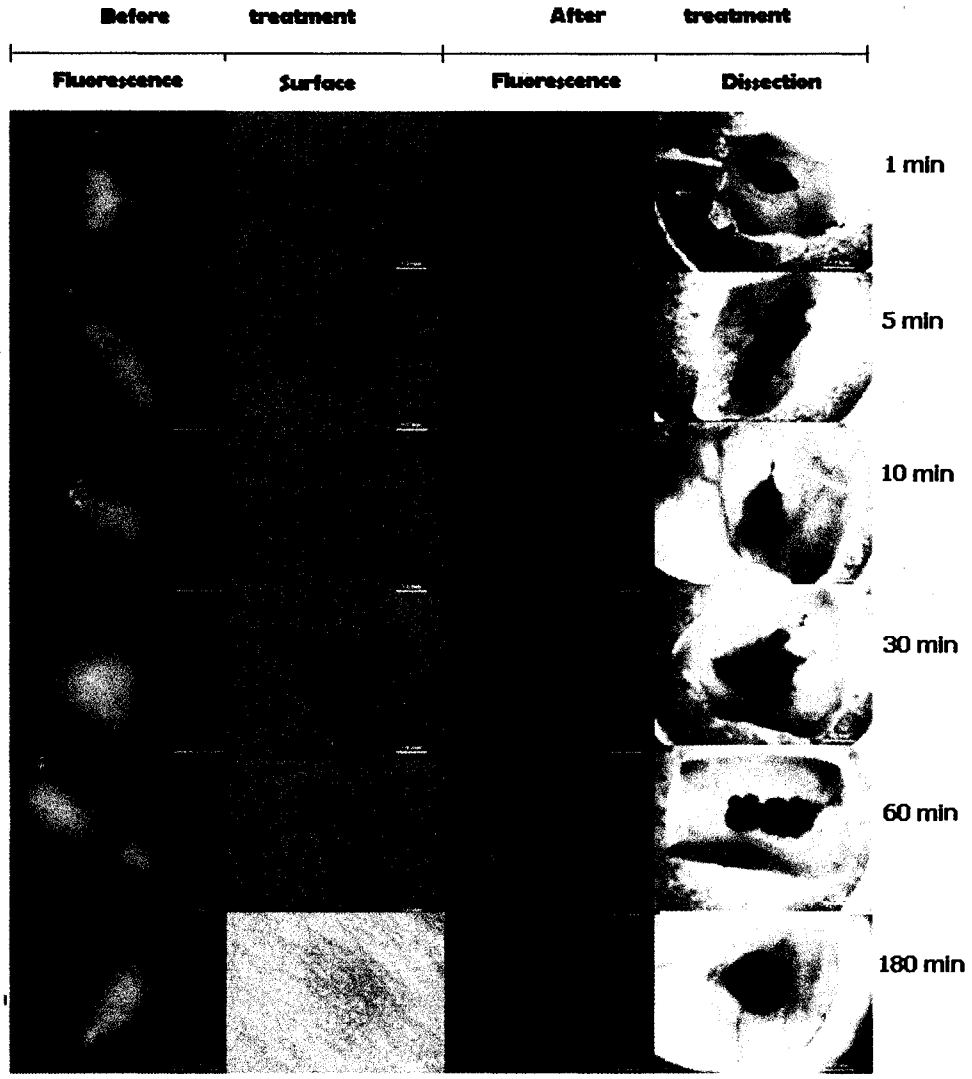

FIGURE 45 - Long pulse effects on fluorescent melanoma tumor cells *in vivo*. Digital imaging was used to quantify the relative fluorescence of B16F10 GFP tumors at the different time points. The images show GFP fluorescence with times between 1-180 minutes. The surface view and the dissected view are also shown in the same time course. Scale bar is 2mm.

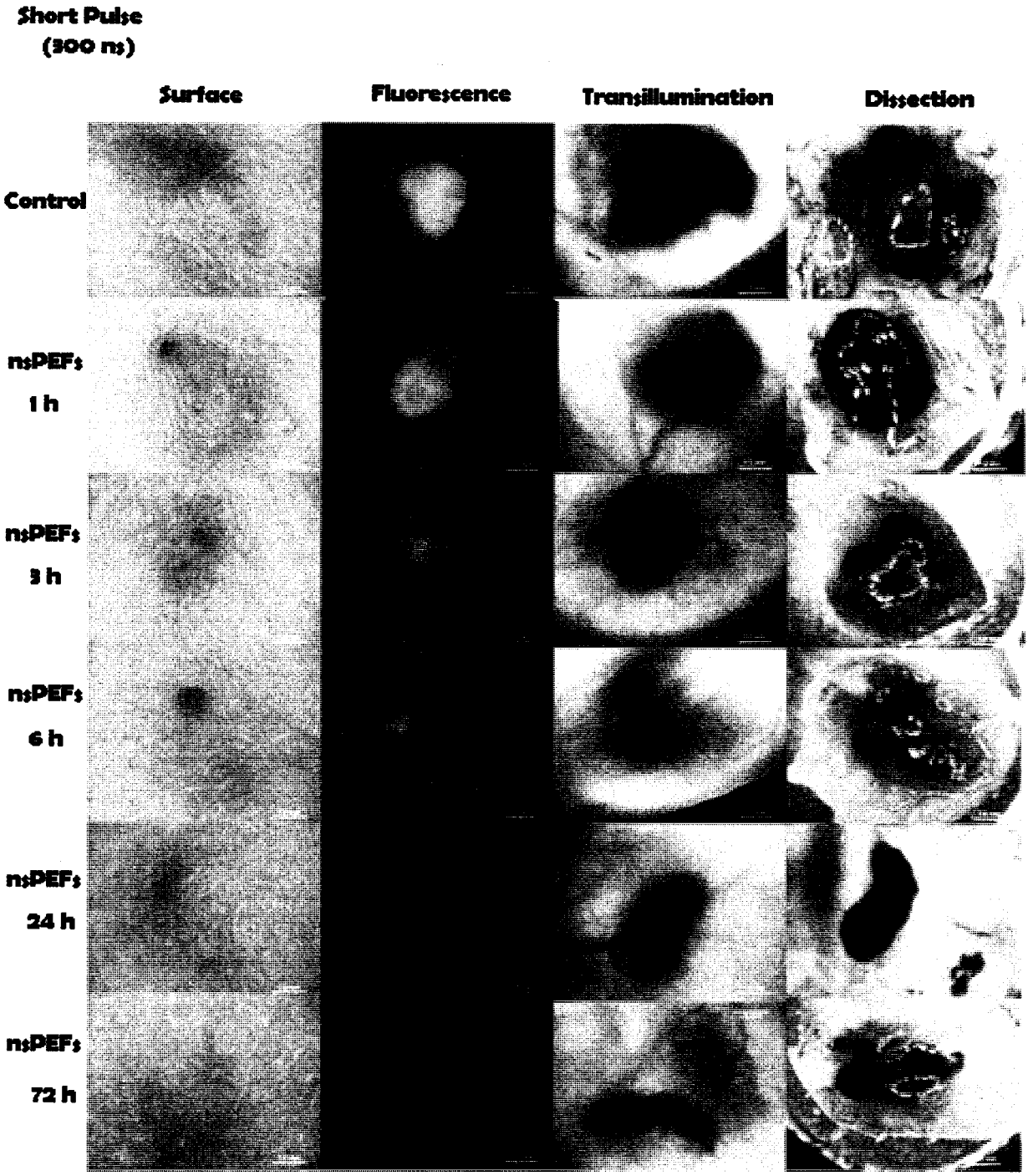

FIGURE 46 - Short pulse effects on fluorescent melanoma tumor cells *in vivo*. Digital imaging was used to quantify the relative fluorescence of B16F10 GFP tumors at the different time points. The images show GFP fluorescence with times between 1-72 hours. Surface views, dissected views, and transillumination views are also shown in the same time course. Scale bar is 2mm.

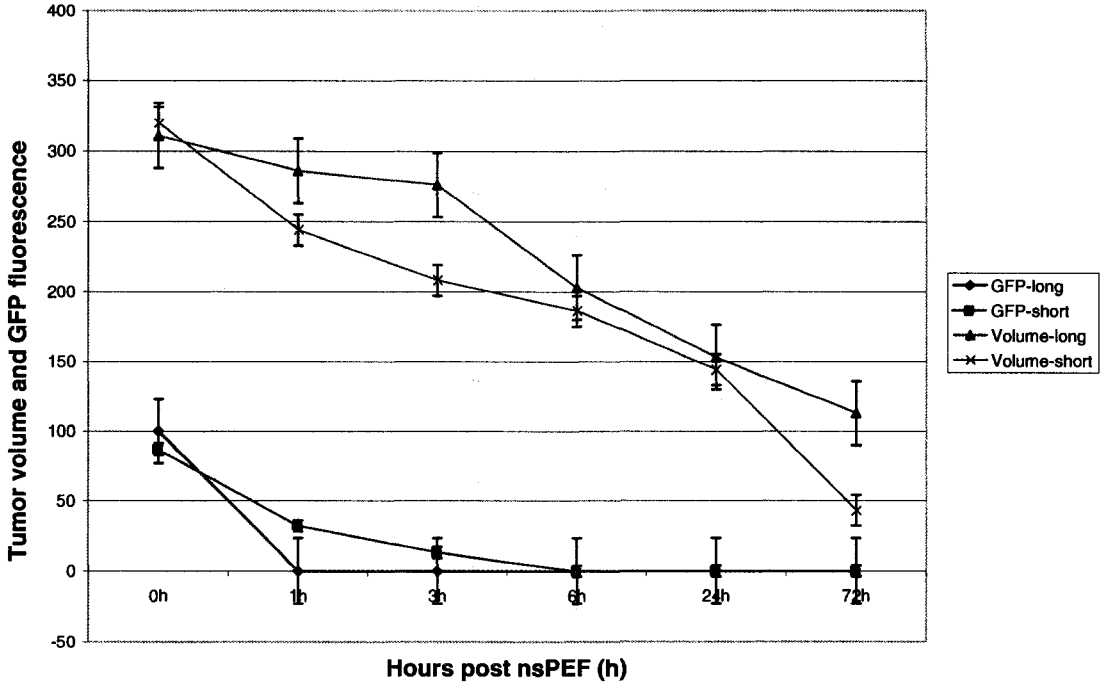

FIGURE 47 - Tumor volume and GFP fluorescence changes before and after PEF treatment. The figure shows effects of the long and the short pulses on tumor volume and GFP fluorescence as a function of time after pulse treatment as indicated in the color code (n=4, $p<0.05$). The long and short pulses were adjusted to the same energy density.

The in vivo tumor didn't hold the scaling law

When cells in culture were exposed to pulse conditions that differed in pulse duration, electric field and/or pulse number, it was found that a linear relationship was observed when the data were plotted for nsPEF effect on calcium mobilization and platelet activation versus the product of the pulse duration, electric field, and the square root of the pulse number. This provided a scaling law that described effects of nsPEFs in vitro. In the experiments here, the scaling law was tested by varying pulse number and electric field under 9 different treatment conditions (Table II -Table VI). The biological effects were evaluated by caspase 3, a marker for apoptosis and CD31, a marker of micro-vessel density for angiogenesis. Tumor volumes were also plotted. A linear relationship was not observed when plotted against this formula for caspase activation, CD31 expression, or tumor volume.

TABLE II - DIFFERENT LEVELS OF ELECTRIC FIELD, ENERGY DENSITY AND PULSE NUMBER

E	Pulse duration	Pulse number
10kV/cm	300	10
20kV/cm	300	100
40kV/cm	300	300

TABLE III - THE RANDOM COMBINATION OF DIFFERENT NSPEF TREATMENT CONDITIONS

Condition	Sample number	E (kV/cm)	τ(ns)	n	$E\tau\sqrt{n}$
1	2	10	300	10	9480
2	2	10	300	100	30000
3	2	10	300	300	51962
4	2	20	300	10	18960
5	4	20	300	100	60000
6	2	20	300	300	103800
7	2	40	300	10	37920
8	8	40	300	100	120000
9	8	40	300	300	207600

TABLE IV-CASPASE ACTIVITY MEASURED BY AC-DEVD-AFC UNDER DIFFERENT NSPEF TREATMENT CONDITIONS

Condition	E (kV/cm)	τ(ns)	n	$E\tau\sqrt{n}$	Caspase-3 pmol/minute/mg protein
1	10	300	10	9480	51
4	20	300	10	18960	91
2	10	300	100	30000	49
7	40	300	10	37920	32
3	10	300	300	51962	83
5	20	300	100	60000	171
6	20	300	300	103800	64
8	40	300	100	120000	129
9	40	300	300	207600	98

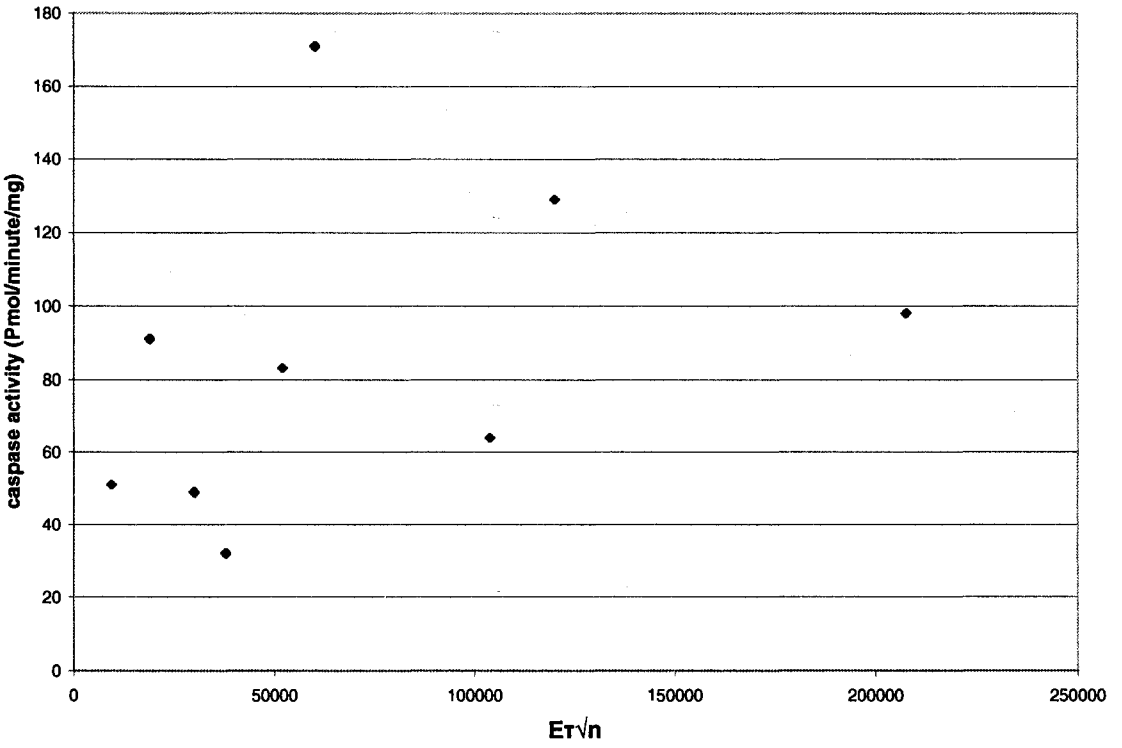

FIGURE 48 - The plot of caspase activity under 9 different nsPEF T_x conditions against the indicated X-axis formula.

TABLE V - CD31 PERCENTAGE OF POSITIVE CELLS IN EVERY FIELD UNDER DIFFERENT nsPEF TREATMENT CONDITIONS

Condition	E (kV/cm)	τ(ns)	n	Eτ √n	CD31
1	10	300	10	9480	13
4	20	300	10	18960	12
2	10	300	100	30000	10
7	40	300	10	37920	11
3	10	300	300	51962	17
5	20	300	100	60000	25
6	20	300	300	103800	15
8	40	300	100	120000	24
9	40	300	300	207600	13

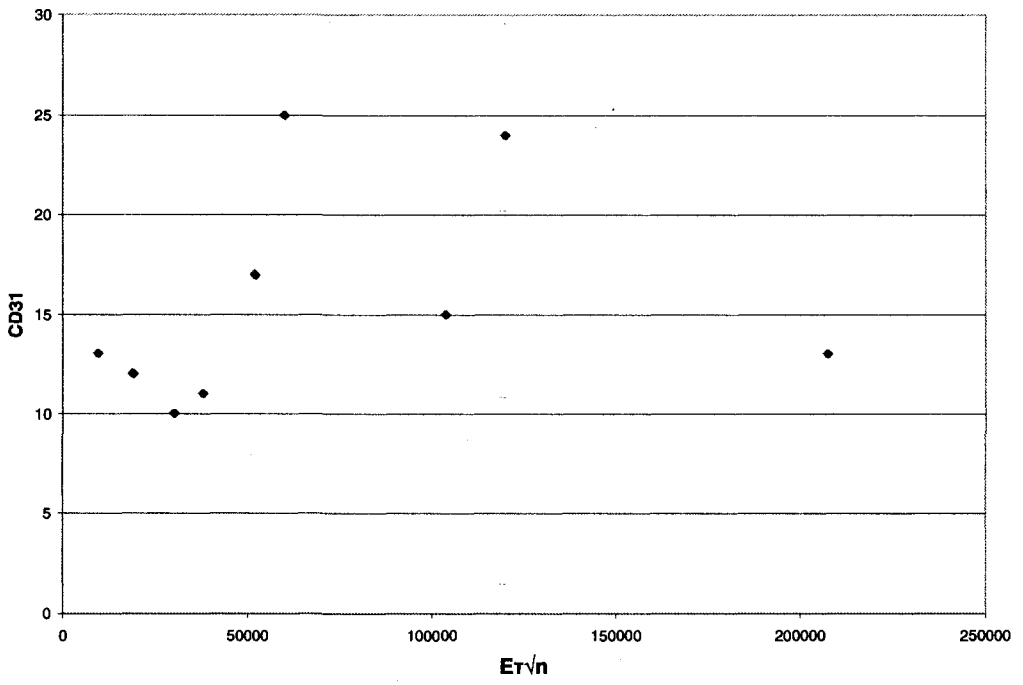

FIGURE 49 - The plot of CD31 under 9 different nsPEF Tx conditions against the indicated X-axis formula.

TABLE VI -TUMOR VOLUME CHANGES UNDER DIFFERENT NSPEF TREATMENT CONDITIONS

Condition	E (kV/cm)	τ(ns)	n	Eτ √n	Tumor volume (mm3)
1	10	300	10	9480	132
4	20	300	10	18960	143
2	10	300	100	30000	110
7	40	300	10	37920	101
3	10	300	300	51962	97
5	20	300	100	60000	55
6	20	300	300	103800	45
8	40	300	100	120000	34
9	40	300	300	207600	45

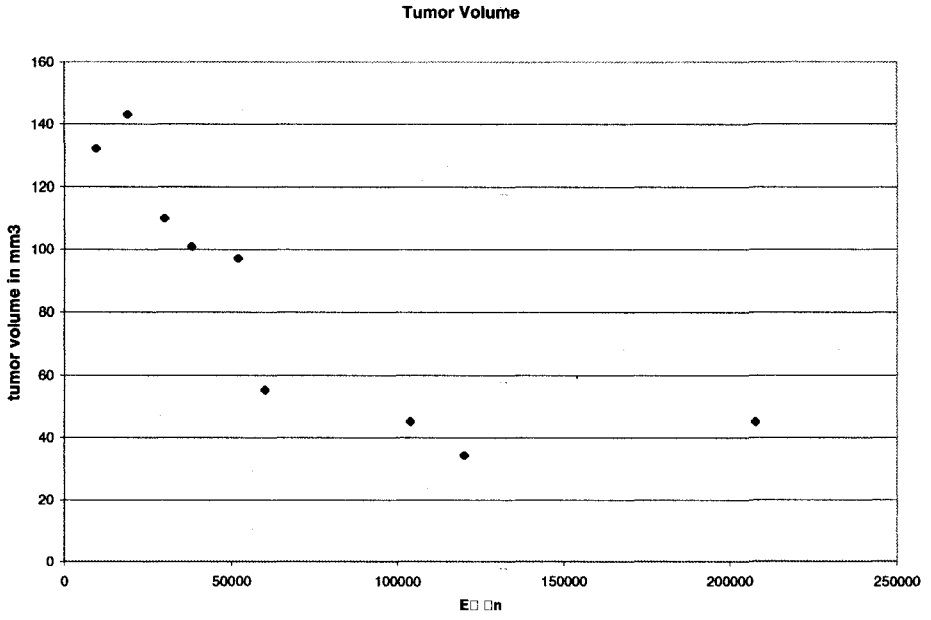

FIGURE 50 - The plot of tumor volume (the mean volume in the first 1-3 days post-treatment) under 9 different nsPEF T_x conditions against the indicated X-axis formula..

Discussion

In these studies the same energy was delivered to two tumors on the same mouse. One treatment will be called a long pulse (150v, 1 ms, 48 pulses) and the other will be called the short pulse (6 kV, 300 ns, 100 pulses).

The energy is written as

$W = \tau \frac{V^2}{R} N$ where W is the energy (joule), τ is the pulse duration, V is the voltage across the electrodes (volt), R is the tissue resistance (Ω), and N is the pulse number. Though there is not an absolute value of energy, but for long pulse (1 ms) at a lower voltage (150 V), 48 pulses was calculated to deliver the same energy to the tissue as short pulse. This was based on differences between electrodes.

Several interesting effects were observed in the study of conventional plasma membrane electroporation pulses defined as long pulses and nsPEF pulses as described as short pulses. The first observation indicates that decreases in tumor volumes are observed in both long and short pulses. However effects of short pulses resulted in greater tumor size decreases than those observed for long pulses. Furthermore, in studies not shown here, the long pulse treated tumors rebounded more rapidly than the short pulse treated

tumors. This indicates that nsPEF treatment of tumors is different than conventional electroporation pulse treatment and is more effective. Long pulses are known to have predominant effects on the plasma membrane with little or no effects on intracellular membrane. In contrast, for shorter pulses, as the pulse duration decreases, greater effects occur on intracellular membranes. Nevertheless, short pulses have effects on the plasma membrane to create nanopore formation in a process termed supra-electroportation. These nanopores are much smaller (~1nm) and more numerous that larger pores formed by classical plasma membrane electroporation pulses or longer pulses. For 300ns pulses it is not clear where this condition fits into the paradigms of plasma membrane or intracellular membrane effects. Based on *in vitro* effects of long and short pulses on propidium iodide uptake in Jurkat cells, 60ns pulses had significantly delayed effect on PI uptake compare to 300ns pulses, suggesting the absence of direct effects on plasma membranes with shorter pulses and more likely due to biological effects, which could be related to apoptosis. In addition, PI may be too large to enter nanopores caused by supra-electropoation. For 300ns pulses in this same paper, there were immediate effects as well as delayed effects on PI uptake, suggesting a mixture of classical plasma membrane electroporation and supra-electroporation. In contrast, 10 and 100 μs pulses caused immediate PI uptake, suggesting conventional electroporation effects. It should be noted that effects of these pulses *in vitro* and *vivo* may be different and that pulses in the referenced study were not corrected for energy density. Nevertheless, this provides an initial understanding of differences between conventional plasma membrane electroporation and nsPEF yielding supr-electroporation.

A second interesting observation occurred for effects of long and short pulses on GFP fluorescence.. The long pulses had immediate effects on GFP causing a rapid quenching effect in minutes. This suggests a direct effect of the long pulses on GFP fluorescence (quenching). In contrast, the short pulses had significantly delayed effects on quenching that were coincident with caspase activation, suggesting the GFP protein was turned-over like other proteins during apoptosis progression.

Finally, the relationships for tumor volume, caspase activation, and micro-vessel formation were not linear with the formula found for *in vivo* effects, which scaled with the produce of the pulse duration, electric field, and square root on the pulse number.

This is not surprising since the square root of pulse number is related to the random walk hypothesis. Random walk would be operative *in vivo* as cells rotate in solution, thus experience pulses from several angles. Such rotation would not be present in vivo tissues. Therefore the randum walk hypothesis would not apply *in vivo*.

In summary, long and short pulses differ in effects on tumor growth and GFP fluorescence (quenching). Short nsPEF pulses have lesser or delayed effects on GFP quenching and great effects on decreases in tumor size. It is likely that long pulses have direct effects on GFP quenching, while short pulses have quenching effects that are coincident with protein turn-over during apoptosis progression. In addition, the scaling law defined for *in vitro* effects on calcium mobilization and platelet activation does not hold for caspase activation, micro-vessel formation and tumor size decreases in tumor tissues *in vivo*. This is expected based on the absence of a random walk effect *in vivo*. However, for some of these studies, the small replicate number indicates a need for more trials to substantiate the dose-effect scaling law or some other coefficients relating nsPEF conditions and biological effects *in vivo*.

CHAPTER VII

CONCLUSIONS

NsPE have been previously used for military and industrial decontamination purposes. NsPEF application in biology gave birth to bio-electrics, which applies ultra-short nsPEF to biological living cells, tissues, organs, and living systems. According to the previous modeling research and *in vitro* studies, the main characteristics of nanosecond pulsed electric fields are their high power and low energy density leading to very little heat production and their special ability to permeabilize intracellular membranes and organelles. The effects of nsPEF T_x on tissues or humans had not been tested until very recently. Initial studies were done *ex vivo* on mouse embryonic fibroblasts. Fibrosarcoma tumors were injected in the flanks of C57Bl6 mice, treated *ex vivo*. Treatment of the fibrosarcoma B10.2 cells indicated a reduced size after nsPEF treatment. Results from *ex vivo* studies indicated caspase activation and induction of DNA fragmentation define by TUNEL. The present studies are based on these initial studies and confirm that nsPEF T_x has the potential to effectively eliminate tumors. In addition the mechanisms of nsPEF effects on B16f10 tumors *in vivo* are revealed.

Transillumination and surface photography showed a consistently decreasing tumor size and eventual self destruction in the treated tumor compared with the untreated melanoma, which kept growing throughout the experiment protocol period. After nsPEF T_x, tumor development was inhibited with sharply decreased volumes on the first 7 days post-nsPEF T_x as compared to control tumors ($p<0.05$). The nsPEF treated tumor weight was reduced to 14.8% of the control group ($p<0.01$). H&E and TEM images both showed that without nsPEF T_x, the melanomas kept a regular outline of tumor cells with a pale nucleus and prominent round nucleolus. Cell cytoplasm was finely dusted with melanin and the cells often formed tumor nests with an active growing center marked by a good blood vessel network and well-organized cancer cell cords marked by invading vessels, dermis and or muscle fibers. In nsPEF treated melanomas, solid tumor nest construction was detached, tumor cords were broken and the space between tumor cells enlarged with shrinking spindle shaped nuclei inside. Regression in size of tumors occurred within 24 hours with surrounding tissue swelling and bleeding. Subcutaneous

tissue and skin were recovered within 7 days. Skin pulsed with nsPEFs produces typical inflammation in the treated area during the first three days but can be resolved in one week. Fontana-Masson stain indicates nsPEF can externalize the melanin. Iron stain suggests nsPEF caused slight to mild hemorrhage in the treated tissue. Histology confirmed that repeated applications of nsPEF did not damage the peripheral healthy skin tissue of treated mice.

NsPEF T_x can significantly reduce subcutaneous murine melanoma development producing tumor contraction and nuclear shrinkage while concurrently but not permanently damaging peripheral healthy skin tissue in the treated area. Furthermore, these studies revealed the mechanisms of nsPEF-induced tumor demise, which included DNA damage as defined by Histone 2AX phosphorylation, apoptosis induction as defined by caspase activation and DNA fragmentation as well as tumor infarction as defined by loss of blood supply to the tumor and the discovory of changes in blood vessel density as defined by CDs 31, 34, and 105, which are markers for large , medium, a micro-vessel formation. Therefore, nsPEF T_x can be used as a highly localized and drug-free, non-thermal physical technique for tumor therapy with known mechanisms of action. Thus these studies pave the way for a fully comprehensive understanding of applications for nsPEF.

NsPEF treated melanomas showed double stranded DNA breaks; H_2AX activation appeared 1 h after the nsPEF treatment. At 3 hours post-nsPEF T_x, H_2AX climbed to a peak and caspases were activated. Caspase enzymes reached their climax at 6 hours post-nsPEF T_x. TUNEL detected apoptosis from 3 hours post-nsPEF T_x and the maximum appeared at 6 hours post-nsPEF T_x. Histological examination of nuclear morphological confirmed the same time sequence of changes seen in caspase and TUNEL assays. Western blot showed BAD expression increased while Bcl-2 expression decreased throughout the post-nsPEF T_x hours. NsPEF treatment activated caspase 9. These data suggest that nsPEF can affect melanoma by inducting apoptosis. A likely conclusion indicates that nsPEF treatment triggered a chain reaction: breaking double stranded DNA, initiating H_2AX phosphorylation for repair, thereby activating caspases and initiating increased Bad and decreased bcl-2 expression resulting in apoptosis with mitochondria involvement. The treated melanomas self destruct as evidenced by

histological changes and the long term study. These results demonstrated that nsPEF T_x induces apoptosis in a time-dependent manner in melanomas *in vivo*.

Both histology and intratumoral MVD assessed by CD31, CD34 and CD105 showed a significant lower vessel number and density in the nsPEF T_x group when compared to the control group. The inhibition rates were 76.9%, 66.7% and 39.9% by CD31, CD34 and CD105, respectively. Western blot indicated protein expression of VEGF and PD-ECGF was lower in the treated melanoma than that in control tumors. The data suggest that nsPEF T_x directly damaged the melanoma cells and pre-existing blood vessels. As a result, tumor-derived blood vessel growth-stimulating factors such as VEGF and PD-ECGF decreased. The balance between pro-angiogenic and anti-angiogenic cytokines was broken and new vessel formation was inhibited which contributed to the tumor self destruction. It is concluded that direct vascular damage on the pre-existing vessels and anti-angiogenic effects on neovasculature are another possible mechanism for tumor self-destruction after nsPEF T_x.

A five-month *in vivo* survival study of tumors exposed to nsPEF tested the long-term effect. All 17 mice in the treated group survived 3-5 months with the melanomas in complete remission while 14 of the 19 control mice died within 3 weeks due to fast tumor growth and big tumor volumes. Tumor volume, survival times and tumor vessel numbers were statistically different ($p<0.001$) between control and treatment groups. Both groups had one case of tumor metastasis but no significant difference existed in tumor metastasis between the groups. *In vivo* images and H&E staining revealed nsPEFs initially disrupt and finally destroy tumor construction and blood supply. IHC and tissue micro-array showed that CD31, a marker for micro vessel density, decreased significantly after nsPEF T_x and western blot analysis confirmed this reduced CD31 protein expression. After the 5-month long survival observation no tumor recurred at the primary site. Therefore nsPEF T_x is safe over a 5-month period.

Initial studies on cells *in vitro* showed that there was a relationship between nsPEF conditions and biological effects that followed the formula: biological response = $E\tau\sqrt{n}$, where E=energy density, τ= pulse duration, and n= pulse number. Our data *in vivo* showed that this scaling law relationship did not hold for tumor tissue response *in vivo*.

The possible reason is tumor tissues are fixed and the random motion effects which exist in cells in media are not present *in vivo*.

This study is the most thorough and systematic animal trial for the nsPEF application in solid tumor *in vivo*. NsPEF T_x induced effects were different from ionization or heating, it can produce broad impacts on the melanomas *in vivo*, ranging from DNA fragmentation, caspase activation, nuclear damage, apoptosis induction, pre-existing local vessel damage, intra-tumoral neovascular inhabitation to systematic histological changes both in short- and long-term experiments. The data reveals nsPEFs act as non-chemical, non-thermal, and non-ligand stimuli that can treat melanomas *in vivo*.

REFERENCES

1. Lachiewicz AM, Berwick M, Wiggins CL, Thomas NE. Epidemiologic support for melanoma heterogeneity using the surveillance, epidemiology, and end results program. J Invest Dermatol 2008;128:1340-2.

2. Qureshi AA, Laden F, Colditz GA, Hunter DJ. Geographic variation and risk of skin cancer in US women. Differences between melanoma, squamous cell carcinoma, and basal cell carcinoma. Arch Intern Med 2008;168:501-7.

3. Katipamula R, Markovic SN. Emerging therapies for melanoma. Expert Rev Anticancer Ther 2008;8:553-60.

4. Tsai S, Sabel MS. Translational research in melanoma. Surg Oncol Clin N Am 2008;17:391-419, ix-x.

5. Agarwala SS, Kirkwood JM. Melanoma: immunotherapeutic approaches. BioDrugs 1999;12:193-208.

6. Padussis JC, Steerman SN, Tyler DS, Mosca PJ. Pharmacokinetics & drug resistance of melphalan in regional chemotherapy: ILP versus ILI. Int J Hyperthermia 2008;24:239-49.

7. Zhang P, Cote AL, de Vries VC, Usherwood EJ, Turk MJ. Induction of postsurgical tumor immunity and T-cell memory by a poorly immunogenic tumor. Cancer Res 2007;67:6468-76.

8. Rass K, Tilgen W. Treatment of melanoma and nonmelanoma skin cancer. Adv Exp Med Biol 2008;624:296-318.

9. Curiel-Lewandrowski C, Atkins MB. Immunotherapeutic approaches for the treatment of malignant melanoma. Curr Opin Investig Drugs 2001;2:1553-63.

10. Fabris C, Vicente MG, Hao E, Friso E, Borsetto L, Jori G, Miotto G, Colautti P, Moro D, Esposito J, Ferretti A, Rossi CR, et al. Tumour-localizing and -photosensitising properties of meso-tetra(4-nido-carboranylphenyl)porphyrin (H2TCP). J Photochem Photobiol B 2007;89:131-8.

11. Delaney G, Barton M, Jacob S. Estimation of an optimal radiotherapy utilization rate for melanoma: a review of the evidence. Cancer 2004;100:1293-301.

12. Shen F, Price JH. Toward complete laser ablation of melanoma contaminant cells in a co-culture outgrowth model via image cytometry. Cytometry A 2006;69:573-81.
13. Steels E, Donckier V, Flamen P, Blocklet D, Sales F, Vereecken P. Long-term benefit of combined radiofrequency ablation and surgery in a patient with AJCC stage IV metastatic melanoma. Clin Exp Dermatol 2007;32:100-1.
14. Rols MP, Bachaud JM, Giraud P, Chevreau C, Roche H, Teissie J. Electrochemotherapy of cutaneous metastases in malignant melanoma. Melanoma Res 2000;10:468-74.
15. Quaglino P, Mortera C, Osella-Abate S, Barberis M, Illengo M, Rissone M, Savoia P, Bernengo MG. Electrochemotherapy with Intravenous Bleomycin in the Local Treatment of Skin Melanoma Metastases. Ann Surg Oncol 2008.
16. Gaudy C, Richard MA, Folchetti G, Bonerandi JJ, Grob JJ. Randomized controlled study of electrochemotherapy in the local treatment of skin metastases of melanoma. J Cutan Med Surg 2006;10:115-21.
17. Byrne CM, Thompson JF. Role of electrochemotherapy in the treatment of metastatic melanoma and other metastatic and primary skin tumors. Expert Rev Anticancer Ther 2006;6:671-8.
18. Sersa G, Stabuc B, Cemazar M, Miklavcic D, Rudolf Z. Electrochemotherapy with cisplatin: clinical experience in malignant melanoma patients. Clin Cancer Res 2000;6:863-7.
19. Sersa G, Cufer T, Cemazar M, Rebersek M, Zvonimir R. Electrochemotherapy with bleomycin in the treatment of hypernephroma metastasis: case report and literature review. Tumori 2000;86:163-5.
20. Yang K, Qin T, Wu H, Yue B, Zou F. [Electrochemotherapy for tumor and mechanism analysis]. Sheng Wu Yi Xue Gong Cheng Xue Za Zhi 2008;25:49-52.
21. Beebe SJ, Fox PM, Rec LJ, Willis EL, Schoenbach KH. Nanosecond, high-intensity pulsed electric fields induce apoptosis in human cells. FASEB J 2003;17:1493-5.
22. Schoenbach KH, Joshi R, Kolb J, Buescher S, Beebe S. Subcellular effects of nanosecond electrical pulses. Conf Proc IEEE Eng Med Biol Soc 2004;7:5447-50.
23. Kolb JF, Kono S, Schoenbach KH. Nanosecond pulsed electric field generators for the study of subcellular effects. Bioelectromagnetics 2006;27:172-87.

24. Pakhomov AG, Kolb JF, White JA, Joshi RP, Xiao S, Schoenbach KH. Long-lasting plasma membrane permeabilization in mammalian cells by nanosecond pulsed electric field (nsPEF). Bioelectromagnetics 2007;28:655-63.

25. Hall EH, Schoenbach KH, Beebe SJ. Nanosecond pulsed electric fields (nsPEF) induce direct electric field effects and biological effects on human colon carcinoma cells. DNA Cell Biol 2005;24:283-91.

26. Chen N, Schoenbach KH, Kolb JF, James Swanson R, Garner AL, Yang J, Joshi RP, Beebe SJ. Leukemic cell intracellular responses to nanosecond electric fields. Biochem Biophys Res Commun 2004;317:421-7.

27. Frey W, White JA, Price RO, Blackmore PF, Joshi RP, Nuccitelli R, Beebe SJ, Schoenbach KH, Kolb JF. Plasma membrane voltage changes during nanosecond pulsed electric field exposure. Biophys J 2006;90:3608-15.

28. Garon EB, Sawcer D, Vernier PT, Tang T, Sun Y, Marcu L, Gundersen MA, Koeffler HP. In vitro and in vivo evaluation and a case report of intense nanosecond pulsed electric field as a local therapy for human malignancies. Int J Cancer 2007;121:675-82.

29. Stacey M, Stickley J, Fox P, Statler V, Schoenbach K, Beebe SJ, Buescher S. Differential effects in cells exposed to ultra-short, high intensity electric fields: cell survival, DNA damage, and cell cycle analysis. Mutat Res 2003;542:65-75.

30. Beebe SJ, White J, Blackmore PF, Deng Y, Somers K, Schoenbach KH. Diverse effects of nanosecond pulsed electric fields on cells and tissues. DNA Cell Biol 2003;22:785-96.

31. Demierre MF. Epidemiology and prevention of cutaneous melanoma. Curr Treat Options Oncol 2006;7:181-6.

32. Hamm C, Verma S, Petrella T, Bak K, Charette M. Biochemotherapy for the treatment of metastatic malignant melanoma: a systematic review. Cancer Treat Rev 2008;34:145-56.

33. De Croock L, Verbraeken H. Metastatic uveal melanoma: diagnosis and treatment. A literature review. Bull Soc Belge Ophtalmol 2002:59-63.

34. Kolb JF, Kono S, Schoenbach KH. Nanosecond pulsed electric field generators for the study of subcellular effects. Bioelectromagnetics 2006;27:172-87.

35. Frey W, White JA, Price RO, Blackmore PF, Joshi RP, Nuccitelli R, Beebe SJ, Schoenbach KH, Kolb JF. Plasma membrane voltage changes during nanosecond pulsed electric field exposure. Biophys J 2006;90:3608-15.

36. Schilling S, Schmid S, Jager H, Ludwig M, Dietrich H, Toepfl S, Knorr D, Neidhart S, Schieber A, Carle R. Comparative Study of Pulsed Electric Field and Thermal Processing of Apple Juice with Particular Consideration of Juice Quality and Enzyme Deactivation. J Agric Food Chem 2008.

37. Tekle E, Oubrahim H, Dzekunov SM, Kolb JF, Schoenbach KH, Chock PB. Selective field effects on intracellular vacuoles and vesicle membranes with nanosecond electric pulses. Biophys J 2005;89:274-84.

38. Hall EH, Schoenbach KH, Beebe SJ. Nanosecond pulsed electric fields (nsPEF) induce direct electric field effects and biological effects on human colon carcinoma cells. DNA Cell Biol 2005;24:283-91.

39. Hall EH, Schoenbach KH, Beebe SJ. Nanosecond pulsed electric fields induce apoptosis in p53-wildtype and p53-null HCT116 colon carcinoma cells. Apoptosis 2007;12:1721-31.

40. Terris MK, Stamey TA. Determination of prostate volume by transrectal ultrasound. J Urol 1991;145:984-7.

41. Ro JY, Lee SS, Ayala AG. Advantage of Fontana-Masson stain in capsule-deficient cryptococcal infection. Arch Pathol Lab Med 1987;111:53-7.

42. Gaitanis G, Chasapi V, Velegraki A. Novel application of the masson-fontana stain for demonstrating Malassezia species melanin-like pigment production in vitro and in clinical specimens. J Clin Microbiol 2005;43:4147-51.

43. Kartashev AH. [Biological mechanism of long-term effect of alternating electric field on the development of mice]. Fiziol Zh 1992;38:81-5.

44. Mori K, Hasegawa T, Sato S, Sugibayashi K. Effect of electric field on the enhanced skin permeation of drugs by electroporation. J Control Release 2003;90:171-9.

45. Vernier PT, Sun Y, Chen MT, Gundersen MA, Craviso GL. Nanosecond electric pulse-induced calcium entry into chromaffin cells. Bioelectrochemistry 2008;73:1-4.

46. Entin I, Plotnikov A, Korenstein R, Keisari Y. Tumor growth retardation, cure, and induction of antitumor immunity in B16 melanoma-bearing mice by low electric field-enhanced chemotherapy. Clin Cancer Res 2003;9:3190-7.

47. Terris MK, Stamey TA. Determination of prostate volume by transrectal ultrasound. J Urol 1991;145:984-7.

48. Nuccitelli R, Pliquett U, Chen X, Ford W, James Swanson R, Beebe SJ, Kolb JF, Schoenbach KH. Nanosecond pulsed electric fields cause melanomas to self-destruct. Biochem Biophys Res Commun 2006;343:351-60.

49. Beebe SJ, Blackmore PF, White J, Joshi RP, Schoenbach KH. Nanosecond pulsed electric fields modulate cell function through intracellular signal transduction mechanisms. Physiol Meas 2004;25:1077-93.

50. Beebe SJ, Fox PM, Rec LJ, Willis EL, Schoenbach KH. Nanosecond, high-intensity pulsed electric fields induce apoptosis in human cells. FASEB J 2003;17:1493-5.

51. Talve LA, Collan YU, Ekfors TO. Nuclear morphometry, immunohistochemical staining with Ki-67 antibody and mitotic index in the assessment of proliferative activity and prognosis of primary malignant melanomas of the skin. J Cutan Pathol 1996;23:335-43.

52. Robertson JD, Gogvadze V, Zhivotovsky B, Orrenius S. Distinct pathways for stimulation of cytochrome c release by etoposide. J Biol Chem 2000;275:32438-43.

53. Kanduc D, Mittelman A, Serpico R, Sinigaglia E, Sinha AA, Natale C, Santacroce R, Di Corcia MG, Lucchese A, Dini L, Pani P, Santacroce S, et al. Cell death: apoptosis versus necrosis (review). Int J Oncol 2002;21:165-70.

54. Ivanov VN, Zhou H, Hei TK. Sequential treatment by ionizing radiation and sodium arsenite dramatically accelerates TRAIL-mediated apoptosis of human melanoma cells. Cancer Res 2007;67:5397-407.

55. Wartenberg M, Wirtz N, Grob A, Niedermeier W, Hescheler J, Peters SC, Sauer H. Direct current electrical fields induce apoptosis in oral mucosa cancer cells by NADPH oxidase-derived reactive oxygen species. Bioelectromagnetics 2008;29:47-54.

56. Chen N, Schoenbach KH, Kolb JF, James Swanson R, Garner AL, Yang J, Joshi RP, Beebe SJ. Leukemic cell intracellular responses to nanosecond electric fields. Biochem Biophys Res Commun 2004;317:421-7.

57. De Croock L, Verbraeken H. Metastatic uveal melanoma: diagnosis and treatment. A literature review. Bull Soc Belge Ophtalmol 2002:59-63.

58. Ioannou YA, Chen FW. Quantitation of DNA fragmentation in apoptosis. Nucleic Acids Res 1996;24:992-3.

59. Muppidi J, Porter M, Siegel RM. Measurement of apoptosis and other forms of cell death. Curr Protoc Immunol 2004;Chapter 3:Unit 3 17.

60. Lu C, Zhu F, Cho YY, Tang F, Zykova T, Ma WY, Bode AM, Dong Z. Cell apoptosis: requirement of H2AX in DNA ladder formation, but not for the activation of caspase-3. Mol Cell 2006;23:121-32.

61. Eggermont AM, Voit C. Management of melanoma: a European perspective. Surg Oncol Clin N Am 2008;17:635-48.

62. Cattell E, Kelly C, Middleton MR. Brain metastases in melanoma: a European perspective. Semin Oncol 2002;29:513-7.

63. Denijn M, Ruiter DJ. The possible role of angiogenesis in the metastatic potential of human melanoma. Clinicopathological aspects. Melanoma Res 1993;3:5-14.

64. Gutman M, Singh RK, Yoon S, Xie K, Bucana CD, Fidler IJ. Leukocyte-induced angiogenesis and subcutaneous growth of B16 melanoma. Cancer Biother 1994;9:163-70.

65. Nuccitelli R, Pliquett U, Chen X, Ford W, James Swanson R, Beebe SJ, Kolb JF, Schoenbach KH. Nanosecond pulsed electric fields cause melanomas to self-destruct. Biochem Biophys Res Commun 2006;343:351-60.

66. Novoselova EG, Ogai VB, Sorokina OV, Novikov VV, Fesenko EE. [Effect of centimeter microwaves and the combined magnetic field on the tumor necrosis factor production in cells of mice with experimental tumors]. Biofizika 2001;46:131-5.

67. Seligson DB. The tissue micro-array as a translational research tool for biomarker profiling and validation. Biomarkers 2005;10 Suppl 1:S77-82.

68. Giacomini P, Imberti L, Aguzzi A, Fisher PB, Trinchieri G, Ferrone S. Immunochemical analysis of the modulation of human melanoma-associated antigens by DNA recombinant immune interferon. J Immunol 1985;135:2887-94.

69. Pisacane AM, Picciotto F, Risio M. CD31 and CD34 expression as immunohistochemical markers of endothelial transdifferentiation in human cutaneous melanoma. Cell Oncol 2007;29:59-66.

70. Mineo TC, Ambrogi V, Baldi A, Rabitti C, Bollero P, Vincenzi B, Tonini G. Prognostic impact of VEGF, CD31, CD34, and CD105 expression and tumour vessel invasion after radical surgery for IB-IIA non-small cell lung cancer. J Clin Pathol 2004;57:591-7.

71. Kawabata K, Nakai S, Miwa M, Sugiura T, Otsuka Y, Shinzato T, Hiki N, Tomimatsu I, Ushida Y, Hosono F, Maeda K. CD31 expression on leukocytes is downregulated in vivo during hemodialysis. Nephron 2001;89:153-60.

72. Goi T, Fujioka M, Satoh Y, Tabata S, Koneri K, Nagano H, Hirono Y, Katayama K, Hirose K, Yamaguchi A. Angiogenesis and tumor proliferation/metastasis of human colorectal cancer cell line SW620 transfected with endocrine glands-derived-vascular endothelial growth factor, as a new angiogenic factor. Cancer Res 2004;64:1906-10.

73. Schneider W, Undeutsch W. [Uncommon blood vessel tumors of the skin. Clinical picture, pathological anatomy and histology as well as classification]. Hautarzt 1967;18:437-45.

74. Gaudy C, Richard MA, Folchetti G, Bonerandi JJ, Grob JJ. Randomized controlled study of electrochemotherapy in the local treatment of skin metastases of melanoma. J Cutan Med Surg 2006;10:115-21.

75. Behrem S, Zarkovic K, Eskinja N, Jonjic N. Endoglin is a better marker than CD31 in evaluation of angiogenesis in glioblastoma. Croat Med J 2005;46:417-22.

76. Vieira SC, Silva BB, Pinto GA, Vassallo J, Moraes NG, Santana JO, Santos LG, Carvasan GA, Zeferino LC. CD34 as a marker for evaluating angiogenesis in cervical cancer. Pathol Res Pract 2005;201:313-8.

77. Duff SE, Li C, Garland JM, Kumar S. CD105 is important for angiogenesis: evidence and potential applications. FASEB J 2003;17:984-92.

78. Fonsatti E, Sigalotti L, Arslan P, Altomonte M, Maio M. Emerging role of endoglin (CD105) as a marker of angiogenesis with clinical potential in human malignancies. Curr Cancer Drug Targets 2003;3:427-32.

79. Dales JP, Garcia S, Andrac L, Carpentier S, Ramuz O, Lavaut MN, Allasia C, Bonnier P, Charpin C. Prognostic significance of angiogenesis evaluated by CD105 expression compared to CD31 in 905 breast carcinomas: correlation with long-term patient outcome. Int J Oncol 2004;24:1197-204.

80. Wang SM, Xu XY, Chen G, Yang LR. [Taohong Siwu decoction II inhibits the angiogenesis and the expressions of VEGF and KDR/FLK-1 in C57BL/6J mice bearing B16 melanoma]. Zhongguo Zhong Yao Za Zhi 2005;30:1866-9.

81. Kitamura T, Asai N, Enomoto A, Maeda K, Kato T, Ishida M, Jiang P, Watanabe T, Usukura J, Kondo T, Costantini F, Murohara T, et al. Regulation of VEGF-mediated angiogenesis by the Akt/PKB substrate Girdin. Nat Cell Biol 2008;10:329-37.

82. Benelli R, Lorusso G, Albini A, Noonan DM. Cytokines and chemokines as regulators of angiogenesis in health and disease. Curr Pharm Des 2006;12:3101-15.

83. Singh RK, Fidler IJ. Regulation of tumor angiogenesis by organ-specific cytokines. Curr Top Microbiol Immunol 1996;213 (Pt 2):1-11.

84. Bremnes RM, Camps C, Sirera R. Angiogenesis in non-small cell lung cancer: the prognostic impact of neoangiogenesis and the cytokines VEGF and bFGF in tumours and blood. Lung Cancer 2006;51:143-58.

85. Jackson MR, Carney EW, Lye SJ, Ritchie JW. Localization of two angiogenic growth factors (PDECGF and VEGF) in human placentae throughout gestation. Placenta 1994;15:341-53.

86. Nuccitelli R, Pliquett U, Chen X, Ford W, James Swanson R, Beebe SJ, Kolb JF, Schoenbach KH. Nanosecond pulsed electric fields cause melanomas to self-destruct. Biochem Biophys Res Commun 2006;343:351-60.

87. Li B, Grambsch P. Sample size calculation in survival trials accounting for time-varying relationship between noncompliance and risk of outcome event. Clin Trials 2006;3:349-59.

88. Jiang Q, Snapinn S, Iglewicz B. Calculation of sample size in survival trials: the impact of informative noncompliance. Biometrics 2004;60:800-6.

89. Kolb JF, Kono S, Schoenbach KH. Nanosecond pulsed electric field generators for the study of subcellular effects. Bioelectromagnetics 2006;27:172-87.

90. Terris MK, Stamey TA. Determination of prostate volume by transrectal ultrasound. J Urol 1991;145:984-7.

91. Macak J, Krc I, Elleder M, Lukas Z, Nadasdy T, Guttnerova J. Balloon cell melanoma of the skin. part I: Histology, immunohistology and histochemistry. Acta Univ Palacki Olomuc Fac Med 1990;126:71-82.

92. Plaza JA, Suster D, Perez-Montiel D. Expression of immunohistochemical markers in primary and metastatic malignant melanoma: a comparative study in 70 patients using a tissue microarray technique. Appl Immunohistochem Mol Morphol 2007;15:421-5.
93. Pisacane AM, Picciotto F, Risio M. CD31 and CD34 expression as immunohistochemical markers of endothelial transdifferentiation in human cutaneous melanoma. Cell Oncol 2007;29:59-66.
94. Boesen EH, Boesen SH, Frederiksen K, Ross L, Dahlstrom K, Schmidt G, Naested J, Krag C, Johansen C. Survival after a psychoeducational intervention for patients with cutaneous malignant melanoma: a replication study. J Clin Oncol 2007;25:5698-703.
95. Mi Y, Sun C, Yao C, Xiong L, Liao R, Hu Y, Hu L. Lethal and inhibitory effects of steep pulsed electric field on tumor-bearing BALB/c mice. Conf Proc IEEE Eng Med Biol Soc 2004;7:5005-8.
96. Beebe SJ, Blackmore PF, White J, Joshi RP, Schoenbach KH. Nanosecond pulsed electric fields modulate cell function through intracellular signal transduction mechanisms. Physiol Meas 2004;25:1077-93.
97. Chen N, Schoenbach KH, Kolb JF, James Swanson R, Garner AL, Yang J, Joshi RP, Beebe SJ. Leukemic cell intracellular responses to nanosecond electric fields. Biochem Biophys Res Commun 2004;317:421-7.
98. Zhang J, Blackmore PF, Hargrave BY, Xiao S, Beebe SJ, Schoenbach KH. Nanosecond pulse electric field (nanopulse): a novel non-ligand agonist for platelet activation. Arch Biochem Biophys 2008;471:240-8.
99. Schoenbach KH, Joshi R, Kolb J, Buescher S, Beebe S. Subcellular effects of nanosecond electrical pulses. Conf Proc IEEE Eng Med Biol Soc 2004;7:5447-50.
100. Botella-Estrada R, Malet G, Revert F, Dasi F, Crespo A, Sanmartin O, Guillen C, Alino SF. Antitumor effect of B16 melanoma cells genetically modified with the angiogenesis inhibitor rnasin. Cancer Gene Ther 2001;8:278-84.
101. de Lorenzo MS, Ripoll GV, Yoshiji H, Yamazaki M, Thorgeirsson UP, Alonso DF, Gomez DE. Altered tumor angiogenesis and metastasis of B16 melanoma in transgenic mice overexpressing tissue inhibitor of metalloproteinases-1. In Vivo 2003;17:45-50.
102. Khosravi Shahi P, Fernandez Pineda I. Tumoral angiogenesis: review of the literature. Cancer Invest 2008;26:104-8.

103. Zimmerman RJ, Gaillard ET, Goldin A. Metastatic potential of four human melanoma xenografts in young athymic mice following tail vein inoculation. Cancer Res 1987;47:2305-10.

104. Winkelmann CT, Figueroa SD, Rold TL, Volkert WA, Hoffman TJ. Microimaging characterization of a B16-F10 melanoma metastasis mouse model. Mol Imaging 2006;5:105-14.

105. Cubillos S, Scallon B, Feldmann M, Taylor P. Effect of blocking TNF on IL-6 levels and metastasis in a B16-BL6 melanoma/mouse model. Anticancer Res 1997;17:2207-11.

106. Elkin M, Vlodavsky I. Tail vein assay of cancer metastasis. Curr Protoc Cell Biol 2001;Chapter 19:Unit 19 2.

107. Parvathenani LK, Buescher ES, Chacon-Cruz E, Beebe SJ. Type I cAMP-dependent protein kinase delays apoptosis in human neutrophils at a site upstream of caspase-3. J Biol Chem 1998;273:6736-43.

108. Lugassy C, Kleinman HK, Engbring JA, Welch DR, Harms JF, Rufner R, Ghanem G, Patierno SR, Barnhill RL. Pericyte-like location of GFP-tagged melanoma cells: ex vivo and in vivo studies of extravascular migratory metastasis. Am J Pathol 2004;164:1191-8.

109. Fukui M, Nakano-Hashimoto T, Okano K, Maruta Y, Suehiro Y, Hamanaka Y, Yamashita H, Imai K, Kawano MM, Hinoda Y. Therapeutic effect of dendritic cells loaded with a fusion mRNA encoding tyrosinase-related protein 2 and enhanced green fluorescence protein on B16 melanoma. Tumour Biol 2004;25:252-7.

APPENDIX

Abbreviations

Abbreviations	The full name
3T3	Mouse pre-adipocytes
AT	ataxia-telangiectasia
BS	Bloom syndrome
BS-LCL	B-cell lymphoblastoid
DMEM	Dulbecco's modified Eagle's medium
DTIC	decarbonizes
FA	Fanconi's anemia
FDA	United States Food and Drug Administration
GFP	green fluorescent protein
H&E	hematoxylin & eosin stain
HCT116	human colon carcinoma cells
HeLa	Human adenocarcinoma of the cervix
HL-60	human promyelocytic leukemia cells
HS578T (BrCa)	Human ductal breast carcinoma
IL-2	Interleukin-2
IACUC	The Institutional Animal Care and Use Committee
IHC	Immunohistochemistry
JURKAT	human, peripheral blood, leukemia, T cell
NsPEF Tx	nanosecond pulsed electric fields treatment
PD-ECGF	platelet-derived endothelial cell growth facto0r
PVDF	polyvinylidene difluoride
SV40	Simian virus 40
TdT	terminal desoxynucleotidyl transferase
TEM	transmission electron microscopy
TUNEL	Terminal deoxynucleotidyl Transferase Biotin-dUTP Nick End Labeling
VEGF	vascular endothelial growth factor
XP	xeroderma pigmentosum
z-IETD-FMK	Z-Ile-Glu-Thr-Asp-fluoromethyl ketone

VITA

Education
Ph.D. Biomedicine (2004-2008)
Joint Ph.D. Program of Eastern Virginia Medical School and Old Dominion University, Norfolk, VA
Ph.D. Organ Transplantation (2003-2006)
Zhejiang University, Hangzhou, Zhejiang, China
M.D. General Surgery (1994-1999)
Xinjiang Medical University, Urumqi, Xinjiang, China

Professional experience
Licensed Surgeon (2003 till now)
Medical Center for Liver Transplantation, School of Medicine, Zhejiang University, Zhejiang, China
Assistant Professor (2006-til now)
Department of General Surgery, School of Medicine, Zhejiang University, Zhejiang, China

Awards:
Curtis Carl Johnson Memorial Award, Bioelectromagnetics (BEMS) Society, 2007
Chinese Government Award, for Outstanding Self-Financed Students Abroad, 2007
The First Class Award, Chinese Overseas Scholars Research Competition (Chunhui Cup) 2006, 2007
Bagley Scholarship, Eastern Virginia Medical School and Old Dominion University, 2005-2006
Medical Research and Development Award, Xinjiang Province, China 2005

Membership:
Student member of The Bioelectromagnetics Society, BEMS
Student member of American Society for Cellular Biology, ASCB
Member of Chinese Medical Association, CMA
Member of Chinese Organ Transplantation Association, COTA

Publication:
1. Yin, S. Li, J. Hu, C. and Chen X., "CD133 Positive Hepatocellular Carcinoma Cells Possess High Capacity for Tumorigenicity", *International Journal of Cancer,* 120(7), 2007, pp.1444-50
2. Swanson, J. Chen, X. and Nuccitelli, R. ,"Melanoma Morphology Change & Apoptosis Induced by Multiple Nanosecond Pulsed Electric Fields", *Conference Proceedings IEEE Xplore*, 2007, pp.1036-39
3. Chen, X. Swanson, R. and Nuccitelli, R., "Nanosecond Pulsed Electric Fields (nsPEFs) Inhibit Melanoma Angiogenesis", *Conference Proceedings IEEE Xplore*, 2007, pp.1040-43
4. Nuccitelli, R. Pliquett, U. and Chen, X., "Nanosecond Pulsed Electric Fields Cause Melanomas to Self-Destruct", *Biochemical and Biophysical Research Communications*. 343(2), 2006, pp.351-60

Grants and Contracts:
1. National Natural Science Foundation, China, Grant No. 3070078, 2008-2010, Principal Investigator
2. Zhejiang Provincial Science Fund for Distinguished Young Medical Faculty, Grant No. 2007QN006, 2007-2009, Principal Investigator
3. Xinjiang Natural Science Foundation, Grant No. XJDX0202-2005-06,2005-2006, Principal Investigator